Nkpa Mba Ogarekpe

The Impacts of Climate Change on Hydrology and Hydropower Production

June 2023

NTNU
Norwegian University of
Science and Technology

Faculty of Engineering
Department of Civil and Environmental Engineering

Master's thesis

2023

Nkpa Mba Ogarekpe

Master's thesis

NTNU
Norwegian University of
Science and Technology

NTNU
Norwegian University of
Science and Technology

NTNU
Norwegian University of
Science and Technology

The Impacts of Climate Change on Hydrology and Hydropower Production

Nkpa Mba Ogarekpe

Hydropower Development
Submission date: June 2023
Supervisor: Knut Alfredsen

Norwegian University of Science and Technology
Department of Civil and Environmental Engineering

NTNU
Norwegian University of
Science and Technology

Faculty of Engineering
Science and Technology
Department of Civil and
Environmental Engineering

M.Sc. THESIS IN HYDROPOWER DEVELOPMENT

Candidate: **Nkpa Mba Ogarepke**

Title: **The impacts of climate change on hydrology and hydropower production.**

1 BACKGROUND

Scenarios show that the expected changes in climate will have impacts on runoff from catchments and thereby have an impact on the potential for hydropower production in the catchment. Previous work show that we can expect both decreases and increases dependent on the location of the site, and that we have considerable uncertainties in the scenarios that needs to be considered. It is therefore necessary to investigate the inflow changes in detail and evaluate the uncertainties in the hydropower production and evaluate how current operation and environmental restrictions will be influenced by these changes. In addition, other factors in the watershed like water use for other purposes and general environmental conditions will also be influenced by changed inflow and altered hydropower production.

The objective of this thesis is to do a detailed evaluation of the changes in climate on a Norwegian hydropower system. This should be done by utilizing the downscaled CMIP5 climate scenarios available from the Norwegian Climate Service Center as input for precipitation and temperature, and then model runoff for the catchment using a hydrological model. This runoff would then be input

for hydropower modelling and assessment of various impacts on production, environmental conditions and other factors related to water use in the catchment. To further evaluate the impacts of climate and hydropower, an unregulated catchment in the neighbourhood of the study catchment should also be modelled and used as a "natural" case for comparison of seasonal flow distribution and low/high flow periods which is typically altered by hydropower production.

2 MAIN QUESTIONS FOR THE THESIS

The thesis shall cover, though not necessarily be limited to the main tasks listed below.

The following main steps will be carried out during the thesis work:

1. A brief literature review should be made to establish the current knowledge on climate impacts on hydropower production, both internationally and particularly for Norwegian systems.
2. Selection of study catchments and the hydrological model to use and preparation of the climate scenarios for the analysis. This involves processing the gridded data from *klimaservicesenter.no* into gridded input data for the target catchments. To properly evaluate uncertainty, it should be aimed at using the full range of climate models available. A comparison of the precipitation and temperature for the historical period and the scenario periods should also be done.
3. Select a hydrological model for the work. Calibrate and validate the model for the historical period with data from 2) and prepare runoff scenarios for the future for all models and emission scenarios for the catchments. Compare modelled runoff between scenarios and models and assess uncertainty. Snow conditions should also be evaluated.
4. Run the nMag hydropower model using input from 3) to produce production scenarios for the historical and scenario periods. Evaluate the model performance and if we need to adjust operational parameters to better utilise the available water.
5. Compare the two catchments related to winter flow, summer low flow, flood

conditions and other key factors in the hydrological regime.

3 SUPERVISION, DATA, AND INFORMATION INPUT

Professor Knut Alfredsen will be the supervisors of the thesis work.

Discussion with and input from colleagues and other research or engineering staff at NTNU, SINTEF, power companies or consultants are recommended. Significant inputs from others shall, however, be referenced in a convenient manner.

The research and engineering work carried out by the candidate in connection with this thesis shall remain within an educational context. The candidate and the supervisors are therefore free to introduce assumptions and limitations, which may be considered unrealistic or inappropriate in contract research or a professional engineering context.

4 REPORT FORMAT AND REFERENCE STATEMENT

The thesis report shall be in the format A4. It shall be typed by a word processor and figures, tables, photos etc. shall be of good report quality. The report shall include a summary, a table of content, a list of literature formatted according to a common standard and other relevant references. A signed statement where the candidate states that the presented work is his own and that significant outside input is identified should be included.

The report shall have a professional structure, assuming professional senior engineers (not in teaching or research) and decision makers as the main target group.

All data and model setups should be compiled, documented, and submitted with the thesis.

The thesis shall be submitted no later than 12th of June 2023.

Trondheim 11th of January 2023

_____

Knut Alfredsen
Professor

ABSTRACT

Climate change impacts catchment hydrology, hence, hydropower production. The study aims to determine the trends in the precipitation and temperature of Forra and Lærdal catchments, the effects of climate change on the hydrology of the catchments, and the effects of climate change on the future energy production of Funna hydropower system. A full range of climate models were utilized to define the uncertainty band. The systematic biases in the Regional Climate Model (RCM) were corrected/adjusted using Quantile mapping method. The potential evaporation of the catchments was computed using the Thornthwaite's method. Hydrological models of the catchments were setup, calibrated and validated using observational gridded climatic datasets. Future flows were simulated for the ten climate models, for RCP4.5 and RCP8.5 scenarios for the periods 2041 – 2070, 2071 – 2099. The effects of future flows on energy production and the environment were simulated using nMAG and HEC-RAS, respectively. The results of the Mann-Kendall trend test revealed that the temperature is projected to increase between the time horizons for both catchments. The climate models do not show a systematic decrease or increase in precipitation between the time horizons considered. On average, the ensemble annual precipitation predicts an increase in future precipitation for both catchments.

The performance of Forra and Lærdal catchment models at calibration yielded NSE R2 values of 0.826 and 0.895, respectively, as well as NSE R2 values of 0.733 and 0.863, respectively, at validation. The snowpack is predicted to reduce between the historical and end of the century periods for both catchments. The average of mean monthly snowpack of Forra catchment, corresponding to the baseline, RCP4.5_2041-2070, RCP4.5_2071-2099, RCP8.5_2041-2070, and RCP8.5_2071-2099 are 140.49 mm, 49.02 mm, 38.03 mm, 37.39 mm, and 11.07 mm, respectively. Also, the mean annual runoff corresponding to the baseline, RCP4.5_2041-2070, RCP4.5_2071-2099, RCP8.5_2041-2070, and RCP8.5_2071-2099 scenarios are 20.67 m^3/s, 21.45 m^3/s, 21.58 m^3/s, 21.33 m^3/s, and 22.68 m^3/s, respectively. In the future, the temporal variability of runoff is likely to change

from the current snowmelt-based spring flood to higher winter runoff.

For Lærdal catchment, the average of the mean monthly snowpack corresponding to the baseline, RCP4.5_2041-2070, RCP4.5_2071-2099, RCP8.5_2041-2070, and RCP8.5_2071-2099 are 316.64 mm, 205.50 mm, 179.51 mm, 171.15 mm, and 108.44 mm, respectively. Also, the mean annual runoff corresponding to the baseline, RCP4.5_2041-2070, RCP4.5_2071-2099, RCP8.5_2041-2070, and RCP8.5_2071-2099 scenarios are 40.89m^3/s, 43.46 m^3/s, 44.24 m^3/s, 43.42 m^3/s, and 47.12 m^3, respectively. In the future, early occurrence of snowmelt-based spring flood will likely become prevalent. A significant increase in runoff is likely to occur for RCP8.5 scenario during the end-of-century period compared to other time horizons. For a designer interested in practicality and applicability of climate change impacts on runoff, the climate change factors for future runoff of Forra and Lærdal catchment are projected to increase by 10% and 15%, respectively, by the end of the 21st century. The ensemble winter low flow will increase while the ensemble summer low flow will decrease in the future for all the scenarios and time horizons for both catchments. A change in the timing of occurrence of low flow will occur, for both catchments, particularly for RCP8.5_2071-2099 scenario.

The reservoir operational strategy, which was designed to maximize the incoming snowmelt spring flood, was evaluated. The average annual energy generation of Funna hydropower system for the baseline scenario was 63.51GWh/year. The hydropower simulations show a marginal decrease in the future energy generation of 0.01–0.02% under the current reservoir operational strategies, for all the scenarios, except RCP8.5_2071-2099. RCP8.5_2071-2099 yielded a marginal increase in hydropower generation of 0.06%. The modification of the operational strategy resulted to the decrease in spill, hence, increase in energy generation. The modified strategies resulted to an increase in the future energy generation of 0.70 – 0.80%, with the highest increase occurring for RCP4.5_2041-2070 scenario. The decision on the future reservoir management strategy must be balanced with other considerations such as target consumers, firm power demand, and environmental constraints.

ACKNOWLEDGEMENT

I thank Prof. Knut Alfredsen for his guidance, zeal, in-depth knowledge, and effective supervision of my thesis. Besides the supervision, he mentored and encouraged me to learn coding as my thesis entailed a lot of data analysis. He guided and advised me on effective time management as well. He provided guidance in respect of the choice of decision-support tools that enhanced the precision and accuracy of the results.

I am greatly indebted to the Department of Civil and Environmental Engineering for the opportunity to study at the Norwegian University of Science and Technology. I am grateful to the Professor-in-Charge of Hydropower Development, Prof. Oddbjørn Bruland, for his mentorship throughout my studies as well as his contributions at certain points during the hydrological modelling phase of this thesis.

Finally, I thank my family for standing by me, their prayers, and encouragement throughout the period of my studies.

Nkpa Mba Ogarekpe

DISCLAIMER

I declare that this thesis is my own and autonomous work. All sources and aids used have been referenced.

Nkpa Mba Ogarekpe

June 2023

TABLE OF CONTENTS

LIST OF FIGURES

LIST OF TABLES

ABBREVIATIONS

AMS	Annual Minimum Series
CMIP	Coupled Model Intercomparison Project
CORDEX	Coordinated Regional Climate Downscaling Experiment
GCM	Global Climate Model
GEV	Generalized Extreme Value distribution
GHG	Green House Gases
Gum	Gumble distribution
HBV	Hydrologiska Byråns Vattenbalansavdelning
IPCC	Intercomparison Project on Climate Change
LP3	Log Pearson type III distribution
NGU	Norges Geologiske Undersøkelse
NSE	Nash-Sutcliffe Efficiency
PEST	Parameter Estimation
PET	Potential evaporation
P3	Pearson type III distribution
RCM	Regional Climate Model
RCP	Representative Concentration Pathway
RCP4.5_2041-2070	Emission scenario 4.5, time horizon 2040-2070
RCP4.5_2071-2099	Emission scenario 4.5, time horizon 2071-2099
RCP8.5_2041-2070	Emission scenario 8.5, time horizon 2040-2070
RCP8.5_2071-2099	Emission scenario 8.5, time horizon 2071-2099
RF	Radiative forcing

1. INTRODUCTION

Climatic variables play a vital role in catchment hydrology. However, the deviations in the erstwhile climatic trends of several regions call for concern. Masson-Delmotte et al. (2021) stated that the global surface temperature of the earth increased from 0.95 to 1.20°C (from 1850–1900 to 2011–2020). Changes in climatic and non-climatic drivers are responsible for climate change (Pörtner et al., 2022). The non-climatic anthropogenic factors worsen the current ecosystem vulnerability to climate change (Pörtner et al., 2022) while global warning, drought, rise in sea level can occur due to changes in the climatic drivers of climate change. Anthropogenic climate change has warmed the atmosphere, ocean, land at an unprecedented scale and has resulted to extreme conditions across the globe (Masson-Delmotte et al., 2021).

The concentrations of well-mixed greenhouse gas (GHG) caused by human activities have continued to increase (Masson-Delmotte et al., 2021). Anthropogenic activities, consequent upon mankind's need for survival, economic prosperity, and power, may perhaps continue to aggravate this trend. Regrettably, this may portend grave danger for the survival of the biota in various ecosystems, in perhaps a few decades to come. At a Global Warming Level of 2ºC, and as early as the mid-21st century, increases in one or more of drought, aridity and fire weather will affect agriculture, health, forestry and ecosystem in a group of regions (Masson-Delmotte et al., 2021). In another group of regions, decreases in snow and/or ice or increases in pluvial/river flooding will affect several sectors including energy production (Masson-Delmotte et al., 2021). Future adverse effects of climate change on periglacial processes in Northern Europe have been reported (Masson-Delmotte et al., 2021).

The response of the catchment to climate change drivers cannot be overemphasized. Climate change drivers impact processes useful to mankind and the environment. Some of these processes include infiltration, runoff, and evapotranspiration. The nexus of climatic drivers (such as precipitation, temperature) and non-climatic drivers (such as land use change, water demand changes) significantly impacts runoff. Climate change impacts on runoff affects

groundwater recharge, biotic components of the river ecosystem, environment, and hydropower production. The availability of water forms the basis for hydropower production, hence, the need to investigate the impact of climate change on the hydrology and hydropower production at the catchment scale.

Forra and Lærdal catchments were selected for a detailed prognoses on the effects of climate change on catchment hydrology as well as the hydropower production. The catchments under review and their environs are not exempted from the myriads of impacts of climate change. Consequently, the need to take proactive measures to mitigate the adverse effects of future climate change in the study area cannot be overstated. Learning to live with climate change necessitates the adoption of adaptative measures to mitigate the impacts arising therefrom. The study aims to evaluate the effects of climate change on the hydrology of the Forra and Lærdal catchments, as well as the effects of climate change on the future energy production of Funna hydropower plant.

1.1 Objectives of the study

Climate change would impact catchment hydrology, hence, hydropower production. It is therefore important to investigate the changes in inflow and the associated uncertainties in the hydropower production occasioned by climate change. In addition, other factors in the watershed like water use for other purposes and general environmental conditions will also be affected by changed inflow and altered hydropower production. The demand for water to satisfy hydropower needs as well as the environmental restrictions underscores the need for this. The specific objectives of the study include:

i. To determine future (2041 – 2070, 2071 – 2099) trends in the climate of Forra and Lærdal catchments considering downscaled climate models obtained from *klimaservicesenter.no*
ii. To calibrate and validate a hydrological model (HBV) for the historical period using observational data.
iii. To simulate runoff and assess uncertainties of various scenarios for the historical and future periods, for 10 GCM-RCM combinations of

climate models for emission scenarios (RCP4.5 and RCP8.5), for Forra and Lærdal catchments.

iv. To simulate and evaluate hydropower production for Stjørdal hydropower system, with emphasis on Funna powerplants for present and future time horizons considering baseline, RCP4.5 and RCP8.5 scenarios, using nMAG.

v. To develop an improved operational schedule for Funna powerplants considering future climate change impacts for RCP4.5 scenario.

vi. To simulate winter low flow from Lærdal catchment using HEC-RAS.

1.2 Study Site

The study area consists of two sites namely Forra catchment and Lærdal catchment. Forra and Lærdal catchments are in Trøndelag and Vestland counties of Norway, respectively (Figure 1.1). Forra catchment is located to the east of Trondheim and lies between longitudes 11.305º and 12.150º East and latitudes 64.675º and 63.448º North (Figure 1.2). Forra, a tributary of Stjørdalselva, is an unregulated river and flows in southwest direction. Høggås bru gauging station, located at a reach of Forra, was utilized as the outlet for the delineation of the Forra catchment (Appendix 1 Figure S.1). Høggås bru gauging station is located at coordinate 11.357º East, 63.493º North. The delineation of the watershed revealed that Forra catchment has an area of 495.12 km^2 and a specific discharge of 41.7 $l/s/km^2$ (nevina.nve.no). Stjørdalselva drains the study area under review and consists of regulated and unregulated tributaries. Stjørdalselva flows in the northwest and west directions at the upper and lower catchments, respectively. The regulated tributaries provide water in various reservoirs and brooks for hydropower production. The Stjørdal hydropower system under review consists of Meråker and Funna hydropower systems (Hailegeorgis et al.). Among all the reservoirs and inter-basin transfers, Fjergen serves as the main reservoir, with a capacity of 204.2 mill m^3 capacity. Fjergen is regulated at a highest regulated water level (HRWL) and lowest regulated water level (LRWL) of 514 masl and 498 masl, respectively. The surface area of Fjergen at HRWL, is 16.34 km^2.

Stjørdalselva discharges at Stjørdalsfjorden. Based on the Koppen's climate classification, Forra catchment predominantly experiences temperate climate (Cfb and Cfc) while the other parts experience continental climates (Dfc). The average monthly precipitation and average monthly temperature were obtained from the observational gridded data over a 30-year period (1971 – 2000). The average lowest and highest monthly temperatures in Forra catchment were in January (-5.9ºC) and July (11.8ºC). Also, the average lowest and highest monthly precipitation were in May (64mm) and October (125 mm). The mean annual discharge as measured at Høggås bru gauging station was 21.42 m^3/s (1971 – 2005).

Lærdal catchment lies between longitudes 7.351º and 8.309º East and latitudes 60.829º and 61.255º North (Figure 1.3). The catchment is drained by Lærdalselva and consists of regulated and unregulated tributaries. Lærdalselva flows in the northwest direction at the lower catchment. There is no gauging station at the outlet of Lærdal catchment under review. However, there are several gauging stations at other locations along the river. Sæltun gauging station, located upstream of the outlet under review, was chosen for the calibration of the corresponding catchment (Appendix 1 Figure S.2) with the aim of transferring the catchment parameters to the entire Lærdal catchment Prior to 1973, the catchment was not regulated, hence, runoff data before regulation was utilized for the calibration of the catchment. Sælthun gauging station is located at coordinate 7.700º East, 61.052º North. The delineation of the watershed revealed that Lærdal catchment has an area of 1182 km^2 and a specific discharge of 30.7 $l/s/km^2$ (Appendix 1 Figure S.3). Lærdalselva discharges at Ardalsfjorden. Based on the Koppen's climate classification, most parts of Lærdal catchment experiences continental climates (Dfb and Dfc) while the other parts experience temperate climate (Cfb). The average lowest and highest monthly temperatures in Lærdal catchment were in February (-9.3ºC) and July (7.7ºC). Also, the average lowest and highest monthly precipitation were in April (37.2mm) and October (84.4 mm). The mean annual discharge as measured at Sælthun gauging station was 23.461 m^3/s (1962 – 1972).

The spatial variability of the topographies of Forra and Lærdal catchments were obtained from https://hoydedata.no/LaserInnsyn/. The 10mx10m grid size Digital Terrain Model revealed that the Forra catchment consists of areas ranging from 95 to 1249 m above mean sea level (Figure 1.2). Lærdal catchment consists of areas ranging from 0 to 1920 m above mean sea level (Figure 1.3). Both catchments consist of strongly dissected mountainous landscapes. The relief of the catchments have considerably steeped valleys, typically suitable for hydropower development.

The geology of the study area was obtained from the Norges geologiske undersøkelse (NGU, 2022). The varieties of rock formations within Forra catchment (Figure 1.4), by percentage of catchment, include Basalt (11.5 %), Phyllite (2.7%), Gabbro (8.4%), Mica slate (29.4 %), Lime mica slate (2.8 %), Rhyolite (0.5 %), and Sandstone (44.6 %). Also, the geology of Lærdal catchment (Figure 1.5) consists of Phyllite (6.8 %), Granite (12.4 %), Tonalite (0.3 %), Amphibolite (36.9 %), Anorthosite (1.6 %), Metagabbro (1.1 %), Granitic gneiss (38.4 %), and Metasandstone (2.4 %). Forra catchment is significantly situated on the Sandstone. Lærdal catchment is predominantly situated on the Granitic Gneiss as well as Amphibolite.

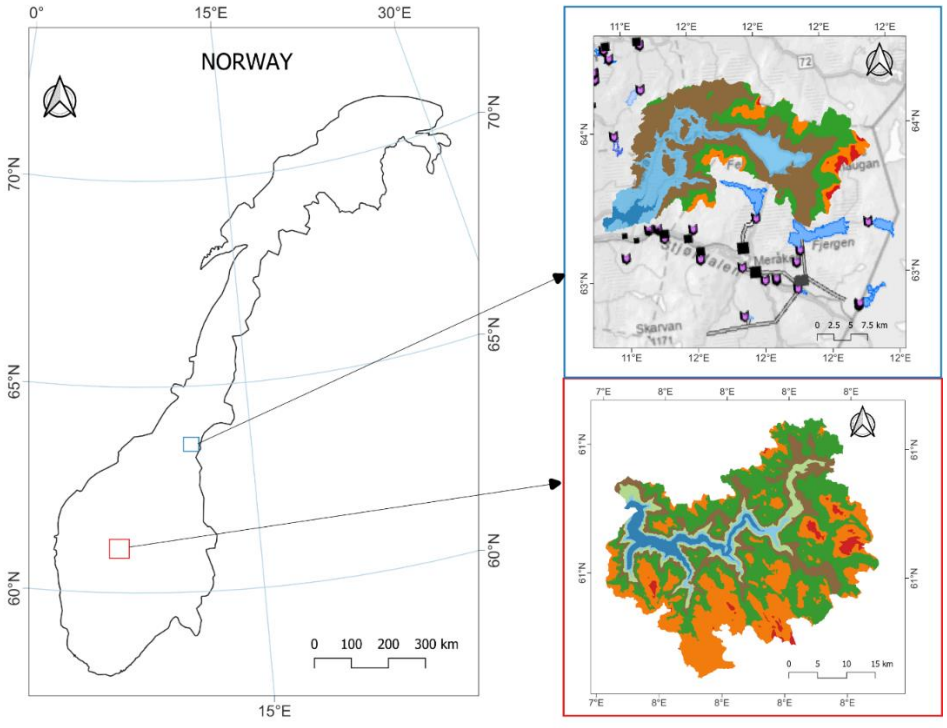

Figure 1.1 Study area located in Trøndelag and Vestland counties of Norway.

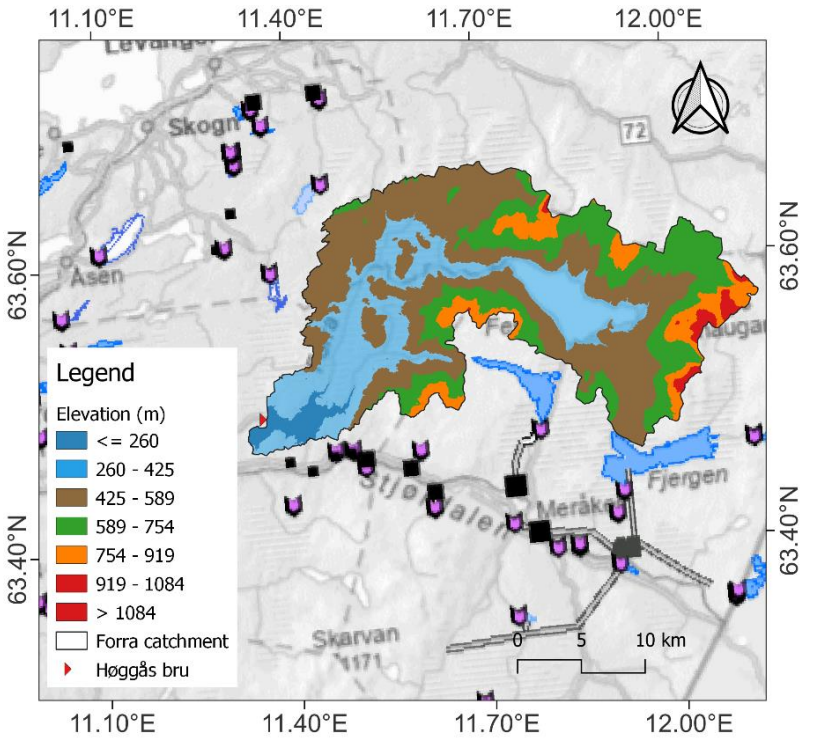

Figure 1.2 Topography of Forra catchments superimposed on hydropower development atlas (from https://atlas.nve.no/), Trøndelag, Norway. Source: https://hoydedata.no/LaserInnsyn/; Author

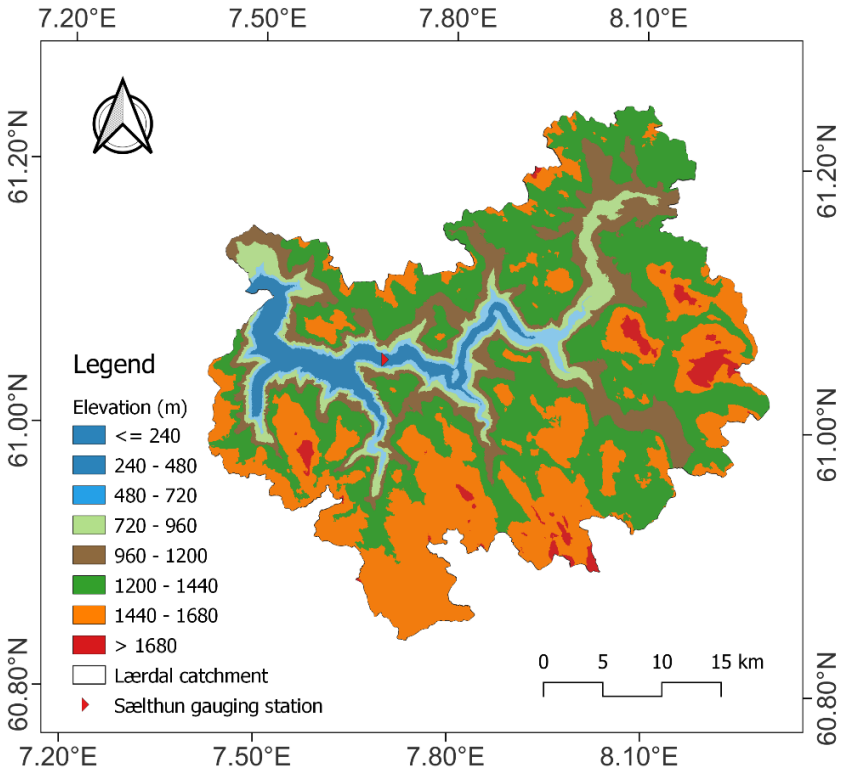

Figure 1.3 Topography of Lærdal catchment, Vestland, Norway. Source: https://hoydedata.no/LaserInnsyn/; Author

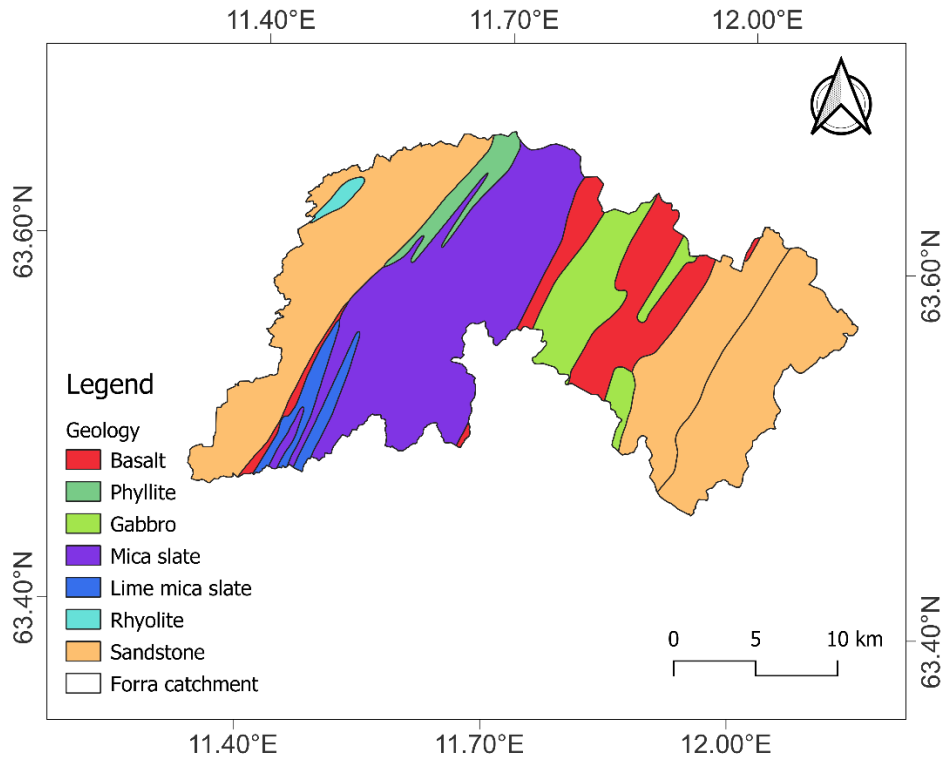

Figure 1.4 Geology of Forra catchment. Source: NGU, 2022; Author.

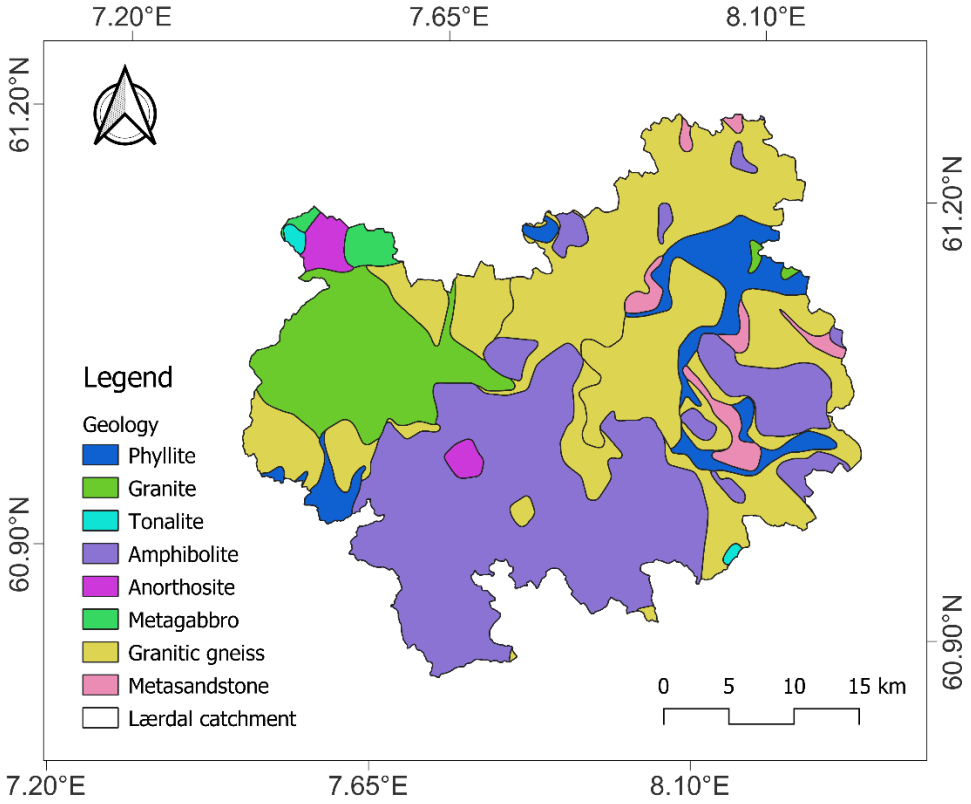

Figure 1.5 Geology of Lærdal catchment. Source: NGU, 2022; Author.

2. LITERATURE REVIEW

This chapter provides an abridged background on the development of climate change studies, climate change drivers as well as theoretical frameworks that underscore the requisite methods used in this study. This section culminates in a brief literature review establishing the current knowledge on climate change impacts on hydrology as well as hydropower production, both internationally and particularly for Norwegian systems.

2.1 Background on the organization of climate change studies

The study of climate change has evolved over the years. Giant strides have been made since the establishment of the Coupled Model Intercomparison Project (CMIP) and the Intercomparison Project on Climate Change (IPCC). CMIP, organized by the World Climate Research Programme, has coordinated various international climate modelling experiments and teams, hence, resulting to better understanding of the past, present, and future climate (Meehl et al., 2014). Since the inception of CMIP, several phases have been executed. Several coordinated experiments have produced climate projections for different sets of scenarios (Meehl et al., 2007). The fifth phase of the Coupled Model Intercomparison Project (CMIP5) provides a database of climate projections for different sets of scenarios from Global Climate Models (GCM) (Perez et al., 2014). The governing processes in the atmosphere, ocean, land surface and sea ice are taken into cognizance in the GCM, hence, making it a using tool in climate change assessment (Wong et al., 2016). For regional studies, the resolution of the GCMs is usually coarse, hence, the need for downscaling to finer scales. Regional Climate Models (RCM) have been developed at relevant scales that enhance the study of regional processes (Giorgi & Gutowski Jr, 2015). Presently, various RCM systems are available. The choice of RCM would depend on flexibility, applicability, as well as sensitivity to paleoclimate climate and future climate simulations (Giorgi & Gutowski Jr, 2015). The Coordinated Regional Climate Downscaling Experiment (CORDEX) has resulted to the production of worldwide high-resolution regional climate projections through a fully

coordinated experiment protocol (Giorgi & Gutowski, 2016). It is noteworthy to state that the systematic errors in climate models usually necessitate post-processing of GCM/RCM outputs to obtain plausible time series at an appropriate scale for use in local impact studies (Wong et al., 2016).

IPCC has prepared several assessment reports on climate change, with the latest being the Sixth Assessment Report. The reports communicate scientific knowledge on climate change, impacts, future risks, and response options (Masson-Delmotte et al., 2022). The IPCC Fifth Assessment Report adopted various Representative Concentration Pathways (RCP) to depict the plausible future climate trajectories of the earth (Stocker et al., 2014). The RCP constitutes the future projections of the climate based on plausible radiative forcings on the earth system.

2.2 Drivers of Climate change

The future climate change projections represents the anthropogenic or natural impacts on climate change over decades and centuries (Collins et al., 2013; Stocker et al., 2014). The drivers of climate change (substances and processes), consequent upon the natural and anthropogenic activities, alter the Earth's energy budget (Stocker et al., 2014). Radiative forcing (RF) is a measure of the change in Earth-atmosphere energy budget due to changes in these drivers (Shine, 2000). RF is usually measured in W/m^2. Some climate change drivers include emissions from well-mixed GHG (CO_2, CH_4, N_2O, halocarbons), emissions of CO_2 alone, emissions of CH_4 alone, stratospheric ozone depleting halocarbons, emission of short-lived gases (e.g., CO, NOx), total aerosols, stratospheric volcanic aerosols, changes in solar irradiance (Stocker et al., 2014). Except for brief period after volcanic eruptions, the contributions of solar irradiance changes and stratospheric volcanic aerosols to the natural net RF are small (Stocker et al., 2014). This implies that anthropogenic activities significantly contribute to the net RF, hence, a major source of concern in the Earth's climate change.

2.3 Theoretical framework for climate change impacts evaluation

2.3.1 Bias correction

The output of GCM/RCM are often flawed with systematic biases, hence the need for bias correction (Buser et al., 2010; Wong et al., 2016). The use of uncorrected climate models' data in impact models may result to unrealistic results (Teutschbein & Seibert, 2010). Post-processing of GCM/RCM outputs (bias correction) results to a plausible time series for local impact studies (Wong et al., 2016). Bias correction entails the identification of possible biases between observed and simulated climate variables, and the subsequent correction of both the historical and projected scenario RCMs runs (Teutschbein & Seibert, 2012).

There are numerous bias correction methods. Several bias correction methods have been used in previous studies; local intensity scaling (Fang et al., 2015; Smitha et al., 2018; Teutschbein & Seibert, 2012), linear scaling (Fang et al., 2015; Teutschbein & Seibert, 2012), variance scaling (Teutschbein & Seibert, 2012), power transformation (Fang et al., 2015), and distribution transfer or quantile mapping (Adera & Alfredsen, 2020; Enayati et al., 2021; Fang et al., 2015; Guo et al., 2019; Teutschbein & Seibert, 2012). In comparison to several bias correction methods, distribution mapping was found to be the best for five catchments in Sweden (Teutschbein & Seibert, 2012). Distribution mapping, local intensity scaling and modified power transformation bias correction methods performed better in correcting the biases in CMIP5 data than the other methods investigated (Smitha et al., 2018).

2.3.2 Climate change impacts study methods

In the past, several methods for which GCM simulated datasets can be used have been reported. GCM simulated temperature have been used directly in hydrological models (Teutschbein & Seibert, 2010). Delta-change method has been used in several climate change impact studies (Hay et al., 2000; Räty et al., 2014). Prior to hydrological climate change impact studies, future precipitation scenarios have been constructed using delta-change methods (Yuan et al., 2016). Delta change method entails the computation of the differences between current and future GCM simulations and superimposing these changes to observed

time-series (Hay et al., 2000; Teutschbein & Seibert, 2010). The delta change method assumes that GCMs reliably simulate relative changes rather than absolute values (Tryhorn & DeGaetano, 2011). Delta-change as well as scaling methods have been used in bias-correcting GCM simulated temperature prior to use in hydrological models (Teutschbein & Seibert, 2010).

2.4 Review of climate change impacts on hydrology and hydropower production

2.4.1 Climate change impact on hydrology

The effects of climate change are enormous. Climate change would likely result to changes in temperatures, floods, drought, precipitation extreme etc. and these would vary in different regions (Stocker et al., 2014). Watershed hydrology is very sensitive to changes in the climate (Hattermann et al., 2015). Impact studies are therefore needed to demonstrate how different regions will be affected by climate change (Andréasson et al., 2004). Several impacts of climate change have been reported on; hydrology (Ficklin et al., 2013; Graham et al., 2007; Hattermann et al., 2015; Lawrence & Haddeland, 2011; Minville et al., 2008); hydropower production (Adera & Alfredsen, 2020; Chernet et al., 2013; Timalsina et al., 2015).

A prognosis of hydrological parameter uncertainty in modelling the projected changes in average annual maximum daily mean runoff in Norwegian catchments was studied (Lawrence & Haddeland, 2011). Lawrence and Haddeland (2011) stated that parameter uncertainty is less important in catchments where spring snowmelt makes predominates contribution to maximum flows. Beyond the issue of hydrological parameters uncertainty is the problem of uncertainty in regional climate models. The inability of CMIP5 ensembles to capture variability in historical precipitation when run in hindcast have been reported (Mohammed et al., 2015). Uncertainties due to GCM and RCM have been found to increase with time horizon of projections (Gelfan et al., 2017). The need for the consideration of an ensemble of climate models cannot be overstated. Due to uncertainty concerns, Shen et al. (2018) underscored the need for the use of multiple GCMs for climate change impacts studies.

Climate change impacts on river flow have been found to vary based on the location of basin (Andréasson et al., 2004; Graham, 2004; Veijalainen, 2012) as well as the choice of GCM/RCM emission scenario (Andréasson et al., 2004; Veijalainen, 2012). Common to all scenarios evaluated, the trend in the river flow have been found to differ between the south and north of Bal basin (Graham, 2004). Climate change would result to the early occurrence of spring flood (Minville et al., 2008; Vicuña et al., 2011) and the modification of its amplitude in Chute-du-Diable watershed (Minville et al., 2008). Early occurrence of spring peak flows, and overall increase in river flow have been reported (Graham et al., 2007). Decrease in summer low flows has been observed as the most notable impact of climate change in a Scottish highland catchment (Capell et al., 2013). Increase in future summer and spring flows are projected to impact river ice conditions (Timalsina et al., 2015).

The enhancement of evapotranspiration losses due to warmer climate alongside the impact on runoff has been emphasized (Vicuña et al., 2011). Warmer climate affected snow accumulation and melt, hence, resulted to changes in the hydrology of catchments in Finland (Veijalainen, 2012). Increase in evapotranspiration and decrease in annual flow of a catchment in midwestern United States of America have been reported (Sunde et al., 2017). Ouyang et al. (2015) stated that there is a possibility of decline in the future discharge due to increase in evapotranspiration, consequent upon increase in air temperature.

2.4.2 Climate change impact on hydropower production

Climate change is likely to alter river flow, hence, impacting water availability and hydropower generation (Berga, 2016). The outcome of climate change impact study by Graham et al. (2007) are indicative of an increase in flow as well as increase in hydropower potential. Increase in annual inflow resulted to an increase in energy generation for the current reservoir operational strategy (Chernet et al., 2013). Based on reservoir hydropower model simulation, Timalsina et al. (2015) stated that the production flows will be increased in the future. The impact of climate change on the hydropower sector might be positive, negative, or inconsequential depending upon several factors (Wasti et

al., 2022). Li et al. (2020) stated that hydropower production does not necessarily increase for wet years due to spill during flooding season.

It is noteworthy to mention the problem of uncertainties in climate models vis-à-vis the effect on hydropower production. In respect of hydropower, uncertainty in predictions of precipitation change is perhaps more important than uncertainty in predictions of temperature change (Markoff & Cullen, 2008). Based on uncertainty modelling, Schaefli et al. (2007) stated that potential climate change has a negative impact on the performance of the system.

The possibility of negative impacts of climate change on hydropower generation underscores the need to harness future flows to enhance hydropower production. The modification of current reservoir operational strategy to minimize spill, hence better utilization of the future flows, has resulted to increased energy production (Adera & Alfredsen, 2020). The modification of the current rule curve was recommended as an adaptation strategy to minimize the impact of climate change on hydropower production (Shrestha et al., 2021).

2.4.3 Minimum flow and implications on the environment

The regulation of rivers, due to hydropower development, results to alterations in downstream flows. Richter et al. (1996) underscored the importance of evaluating the anthropogenic induced hydrologic alteration of wetland, aquatic, and riparian ecosystem in relation to the biotic implications, ecosystem restoration and management plan. Smakhtin (2001) emphasized the need for the prognoses of low-flow changes in a changing climate. Among numerous methods for the determination of minimum flow, the wetted perimeter-discharge relationship is sometimes used (Gippel & Stewardson, 1998). The implementation of an enhanced minimum flow regime resulted to an increase in species richness (Travnichek et al., 1995). Increase in flow velocity, achieved through increase in minimum flow, relatively resulted to an abundance of species preferring fast-flowing and/or deep microhabitats (Lamouroux et al., 2006). The assessment of minimum flow changes impacts on invertebrates and fish fauna has been reported (Harby et al., 2007). While some species were favoured by increased minimum flow others were not (Harby et al., 2007).

3. MATERIALS

3.1 Observational Gridded Climatic Data

Observational gridded precipitation and temperature data were obtained from thredds.met.no. The dataset constitutes a valuable meteorological input for snow and hydrological simulations and is presented on a 1 km of grid spacing (Lussana et al., 2018). The observational gridded datasets, spanning the period 1971 – 2000, were obtained in obtained in NetCDF format and were subsequently extracted using an R script written by Abebe Adera at NTNU. To lay emphasis on the catchments under review, the extracted grid points were clipped to the Forra and Lærdal catchments (Figures 3.1). The average daily precipitation and daily temperature of Forra catchment range from 0 – 54.93 mm and –28.87 to 22.15ºC, respectively. The observational gridded dataset of temperature and precipitation as well as the potential evaporation were required to simulate the daily streamflow for the catchment. The potential evaporation data are herewith presented in Appendix 2.

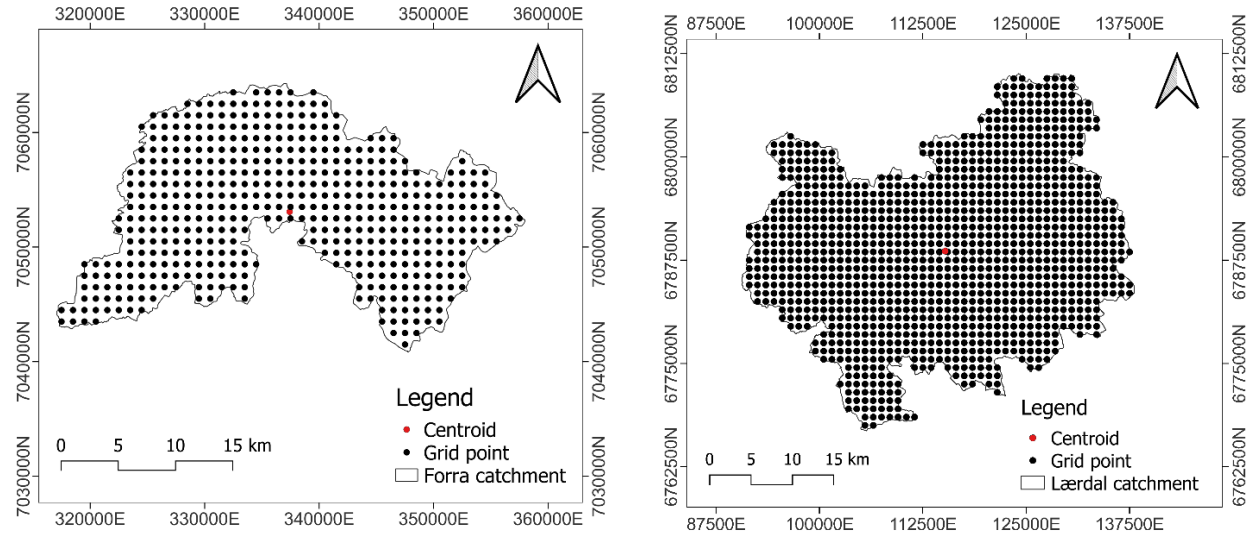

a. **b.**

Figure 3.1 Grid points of climatic data for catchments under review **a**. Forra **b**. Lærdal

3.2 Climate Models

The climate models under review were obtained from Klima i Norge 2100'. 'Klima i Norge 2100' come from an ensemble of ten EURO-CORDEX runs (Jacob et al., 2014; see also http://www.eurocordex.net/), resulting from five Global

Climate Models (GCMs) and four Regional Climate Models (RCMs) combinations (Wong et al., 2016). The datasets were obtained from https://nedlasting.nve.no/klimadata/kss. 'Klima i Norge 2100' utilized only the EUR-11 outputs, which have a spatial resolution of approximately 12.5 x 12.5 km (Wong et al., 2016). The coarse resolution of the RCM was downscaled to finer resolution 1 x 1km (Wong et al., 2016). The downscaled daily gridded temperature and precipitation datasets, corresponding to future periods, were obtained for emission scenarios RCP4.5 and RCP8.5 for the unregulated catchment. The historical data, spanning the periods 1971 – 2000, and future scenarios were obtained in NetCDF format and were subsequently extracted using an R script. The future period was divided into two sub-periods: medium term or mid-century (2041 – 2070) and long term or end of century (2071 – 2099). Hence, the future emission pathways under review were abbreviated for the medium and long terms as follows: RCP4.5_2041-2070, RCP4.5_2071-2099, RCP8.5_2041-2070, and RCP8.5_2071-2099. The output of GCM/RCM are often flawed with systematic bias, hence the need for bias correction (Buser et al., 2010; Wong et al., 2016). The summary of GCM/RCM combinations used in this study is shown in Table 3.1.

Table 3.1 Summary of climate models used in the study.

Global Climate Model	**Regional Climate Model**	**Institution**
CNRM	CCLM	Climate Limited area Modelling Community
CNRM	RCA	Swedish Meteorological and Hydrological Institute
EC-EARTH	CCLM	Climate Limited area Modelling Community
EC-EARTH	HIRHAM	Danish Meteorological Institute
EC-EARTH	RACMO	Royal Netherlands Meteorological Institute
EC-EARTH	RCA	Swedish Meteorological and Hydrological Institute
HADGEM	RCA	Swedish Meteorological and Hydrological Institute

IPSL	RCA	Swedish Meteorological and Hydrological Institute
MPI	CCLM	Climate Limited area Modelling Community
MPI	RCA	Swedish Meteorological and Hydrological Institute

3.3 Bias Correction and bias adjustment

Bias-correction entails the removal of systematic biases in simulated values relative to observed data, which, in principle, reflect the 'true values' (Wong et al., 2016). Therefore, a comparison of the monthly average temperature and monthly average precipitation of the historical datasets of the ten climate models to the observational data was carried out. This was considered as a preliminary measure to determine the extent of comparability of the predictions of the climate models to the observed datasets. The systematic errors in the datasets necessitated the correction of the bias between the climate models and the observed datasets for the historical period (1971 – 2000). The quantile mapping approach was adopted for the bias correction of the historical datasets of the climate models. The bias correction and adjustment as well as design flood computation were carried out using R script written by Knut Alfredsen at NTNU.

3.4 Hydrological model setup, calibration, and validation

HBV model was set up using observational gridded average precipitation and average temperature from https://thredds.met.no/thredds/catalog/senorge/ for the period 1971-2000. The data needs of HBV model include daily temperature, precipitation, and potential evaporation (Bergström, 1976). Hence, the potential evaporation, confined parameters, unconfined parameters, sensitive and insensitive model parameters for Forra and Lærdal catchments were utilized to setup the respective models. Streamflow data from Høggås bru gauging station, located at an unregulated reach of Forra river, was utilized as the outlet for the calibration of the Forra catchment. Also, streamflow data from Sælthun gauging station was utilized for the calibration of a section of Lærdal catchment.

The elevation of the centroid, monthly mean potential evaporation, average daily precipitation and temperature of the respective catchments were utilized as

inputs in setting up the HBV model. Site-specific confinement parameters of the catchments were utilized while default model parameters were used to initialize and run the model. Measured runoff timeseries from Høggås bru and Sælthun gauging stations were obtained from Sildre (www.sildre.nve.no). The nexus of the models' parameters and the measured runoff enhanced the autocalibration of the catchment using the Parameter Estimation (PEST) algorithm. The split sample approach was applied in determining the data range for calibration and validation. Care was taken to ensure that the datasets for the calibration and validation covered the variability of melt and rain floods. The model, for Forra catchment, was calibrated and validated using discharge datasets ranging from 01.09.1971 – 31.08.1976 and 01.09. 1976 – 31.08.2000, respectively. The model, for Lærdal catchment, was calibrated and validated using discharge datasets ranging from 01.09.1961 – 31.08.1966 and 01.09.1966 – 31.08.1973, respectively. Calibration parameters obtained via the calibration of a section of Laerdal catchment, due to location of gauging station, were transferred for the simulation of the flow of the entire Lærdal catchment (Appendix 1 Figure S.2). The respective calibration parameters of both models were utilized for the simulation of flow consequent upon the future input parameters of the catchments.

3.5 Future hydropower production

The determination of future production is dependent on the estimation of future discharge for requisite hydropower production modules. The hydropower system under review consists of the following hydropower systems, Meråker, and Funna. Future flows, at various modules, were obtained from simulated discharge at Høggås bru (outlet of Forra catchment). The discharges at the modules were obtained for the future periods (2041 – 2070 and 2071 – 2099) for greenhouse gases concentration trajectories of RCP4.5 and RCP8.5. nMAG was used for the simulation of the average annual power production and spill vis-à-vis the reliability of firm power supply corresponding to the various future scenarios.

4. METHODS

The climate models' datasets were categorized into three sub-periods: the historical period (1971 – 2000), medium-term or mid-century period (2041 – 2070) and long-term or end of century (2071 – 2099). Observational gridded precipitation and temperature data, obtained for the period 1971 – 2000, were utilized for the correction of the systematic biases in the climate models. To account for the future period, the scenarios were designated as RCP4.5_2041-2070, RCP4.5_2071-2099, RCP8.5_2041-2070, RCP8.5_2071-2099. The observed climatic data vis-à-vis the climate models' datasets were utilized for the bias correction and bias adjustment of the climate models for the historical and future periods, respectively, using quantile mapping coded in an R script. The future scenarios were bias adjusted. The potential evaporation (PET) was computed using Thornthwaite method (Thornthwaite, 1948). The monthly PET was computed and subsequently, the average monthly PET was computed (Appendix 2). The PET was computed using the Thornthwaite method and was implemented using an R script (Appendix 3). The direct and delta change approaches were adopted for the determination of the effect of climate change on runoff. Climate datasets resulting from five General Circulation Models (GCMs) and four Regional Climate Models (RCMs) combinations were obtained from https://nedlasting.nve.no/klimadata/kss.

4.1 Climate change impact modelling

To determine the impacts of climate change on Forra and Laerdal catchments, the bias corrected/adjusted data were utilized for the climate change impact modelling using HBV setup in Section 3.4.

4.1.1 Direct method

The bias corrected datasets of the historical RCMs were run in hindcast. This was carried out to test how well the climate models datasets, for the historical period, would simulate or match the observed runoff. The ability of the RCM to match or otherwise, observed runoff was carried out by inputting the precipitation, temperature, and PET of the RCM into the calibrated model in Section 3.4. The

performance of the RCMs was evaluated using NSE R2 and accumulated difference metrics.

4.1.2 Delta change

The computation of the delta changes was based on the corrected average monthly precipitation and temperature for the historical and future scenarios. The delta changes were computed to account for the GCM inadequacies by determining the differences between current and future GCM simulations and add these changes to observed time-series (e.g., Gleick, 1986; Arnell, 1996). Delta changes were computed using Equations (4.1) and (4.2).

$$\Delta T = T_{Future} - T_{Current} \tag{4.1}$$

$$\Delta P = \frac{(P_{Future} - P_{current})}{P_{current}} + 1 \tag{4.2}$$

The observed bias corrected average temperature and the latitude corresponding to the centroid of the catchment were utilized for the computation of the potential evaporation for the historical period. The elevations at the centroid of the respective catchments were extracted using the geometry tool of QGIS. The potential evaporation corresponding to the centroid were computed for the future climate for RCP4.5_2041-2070, RCP4.5_2071-2099, RCP8.5_2041-2070, and RCP8.5_2071-2099, scenarios using the corrected average temperature of respective scenarios. The computation of the potential evaporation was implemented using an R script.

The future effects of climate change, for RCP4.5 and RCP8.5, were simulated via the perturbation of the observed time-series of precipitation and temperature using the delta values. The observed precipitation values were multiplied with the respective delta values of precipitation for respective months while delta temperature values were added to the observed temperature time series to account for the medium and long-term effects of climate change. Subsequently, the timeseries of the delta-perturbed observed precipitation and temperature for different climate models as well as the corresponding potential evaporation were simulated in the calibrated HBV models of Forra and Lærdal catchments. The simulated runoff from the calibrated models (baseline) were compared with

the simulated runoff of the various climate models for RCP4.5_2041-2070, RCP4.5_2071-2099, RCP8.5_2041-2070, and RCP8.5_2071-2099.

4.2 Hydropower system simulation

The simulation of the hydropower system was carried out using nMAG. Validated nMAG model was obtained from previous studies (Hailegeorgis, unpublished data). To account for the effect of climate change on the regulated rivers, streamflow simulations at Høggås bru (outlet of Forra catchment) were used as input in the nMAG model. Hence, the effect of climate change on runoff of the adjacent hydropower schemes were obtained for various modules via scaling in nMAG. A prognosis of 100GW firm power was carried out with a view to determining the average annual production, for various scenarios (baseline, RCP4.5 and RCP8.5), as well as spill.

4.3 Computation and hydraulic simulation of future low flow effects on the environment

The future low flow, winter low flow, summer low flow of Forra and Lærdal catchments were computed using the 7Q10 method. Also, the design flood was computed using the generalized extreme value (GEV) distribution. The 200- and 1000-year return period design floods were computed based on the 28 years flow for the baseline and projected scenarios. The effects of future winter low flow on the environment were simulated using HEC-RAS. Validated HEC-RAS model was obtained from previous studies (Alfredsen et al., 2019). The impact of climate change on the water covered area of a reach of Lærdalselva was investigated.

The computation of the low flows, using the 7Q10 method, was carried out using the following steps:

a. Computation of the D-day (7-day) averages.
b. Determination of the annual minimum series (AMS) obtained from 7-day averages of runoff.
c. Frequency analysis to find low flow (non-exceedance).
d. Fitting of AMS obtained from the 7-day averages to find 10-year return period low flow using Log-Pearson type III distribution.

The requisite equations for the computation of the 7Q10 were all coded in R. The approach adopted by the US Water Resources Council (Committee, 1967) was utilized in the fitting of the non-exceedance probability analysis. Equations (4.1 – 4.3) were utilized in the fitting of the non-exceedance probability analysis, hence, determining the low flow corresponding to a 10-year recurrence interval.

$$\log x = \overline{log\ x} + K\sigma_{\log x} \tag{4.1}$$

Where K is the frequency factor, σ is the standard deviation.

$$\overline{\log x} = \frac{\sum \log x}{n} \tag{4.2}$$

$$\sigma_{\log x} = \sqrt{\frac{\sum(\log x - \overline{\log x})^2}{n-1}} \tag{4.3}$$

Where n is the number of data

The frequency factor was computed using Equation (4.4) (Stedinger, 1993).

$$K = \frac{2}{\gamma}\left[1 + \frac{\gamma Z}{2} - \frac{\gamma^2}{36}\right]^3 - \frac{2}{\gamma} \tag{4.4}$$

Where γ is the skew coefficient, z is the p th quantile of the zero-mean and unit-variance standard normal distributions.

The skew coefficient was determined using Equation (4.5).

$$\gamma = \frac{n\sum(\log x - \overline{\log x})^3}{(n-1)(n-2)(\sigma_{\log x})^3} \tag{4.5}$$

The use of Equations (4.1) to (4.5) enhanced the computation of low flow corresponding to 10 years recurrence interval.

4.4 Framework for the study on the impact of climate change on hydrology and hydropower production

The pictorial representation of the framework for the study, shown in Figure 4.1, can be summarized as follows:

a. Obtain observational gridded climatic data and climate model datasets.
b. Ascertain the need, or otherwise, for the bias correction of the historical climate model data.
c. Carry out bias correction of the historical climate model data using Quantile mapping. Bias adjustment of the future climate model was carried out.

d. Calibration and validation of the catchment using the observed data.
e. Ascertain the appropriateness, or otherwise, for use of direct method. If not appropriate, use delta change method.
f. Computation of the average monthly precipitation and temperature for the historical and future scenarios using the bias corrected data.
g. Compute of delta changes in temperature and precipitation.
h. Simulate future effect of climate change, for mid-century and end-of-century periods for RCP4.5 and RCP8.5 scenarios, via the perturbation of the observed time-series of precipitation and temperature. The observed precipitation values were multiplied with the respective ΔP for various months while respective ΔT values were added to the observed temperature time series.
i. Simulation of the future flows and snowpack from Forra catchment using the model in Step d and the perturbations of the observed time-series of precipitation and temperature for RCP4.5 and RCP8.5 scenarios for the mid-century (2041 – 2071) and end of century (2071 – 2099).
j. Comparison of simulated runoff from the calibrated model (baseline) with the simulated runoff of the various climate models for RCP4.5_2041-70, RCP4.5_2071-99, RCP8.5_2041-70, and RCP8.5_2071-99.
k. Simulation and evaluation of various scenarios of hydropower production for Funna powerplant for the current operational strategy using nMAG.
l. Simulation and evaluation of hydropower system using improved operational strategies using nMAG.
m. Simulation of winter low flow from Lærdal catchment using HEC-RAS.

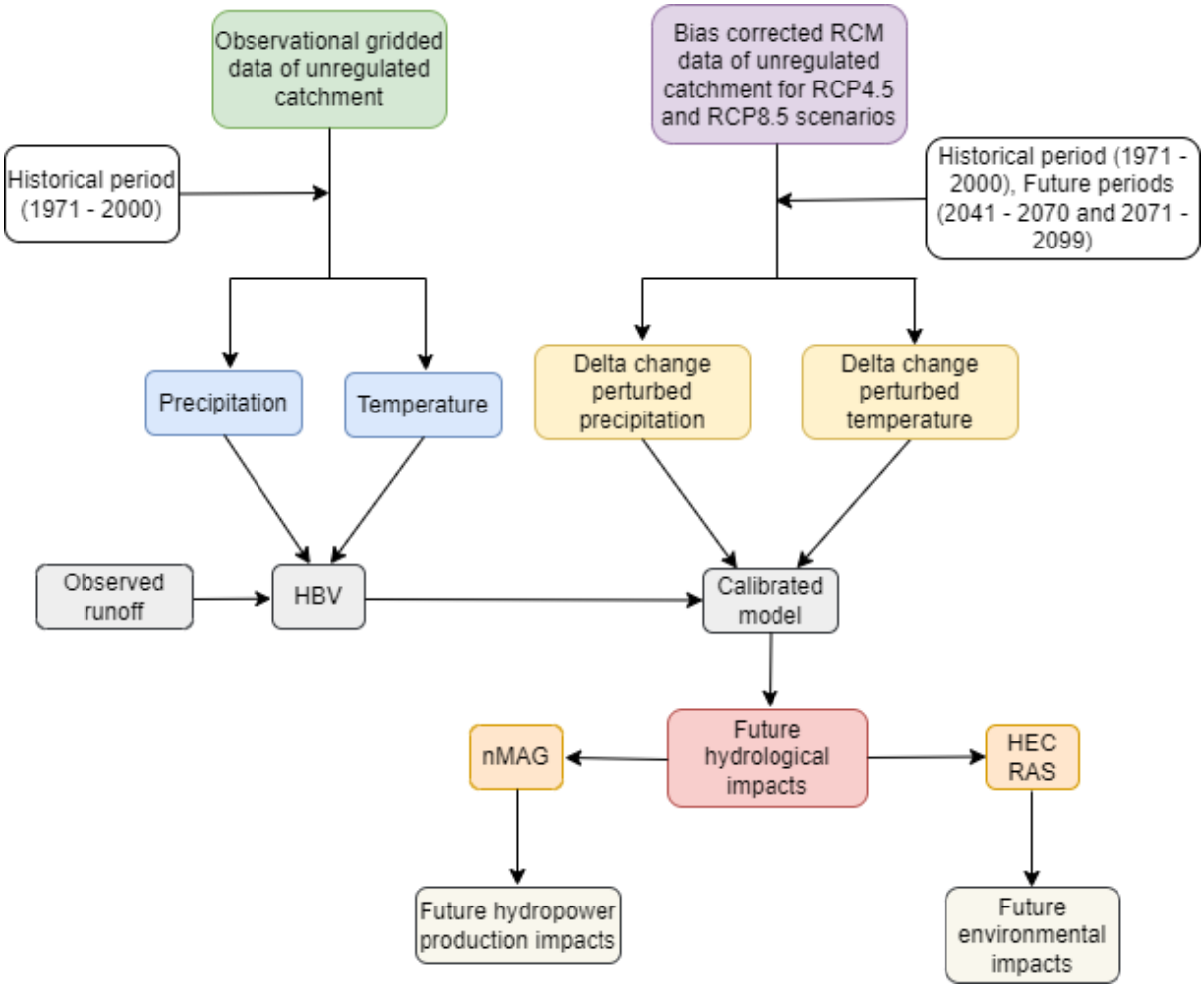

Figure 4.1 Climate change modelling framework

5. RESULTS AND DISCUSSION

5.1 Future climate of Forra and Lærdal catchments

5.1.1 Predictions of future precipitation and temperature of Forra and Lærdal catchments based on baseline, RCP4.5, and RCP8.5 scenarios.

The results of the mean monthly precipitation of the raw and bias-corrected climate models' datasets, for Forra catchment, for various time horizons are shown in Figure 5.1. Prior to bias correction of the 10 climate models datasets for the historical period, the minimum and maximum mean monthly precipitation values are 73.4 mm and 185.7 mm, respectively (Figure 5.1). Also, the minimum and maximum temperature values, for the 10 climate models prior to correction, are -6.8ºC and 11.9ºC, respectively (Figure 5.1). The minimum and maximum mean monthly precipitation and mean monthly temperature values after bias correction are 51.7 mm and 131.4 mm (Figure 5.1) and -6.7ºC and 12.6ºC (Figure 5.1), respectively. The observed minimum and maximum precipitation and temperature values (obtained from https://thredds.met.no/) are 64.1 mm and 124.7 mm (Figure 5.1) and -5.9ºC and 11.8ºC (Figure 5.2), respectively. The minimum and maximum corrected average monthly precipitation values corresponding to the RCP4.5_2041-2070 and RCP4.5_2071-2099 are 47.2mm and 152.9 mm and 55.2mm and 164.8mm, respectively (Figure 5.1). The minimum and maximum corrected average monthly precipitation values corresponding to the RCP8.5_2041-2070 and RCP8.5_2071-2099 are 49.2mm and 164.3mm and 55.7mm and 170.2mm, respectively (Figure 5.1). The minimum and maximum corrected average monthly temperature values corresponding to RCP4.5_2041-2070 and RCP4.5_2071-2099 are -5.1ºC and 15.8ºC and -3.8ºC and 16.3ºC, respectively (Figure 5.2). The minimum and maximum corrected average monthly temperature values corresponding to the RCP8.5_2041-2070 and RCP8.5_2071-2099 are -4.2ºC and 16.3ºC and -2.3ºC and 18.0ºC, respectively (Figure 5.2).

The results of the observed average monthly precipitation and the average monthly precipitation of the raw climate models, for Forra **c**atchment, revealed

that the later overestimated the mean monthly precipitation for the historical period (Figures 5.1). The corrected values revealed that the bias correction significantly improved the precipitation values of the climate models compared to the temperature, for the historical period. A comparison of the temperature of Forra catchment for the historical and mid-century time horizons revealed that an increase of 1.52ºC and 3.23ºC in the minimum and maximum average monthly temperature would occur, respectively, for RCP4.5 scenario. The minimum and maximum average monthly temperature would increase by 1.30ºC and 0.47ºC, respectively, between the mid-century and end-of-century periods for RCP4.5. The increase in the minimum and maximum average monthly temperature between the historical period and mid-century period, for RCP8.5 scenario, considering the ten climate models, are 2.49ºC and 3.69ºC, respectively. The minimum and maximum average monthly temperature would increase by 1.87ºC and 1.71ºC, respectively, between mid-century and end-of-century periods for RCP8.5. Therefore, RCP4.5 and RCP8.5 scenarios would comparatively result to higher temperature increase between the historical period (1971 – 2000) and the medium term (2041 – 2070) than between the medium term (2041 - 2070) and long term (2071 - 2099). The impact of climate change on the precipitation of Forra catchment was also evaluated considering average monthly timestep for the 10 climate models. The minimum average monthly precipitation, considering all the models, decreased by 4.45 mm while the maximum average monthly precipitation increased by 21.57 mm, between the periods (1971 – 2000) and (2041 – 2070) for RCP4.5 scenario. The minimum and maximum average monthly precipitation would increase by 7.99 mm and 11.86mm, respectively, between 2041 - 2070 and 2071 - 2099 for RCP4.5. The minimum average monthly precipitation, considering all the models, decreased by 2.44 mm while the maximum average monthly precipitation increased by 32.90 mm, between the periods (1971 – 2000) and (2041 – 2070) for RCP8.5 scenario. The minimum and maximum average monthly precipitation would increase by 6.44 mm and 5.95 mm, respectively, between 2041 - 2070 and 2071 - 2099 for RCP8.5. Therefore, minimum average monthly precipitation would

decrease for RCP4.5 and RCP8.5 scenarios between the historical period (1971 – 2000) and the medium term (2041 – 2070). However, the maximum average monthly precipitation would increase for RCP4.5 and RCP8.5 scenarios between the historical period (1971 – 2000) and the medium term (2041 – 2070) as well as between the medium term (2041 – 2070) and the long-term (2071 – 2099) (Figure 5.1).

The future climatic variables of Forra catchment were compared on an annual timescale. On average, the ensemble mean predicts an increase in average annual temperature of 2.1ºC and 2.8ºC corresponding to the mid-century and end-of-century periods, respectively, for RCP4.5 scenario as well as 2.8ºC and 4.6ºC for RCP8.5. On average, the ensemble mean predicts an increase in average annual precipitation of 7.2 mm and 9.2 mm as well as 8.4 mm and 17.9 mm, for the RCP4.5 and RCP8.5, respectively, for the mid-century and end-of-century periods.

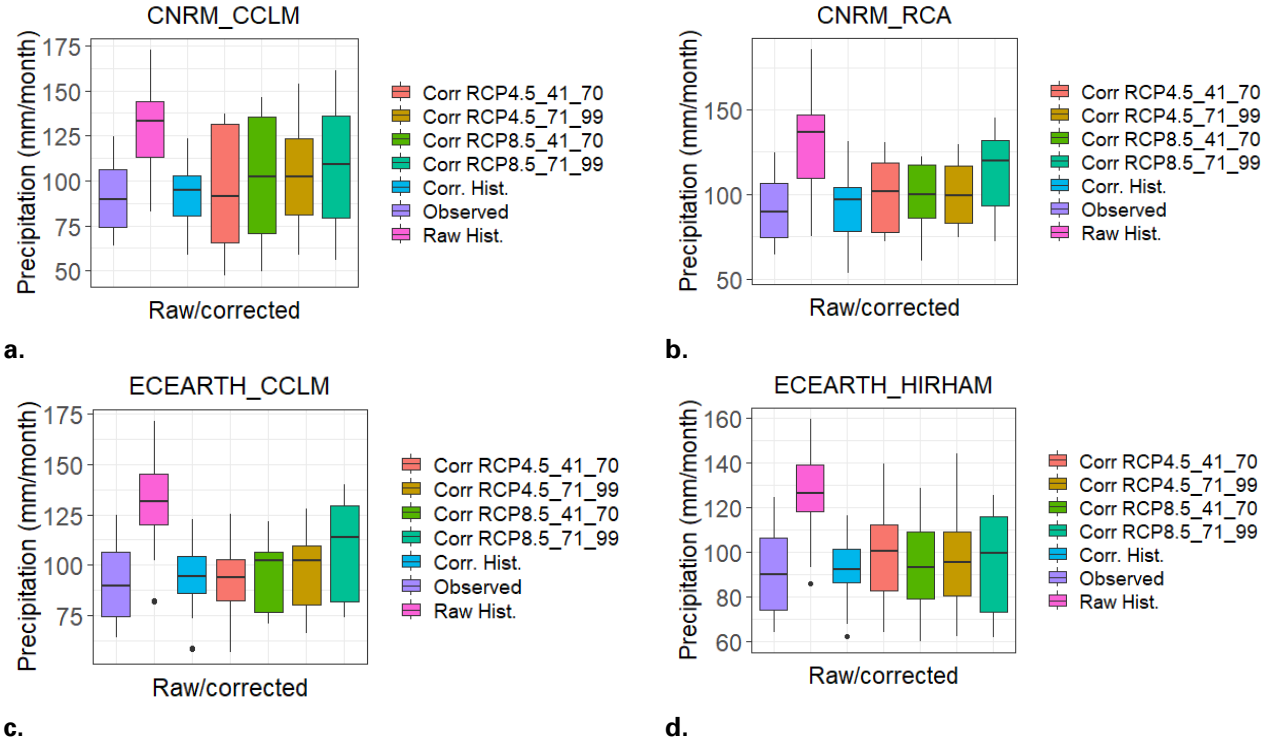

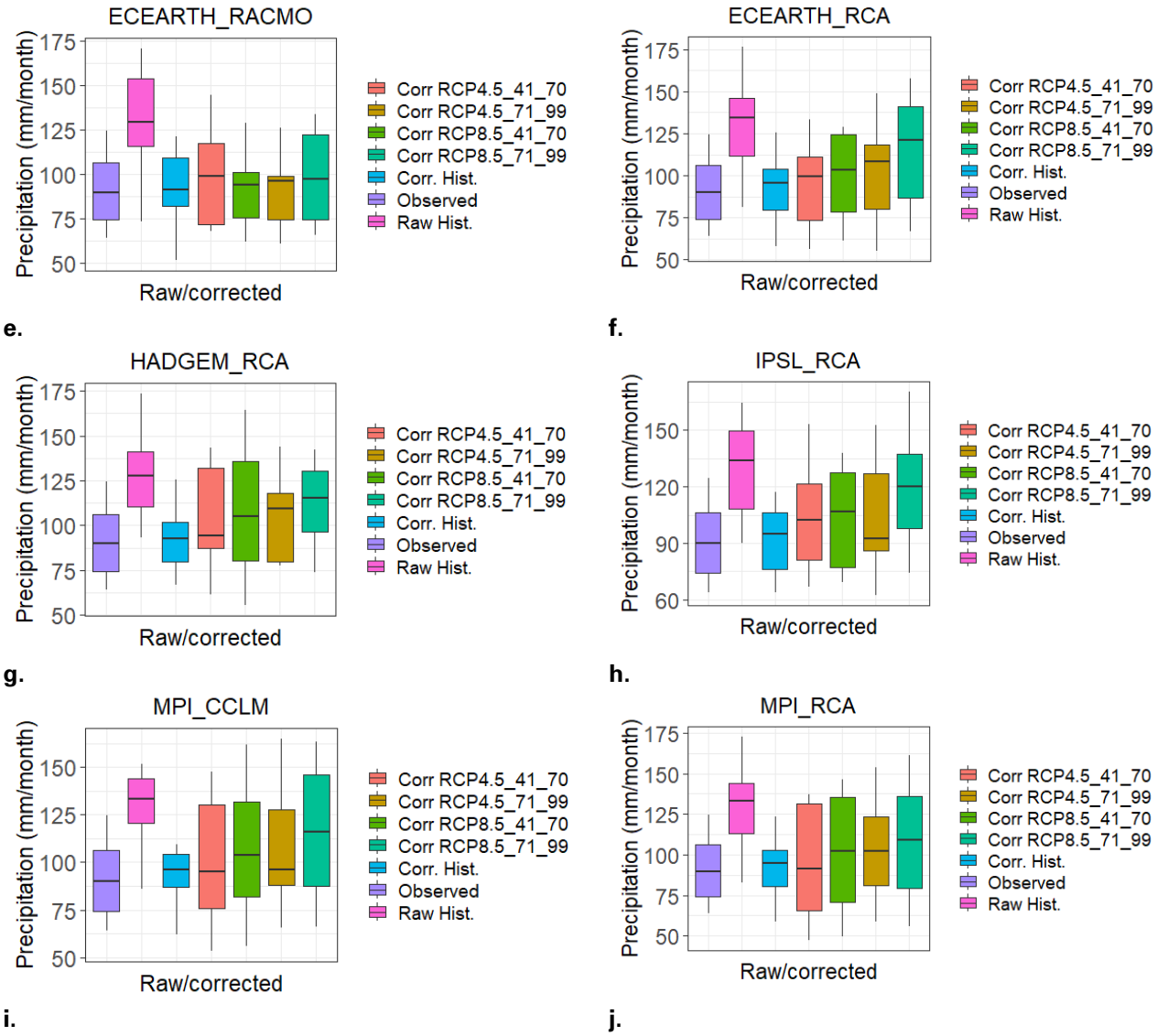

Figure 5.1 Box-scatter plots of mean monthly precipitation of Forra catchment for observed, raw, and corrected climate models for various time horizons

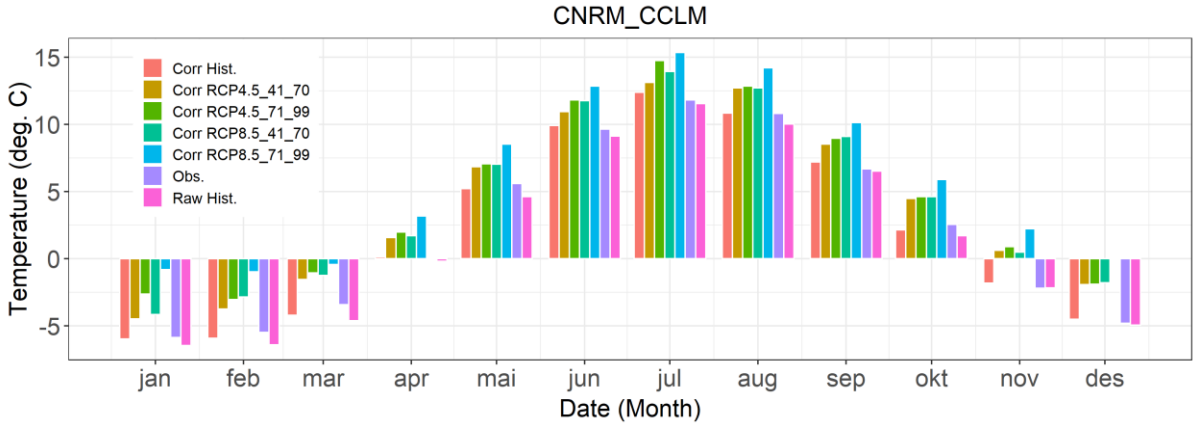

a.

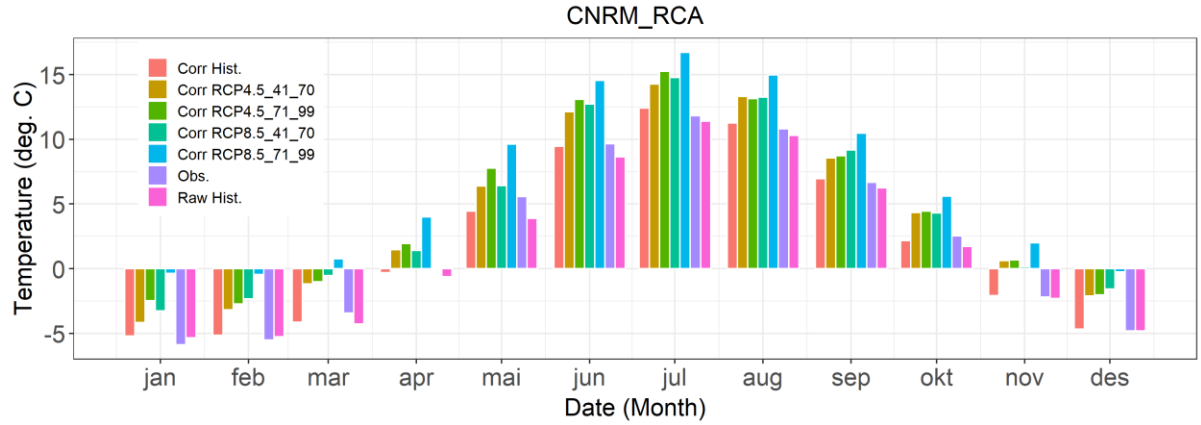
CNRM_RCA
Corr Hist.
Corr RCP4.5_41_70
Corr RCP4.5_71_99
Corr RCP8.5_41_70
Corr RCP8.5_71_99
Obs.
Raw Hist.
Temperature (deg. C)
15
10
5
0
-5
jan
feb
mar
apr
mai
jun
jul
aug
sep
okt
nov
des
Date (Month)

b.

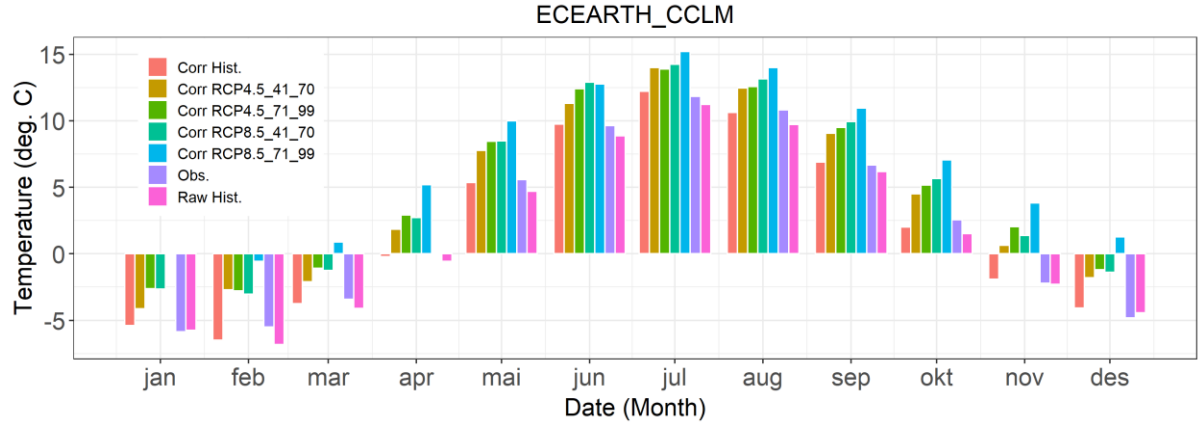
ECEARTH_CCLM
Corr Hist.
Corr RCP4.5_41_70
Corr RCP4.5_71_99
Corr RCP8.5_41_70
Corr RCP8.5_71_99
Obs.
Raw Hist.
Temperature (deg. C)
15
10
5
0
-5
jan
feb
mar
apr
mai
jun
jul
aug
sep
okt
nov
des
Date (Month)

c.

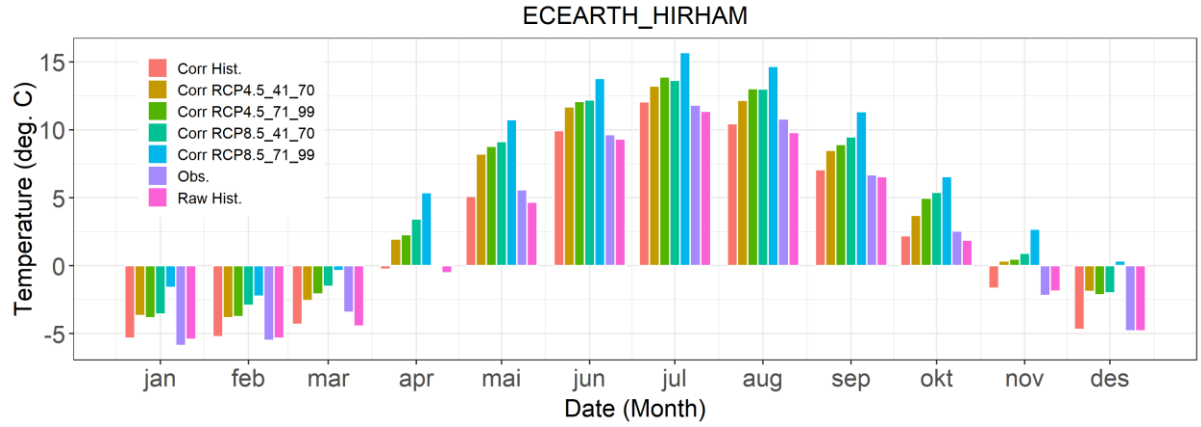
ECEARTH_HIRHAM
Corr Hist.
Corr RCP4.5_41_70
Corr RCP4.5_71_99
Corr RCP8.5_41_70
Corr RCP8.5_71_99
Obs.
Raw Hist.
Temperature (deg. C)
15
10
5
0
-5
jan
feb
mar
apr
mai
jun
jul
aug
sep
okt
nov
des
Date (Month)

d.

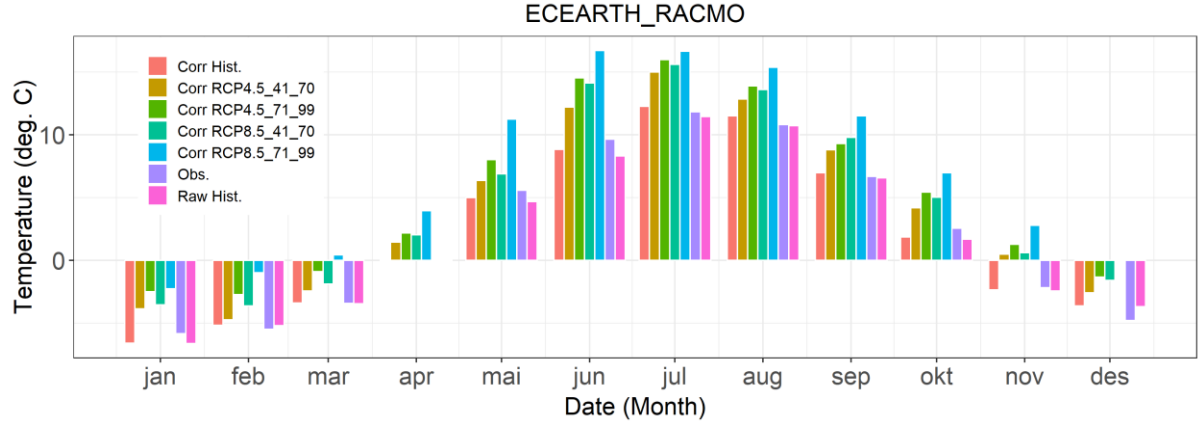
ECEARTH_RACMO
Corr Hist.
Corr RCP4.5_41_70
Corr RCP4.5_71_99
Corr RCP8.5_41_70
Corr RCP8.5_71_99
Obs.
Raw Hist.
Temperature (deg. C)
10
0
jan
feb
mar
apr
mai
jun
jul
aug
sep
okt
nov
des
Date (Month)

e.

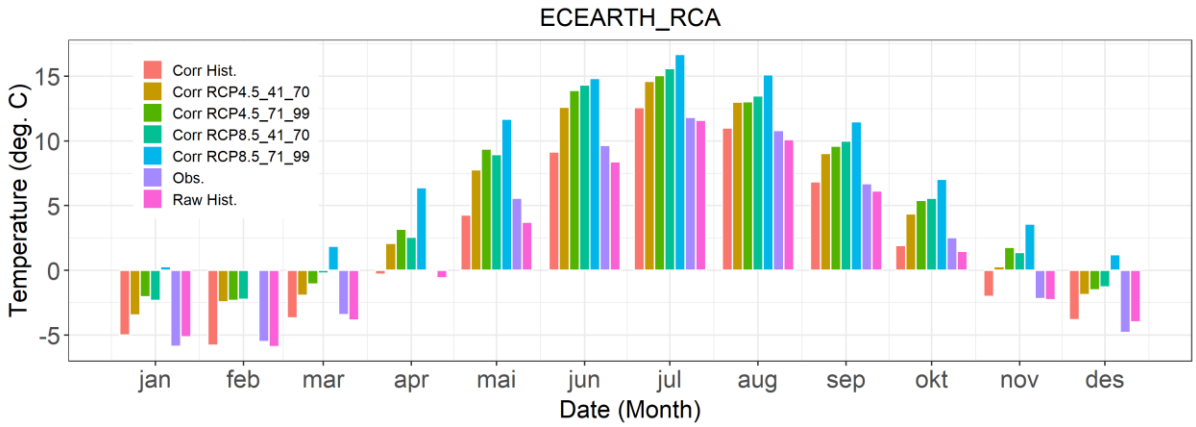
ECEARTH_RCA
Corr Hist.
Corr RCP4.5_41_70
Corr RCP4.5_71_99
Corr RCP8.5_41_70
Corr RCP8.5_71_99
Obs.
Raw Hist.
Temperature (deg. C)
15
10
5
0
-5
jan
feb
mar
apr
mai
jun
jul
aug
sep
okt
nov
des
Date (Month)

f.

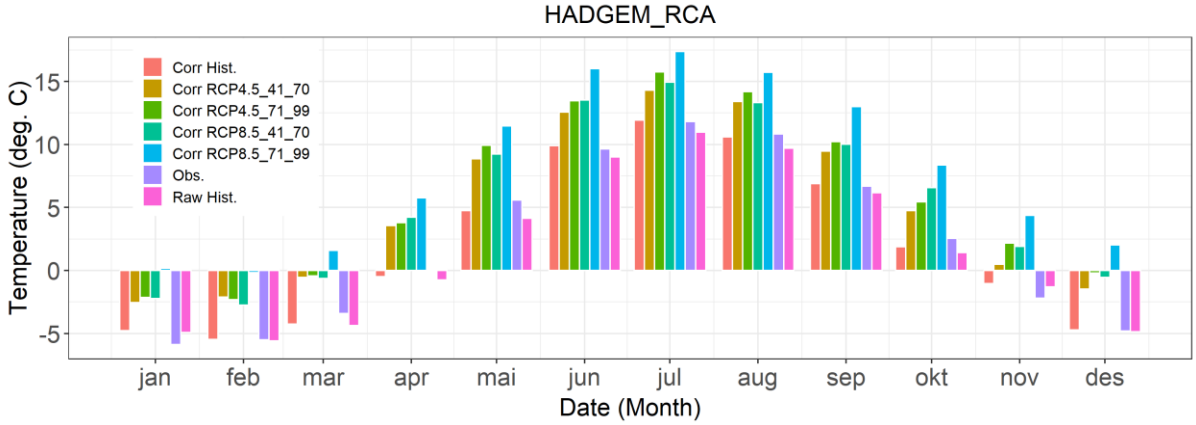
HADGEM_RCA
Corr Hist.
Corr RCP4.5_41_70
Corr RCP4.5_71_99
Corr RCP8.5_41_70
Corr RCP8.5_71_99
Obs.
Raw Hist.
Temperature (deg. C)
15
10
5
0
-5
jan
feb
mar
apr
mai
jun
jul
aug
sep
okt
nov
des
Date (Month)

g.

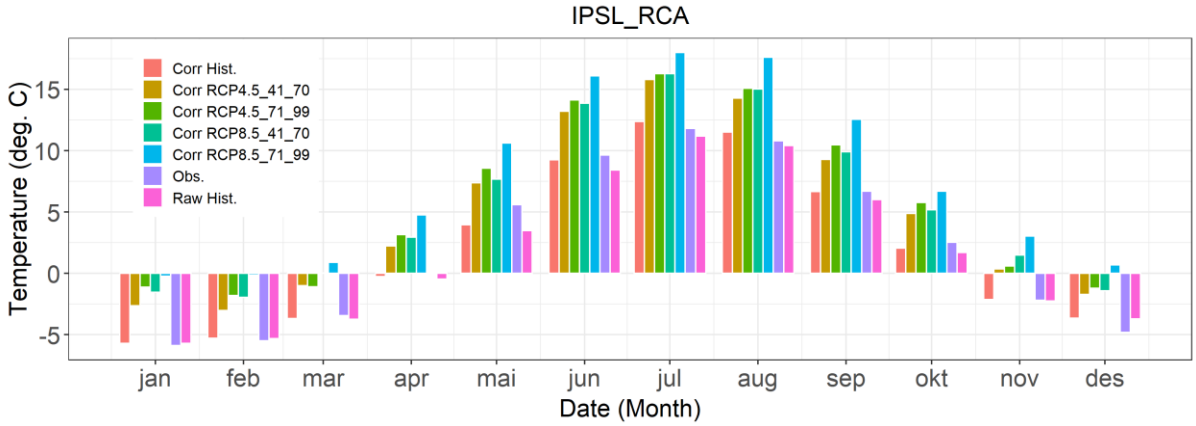
IPSL_RCA
Corr Hist.
Corr RCP4.5_41_70
Corr RCP4.5_71_99
Corr RCP8.5_41_70
Corr RCP8.5_71_99
Obs.
Raw Hist.
Temperature (deg. C)
15
10
5
0
-5
jan
feb
mar
apr
mai
jun
jul
aug
sep
okt
nov
des
Date (Month)

h.

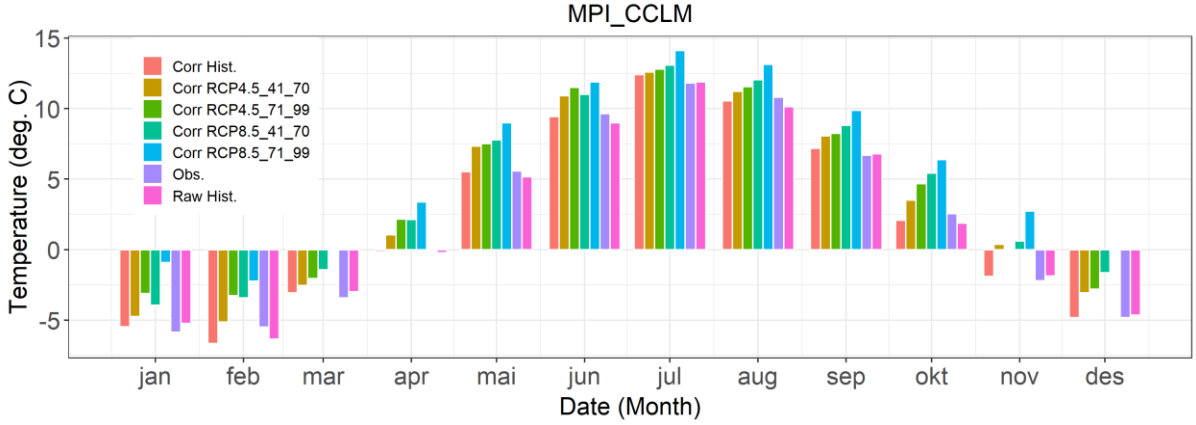
MPI_CCLM
Corr Hist.
Corr RCP4.5_41_70
Corr RCP4.5_71_99
Corr RCP8.5_41_70
Corr RCP8.5_71_99
Obs.
Raw Hist.
Temperature (deg. C)
15
10
5
0
-5
jan
feb
mar
apr
mai
jun
jul
aug
sep
okt
nov
des
Date (Month)

i.

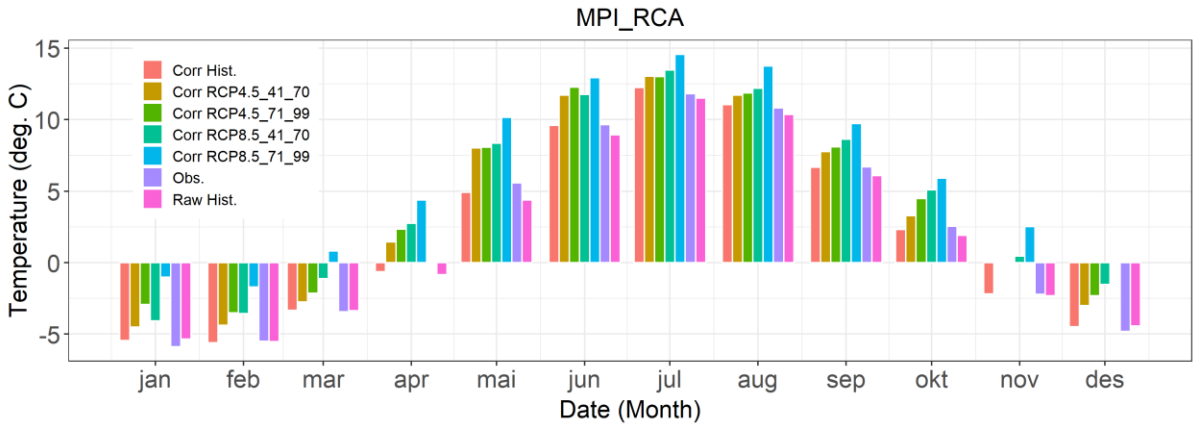

j.

Figure 5.2 Histogram of mean monthly temperature of Forra catchment for observed, raw, and corrected climate models for various time horizons. **a.** CNRM_CCLM **b.** CNRM_RCA **c.** ECEARTH_CCLM **d.** ECEARTH_HIRHAM **e.** ECEARTH_RACMO **f.** ECEARTH_RCA **g.** HADGEM_RCA **h.** IPSL_RCA **i.** MPI_CCLM **j.** MPI_RCA

The results of the mean monthly precipitation of the raw and bias-corrected climate models' datasets, of Lærdal catchment, for various time horizons are shown in Figure 5.3. Prior to bias correction of the 10 climate models datasets for the historical period, the minimum and maximum mean monthly precipitation values are 59.9 mm and 181.1 mm, respectively (Figure 5.3). Also, the minimum and maximum temperature values, for the 10 climate models prior to correction, are -8.2ºC and 8.3ºC, respectively (Figure 5.3). The minimum and maximum mean monthly precipitation and mean monthly temperature values after bias correction are 35.1 mm and 103.9 mm (Figure 5.3) and -9.9ºC and 8.4ºC (Figure 5.3), respectively. The observed minimum and maximum precipitation and temperature values (obtained from https://thredds.met.no/) are 37.2 mm and 84.4 mm (Figure 5.3) and -9.3ºC and 7.7ºC (Figure 5.2), respectively. The minimum and maximum corrected average monthly precipitation values corresponding to the RCP4.5_2041-2070 and RCP4.5_2071-2099 are 32.1 mm and 110.0 mm and 38.7 mm and 117.2 mm, respectively (Figure 5.3). The minimum and maximum corrected average monthly precipitation values corresponding to the RCP8.5_2041-2070 and RCP8.5_2071-2099 are 31.5 mm and 120.0mm and 38.4 mm and 134.8 mm, respectively (Figure 5.3). The minimum and maximum corrected average monthly temperature values corresponding to RCP4.5_2041-

2070 and RCP4.5_2071-2099 are -9.0ºC and 11.2ºC and -7.2ºC and 13.9ºC, respectively (Figure 5.4). The minimum and maximum corrected average monthly temperature values corresponding to the RCP8.5_2041-2070 and RCP8.5_2071-2099 are -7.8ºC and 13.0ºC and -6.0ºC and 17.5ºC, respectively (Figure 5.4).

The results of the observed average monthly precipitation and the average monthly precipitation of the raw climate models reveals that the later overestimate the mean monthly precipitation for the historical period 1971-2000 (Figures 5.3). The corrected values revealed that the bias correction significantly improved the precipitation and temperature values of the climate models for the historical period. A comparison of the temperature of Lærdal catchment for the historical and mid-century time horizons revealed that an increase of 0.97ºC and 2.84ºC in the minimum and maximum average monthly temperature would occur, respectively, for RCP4.5 scenario. The minimum and maximum average monthly temperature would increase by 1.75ºC and 2.68ºC, respectively, between the mid-century and end-of-century periods for RCP4.5. The increase in the minimum and maximum average monthly temperature between the historical period and mid-century period, for RCP8.5 scenario, considering the ten climate models, are 2.16ºC and 4.67ºC, respectively. The minimum and maximum average monthly temperature would increase by 1.81ºC and 4.49ºC, respectively, between mid-century and end-of-century periods for RCP8.5. Therefore, RCP4.5 and RCP8.5 scenarios result to marginally higher temperature increases between the historical period (1971 – 2000) and the medium term (2041 – 2070) than between the medium term (2041 - 2070) and long term (2071 - 2099). The impact of climate change on the precipitation of Lærdal Catchment was also evaluated considering average monthly timestep for the 10 climate models. The minimum average monthly precipitation, considering all the models, decreased by 2.93 mm while the maximum average monthly precipitation increased by 6.10 mm, between the periods (1971 – 2000) and (2041 – 2070) for RCP4.5 scenario. The minimum and maximum average monthly precipitation would increase by 6.53 mm and 7.26 mm, respectively, between 2041 - 2070 and 2071 - 2099 for

RCP4.5. The minimum average monthly precipitation, considering all the models, decreased by 3.56mm while the maximum average monthly precipitation increased by 16.17 mm, between the periods (1971 – 2000) and (2041 – 2070) for the historical datasets and RCP8.5 scenario. The minimum and maximum average monthly precipitation would increase by 6.94 mm and 14.81 mm, respectively, between 2041 - 2070 and 2071 - 2099 for RCP8.5. Therefore, minimum average monthly precipitation would decrease for RCP4.5 and RCP8.5 scenarios between the historical period (1971 – 2000) and the medium term (2041 – 2070). However, the maximum average monthly precipitation would increase for RCP4.5 and RCP8.5 scenarios between the historical period (1971 – 2000) and the medium term (2041 – 2070) as well as between the medium term (2041 – 2070) and the long-term (2071 – 2099) (Figures 5.3).

The future climatic variables of Lærdal catchment were compared on an annual timescale. On average, the ensemble mean predicts an increase in average annual temperature of 2.0ºC and 2.7ºC corresponding to the mid-century and end-of-century periods, respectively, for RCP4.5 scenario as well as 2.8ºC and 4.6ºC for RCP8.5. On average, the ensemble mean predicts an increase in average annual precipitation of 4.6 mm and 6.7 mm as well as 5.2 mm and 14.4 mm, for the RCP4.5 and RCP8.5, respectively, for the mid and end-of-century periods.

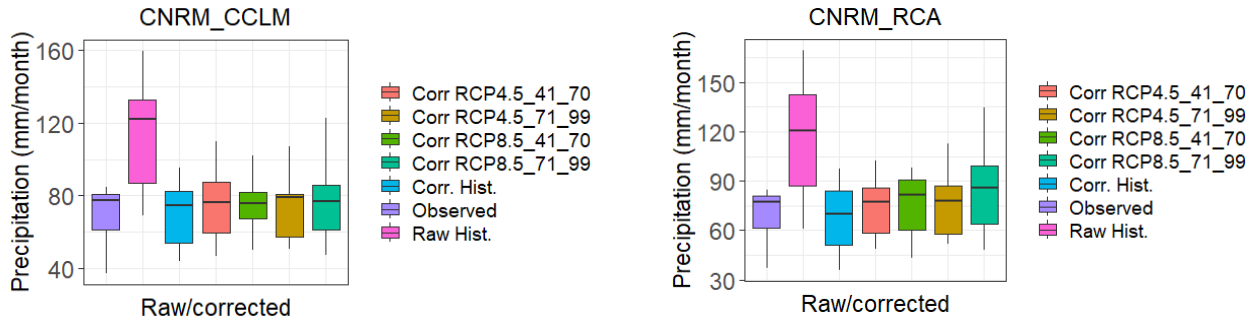

a. **b.**

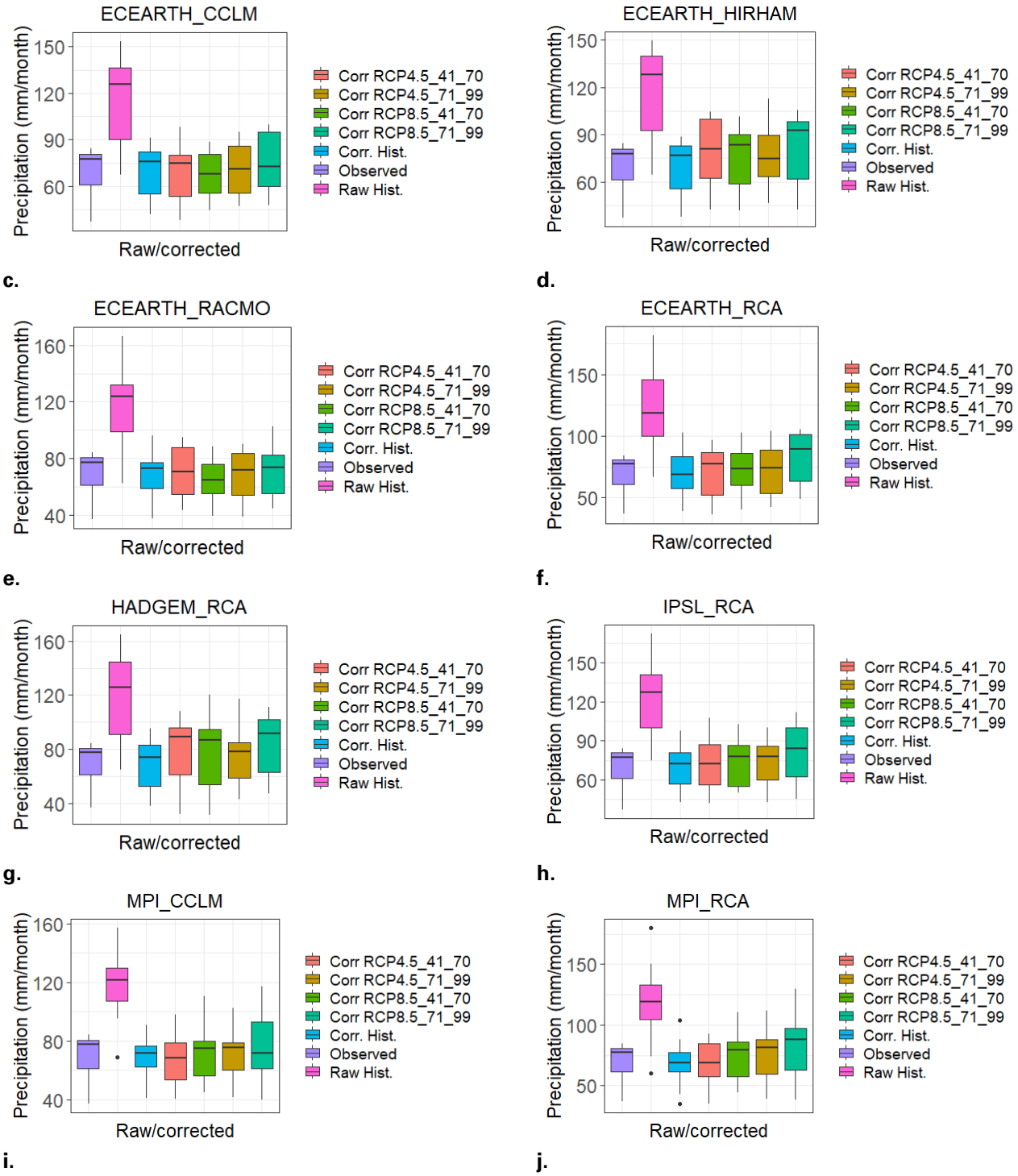

Figure 5.3 Box-scatter plots of mean monthly precipitation of Lærdal catchment for observed, raw, and corrected climate models for various time horizons. **a.** CNRM_CCLM **b.** CNRM_RCA **c.** ECEARTH_CCLM **d.** ECEARTH_HIRHAM **e.** ECEARTH_RACMO **f.** ECEARTH_RCA **g.** HADGEM_RCA **h.** IPSL_RCA **i.** MPI_CCLM **j.** MPI_RCA

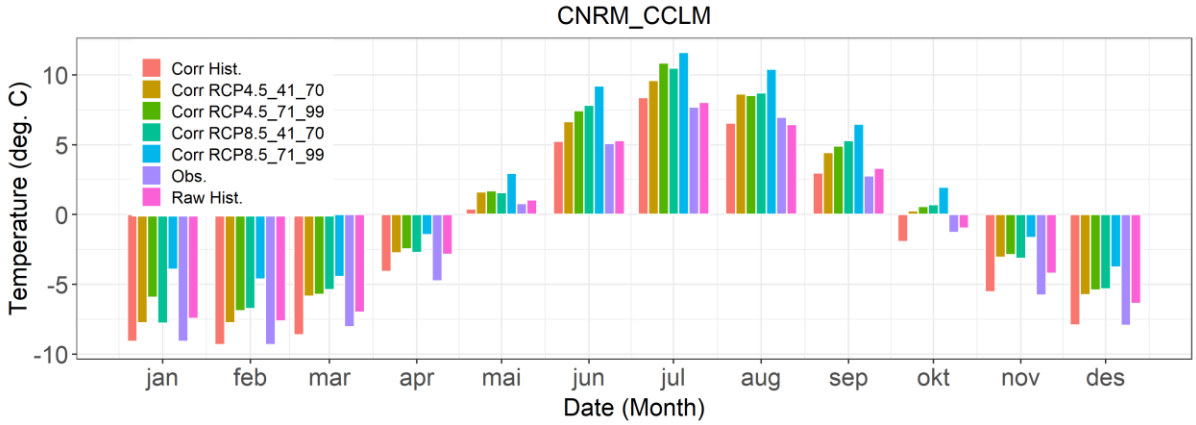
CNRM_CCLM
Corr Hist.
Corr RCP4.5_41_70
Corr RCP4.5_71_99
Corr RCP8.5_41_70
Corr RCP8.5_71_99
Obs.
Raw Hist.
Temperature (deg. C)
10
5
0
-5
-10
jan
feb
mar
apr
mai
jun
jul
aug
sep
okt
nov
des
Date (Month)

a.

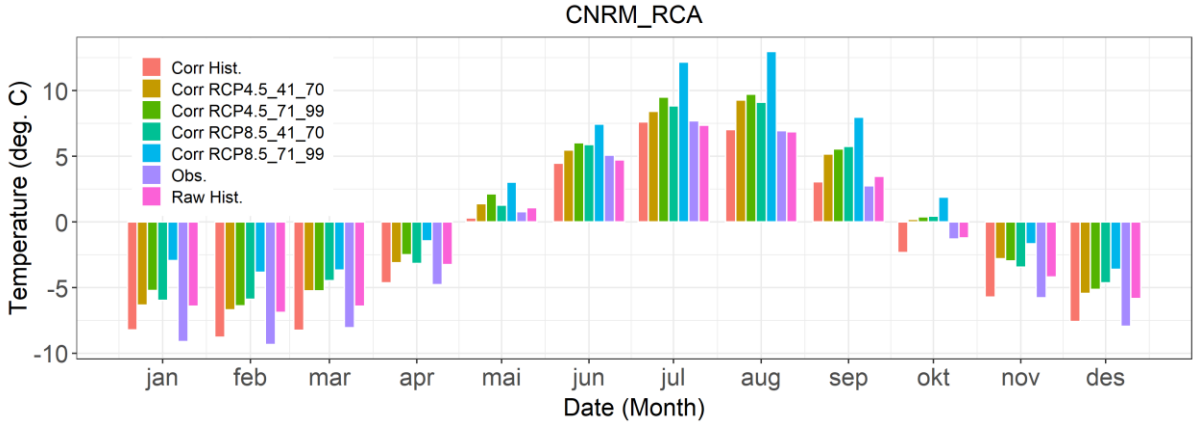
CNRM_RCA
Corr Hist.
Corr RCP4.5_41_70
Corr RCP4.5_71_99
Corr RCP8.5_41_70
Corr RCP8.5_71_99
Obs.
Raw Hist.
Temperature (deg. C)
10
5
0
-5
-10
jan
feb
mar
apr
mai
jun
jul
aug
sep
okt
nov
des
Date (Month)

b.

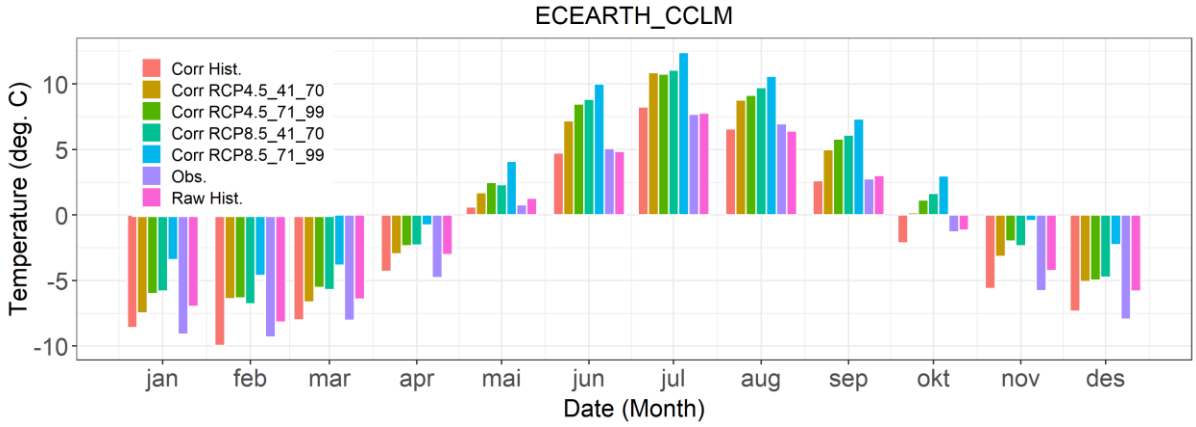
ECEARTH_CCLM
Corr Hist.
Corr RCP4.5_41_70
Corr RCP4.5_71_99
Corr RCP8.5_41_70
Corr RCP8.5_71_99
Obs.
Raw Hist.
Temperature (deg. C)
10
5
0
-5
-10
jan
feb
mar
apr
mai
jun
jul
aug
sep
okt
nov
des
Date (Month)

c.

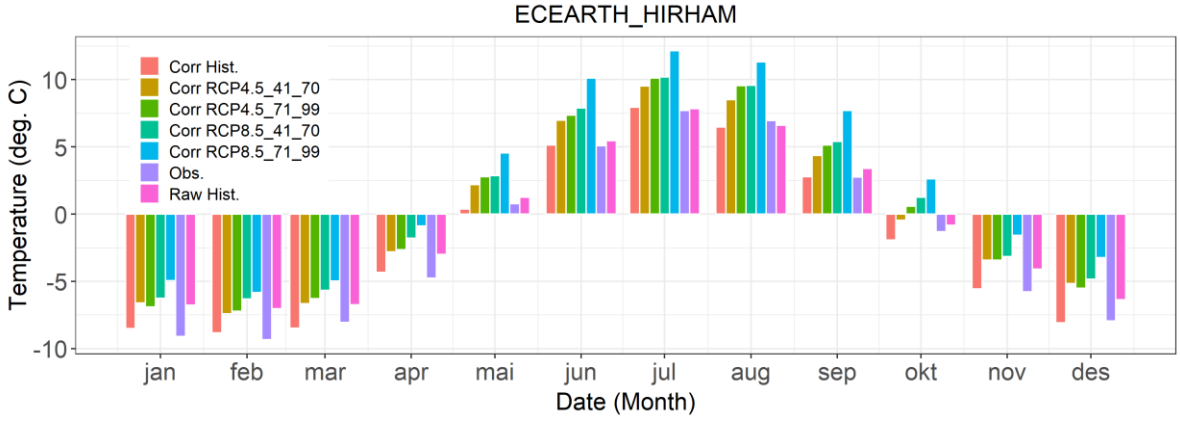
ECEARTH_HIRHAM
Corr Hist.
Corr RCP4.5_41_70
Corr RCP4.5_71_99
Corr RCP8.5_41_70
Corr RCP8.5_71_99
Obs.
Raw Hist.
Temperature (deg. C)
10
5
0
-5
-10
jan
feb
mar
apr
mai
jun
jul
aug
sep
okt
nov
des
Date (Month)

d.

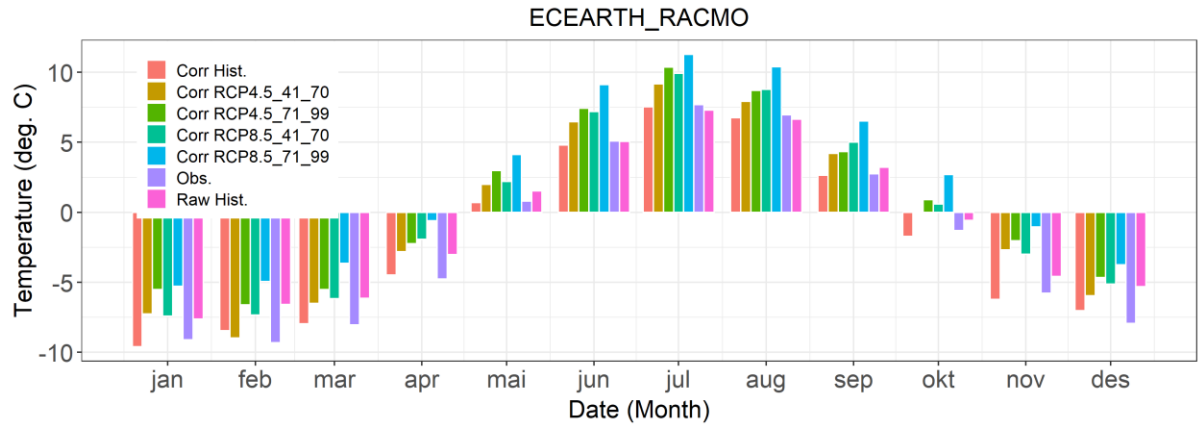
ECEARTH_RACMO
Corr Hist.
Corr RCP4.5_41_70
Corr RCP4.5_71_99
Corr RCP8.5_41_70
Corr RCP8.5_71_99
Obs.
Raw Hist.
Temperature (deg. C)
10
5
0
-5
-10
jan
feb
mar
apr
mai
jun
jul
aug
sep
okt
nov
des
Date (Month)

e.

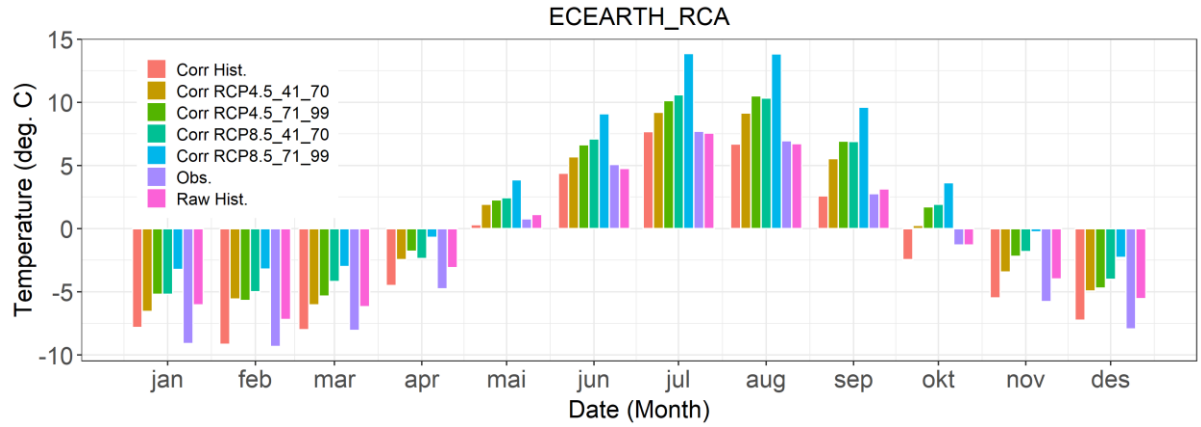
ECEARTH_RCA
Corr Hist.
Corr RCP4.5_41_70
Corr RCP4.5_71_99
Corr RCP8.5_41_70
Corr RCP8.5_71_99
Obs.
Raw Hist.
Temperature (deg. C)
15
10
5
0
-5
-10
jan
feb
mar
apr
mai
jun
jul
aug
sep
okt
nov
des
Date (Month)

f.

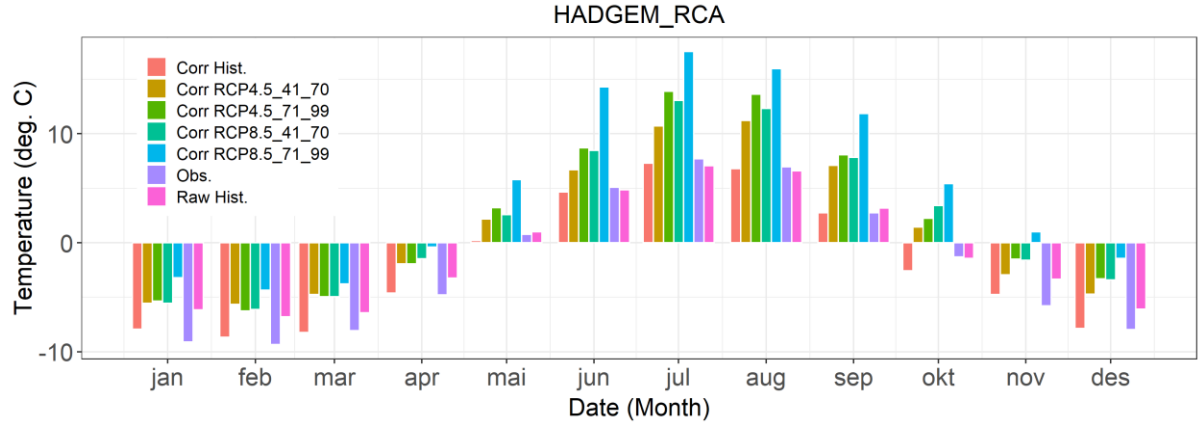
HADGEM_RCA
Corr Hist.
Corr RCP4.5_41_70
Corr RCP4.5_71_99
Corr RCP8.5_41_70
Corr RCP8.5_71_99
Obs.
Raw Hist.
Temperature (deg. C)
10
0
-10
jan
feb
mar
apr
mai
jun
jul
aug
sep
okt
nov
des
Date (Month)

g.

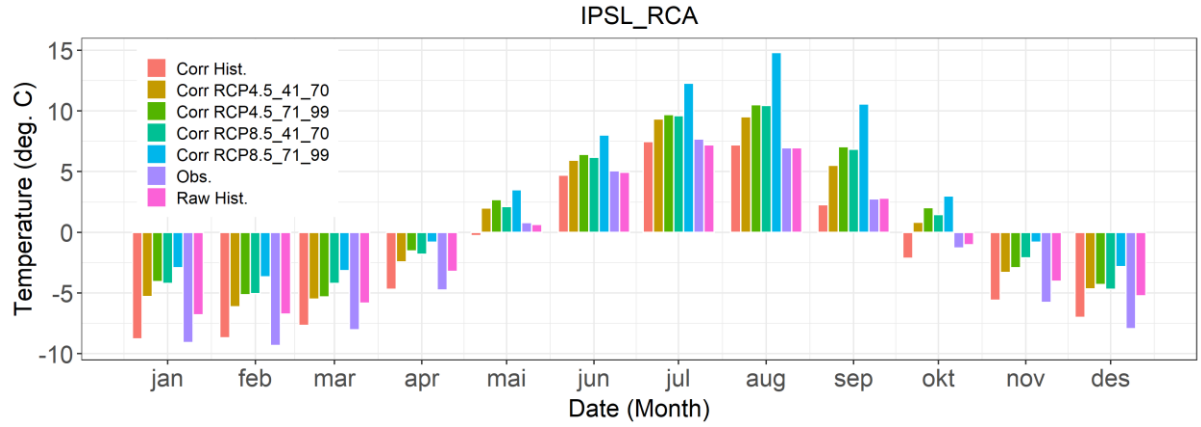
IPSL_RCA
Corr Hist.
Corr RCP4.5_41_70
Corr RCP4.5_71_99
Corr RCP8.5_41_70
Corr RCP8.5_71_99
Obs.
Raw Hist.
Temperature (deg. C)
15
10
5
0
-5
-10
jan
feb
mar
apr
mai
jun
jul
aug
sep
okt
nov
des
Date (Month)

h.

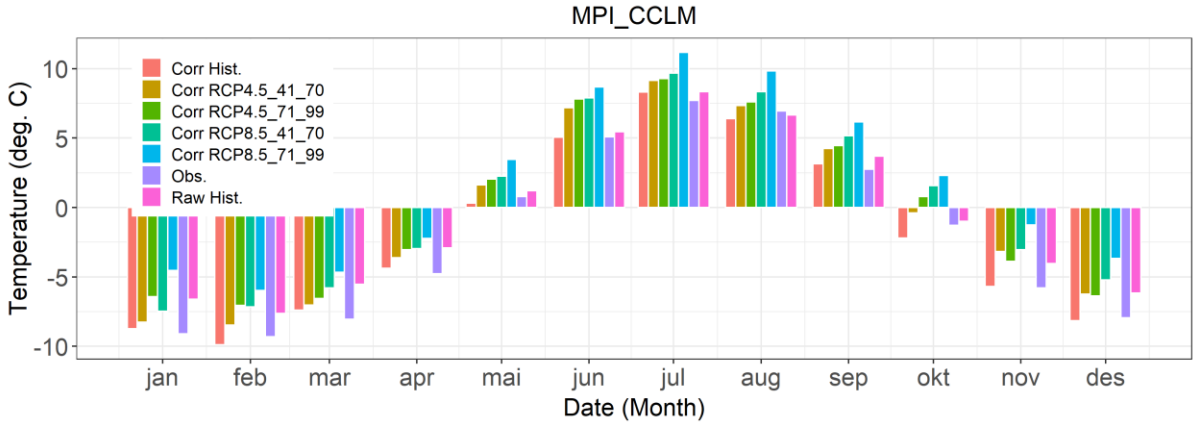

i.

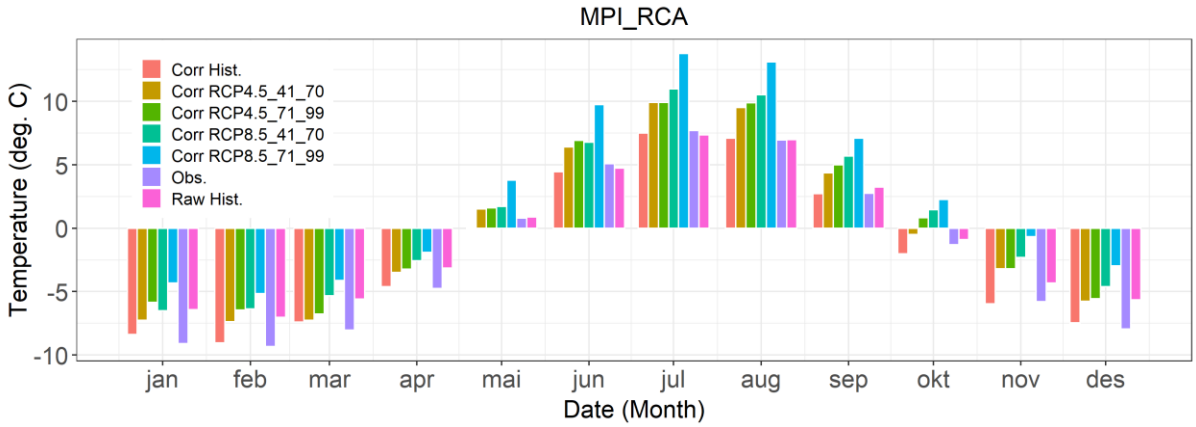

j.

Figure 5.4 Histogram of mean monthly temperature of Lærdal catchment for observed, raw, and corrected climate models for various time horizons. **a.** CNRM_CCLM **b.** CNRM_RCA **c.** ECEARTH_CCLM **d.** ECEARTH_HIRHAM **e.** ECEARTH_RACMO **f.** ECEARTH_RCA **g.** HADGEM_RCA **h.** IPSL_RCA **i.** MPI_CCLM **j.** MPI_RCA

5.1.2 Trend analysis of future precipitation and temperature of Forra and Lærdal catchments based on historical, RCP4.5, and RCP8.5 scenarios.

The impacts of climate change on Forra and Lærdal catchments were evaluated using the Mann-Kendall trend test. The statistical evaluation of the climatic trends was carried out between the periods of 1971 – 2000 and 2041 - 2070 as well as 2041 – 2070 and 2071 – 2099 using the annual temperature and annual precipitation datasets of the climate models.

For Forra catchment, three out of ten models predict that the precipitation of the watershed will significantly increase between the historical period (1971 – 2000) and medium term (2041-2070) for RCP4.5 (Table 5.1). On the other hand, seven

models predict that there will be no significant change in the precipitation (Table 5.1). For the period between the medium term (2041-2070) and the long term (2071 – 2099), all ten models predict that there would be no significant change in the precipitation of the Forra watershed for RCP4.5 (Table 5.2). Four out of ten models predict that the precipitation of Forra catchment would significantly increase between the historical period (1971 – 2000) and medium term (2041-2070) for RCP8.5 (Table 5.3). The remaining six models predict that there would be no significant change in the precipitation of the watershed in the medium term (Table 5.3). For the period between the medium term (2041-2070) and the long term (2071 – 2099), Six out of Ten models predict that the precipitation of Forra catchment would significantly increase for RCP8.5 (Table 5.4). However, the remaining four models predict that there would be no significant change in the precipitation of the watershed in the long-term (Table 5.4). For temperature, all the models predict that the temperature would significantly increase between the periods of 1971 – 2000 and 2041 - 2070 as well as 2041 – 2070 and 2071 – 2099 for both RCP4.5 and RCP8.5 scenarios (Tables 5.5 – 5.8).

Table 5.1 Mann-Kendall trend test for corrected annual precipitation RCP4.5_2041-2070 and historical period of climate models for Forra catchment.

Climate Model	Kendall's Tau	Standardized test statistic	p-value	Alpha	Trend
CNRM_CCLM	0.08	0.92	0.36	0.05	Not significant
CNRM_RCA	0.15	1.72	0.09	0.05	Not significant
ECEARTH_CCLM	-0.09	-1.07	0.29	0.05	Not significant
ECEARTH_HIRHAM	0.14	1.52	0.13	0.05	Not significant
ECEARTH_RACMO	0.14	1.61	0.11	0.05	Not significant
ECEARTH_RCA	0.00	-0.01	0.99	0.05	Not significant
HADGEM_RCA	0.24	2.71	0.01	0.05	Significantly increasing
IPSL_RCA	0.17	1.91	0.06	0.05	Not significant
MPI_CCLM	0.27	3.08	0.00	0.05	Significantly increasing
MPI_RCA	0.19	2.19	0.03	0.05	Significantly increasing

Table 5.2 Mann-Kendall trend test for corrected annual precipitation RCP4.5_2041-2070 and RCP4.5_2071-2099 for Forra catchment.

Climate Model	Kendall's Tau	Z	p-value	Alpha	Trend
CNRM_CCLM	0.079	0.876	0.381	0.050	Not significant
CNRM_RCA	-0.016	-0.170	0.865	0.050	Not significant
ECEARTH_CCLM	0.056	0.615	0.539	0.050	Not significant
ECEARTH_HIRHAM	-0.314	-0.029	0.754	0.050	Not significant
ECEARTH_RACMO	-0.174	-1.936	0.053	0.050	Not significant
ECEARTH_RCA	0.163	1.818	0.069	0.050	Not significant
HADGEM_RCA	-0.019	-0.203	0.839	0.050	Not significant
IPSL_RCA	0.046	0.510	0.610	0.050	Not significant
MPI_CCLM	0.074	0.824	0.410	0.050	Not significant
MPI_RCA	0.134	1.491	0.136	0.050	Not significant

Table 5.3 Mann-Kendall trend test for corrected annual precipitation RCP8.5_2041-2070 and historical period of climate models for Forra catchment.

Climate Model	Kendall's Tau	Z	p-value	Alpha	Trend
CNRM_CCLM	0.075	0.836	0.403	0.050	Not significant
CNRM_RCA	0.131	1.473	0.141	0.050	Not significant
ECEARTH_CCLM	0.098	1.103	0.270	0.050	Not significant
ECEARTH_HIRHAM	0.080	0.899	0.369	0.050	Not significant
ECEARTH_RACMO	0.068	0.759	0.448	0.050	Not significant
ECEARTH_RCA	0.142	1.601	0.109	0.050	Not significant
HADGEM_RCA	0.334	3.769	0.000	0.050	Significantly increasing
IPSL_RCA	0.268	3.017	0.003	0.050	Significantly increasing
MPI_CCLM	0.356	4.012	0.000	0.050	Significantly increasing
MPI_RCA	0.302	3.399	0.001	0.050	Significantly increasing

Table 5.4 Mann-Kendall trend test for corrected annual precipitation RCP8.5_2041-2070 and RCP8.5_2071-2099 for Forra catchment.

Climate Model	Kendall's Tau	Z	p-value	Alpha	Trend
CNRM_CCLM	0.231	2.577	0.010	0.050	Significantly increasing
CNRM_RCA	0.347	3.871	0.000	0.050	Significantly increasing
ECEARTH_CCLM	3.074	0.275	0.002	0.050	Significantly increasing
ECEARTH_HIRHAM	0.029	0.314	0.754	0.050	Not significant
ECEARTH_RACMO	0.059	0.654	0.513	0.050	Not significant
ECEARTH_RCA	0.264	2.943	0.003	0.050	Significantly increasing
HADGEM_RCA	0.067	0.746	0.456	0.050	Not significant
IPSL_RCA	0.297	3.322	0.001	0.050	Significantly increasing
MPI_CCLM	0.181	2.014	0.044	0.050	Significantly increasing
MPI_RCA	0.113	1.256	0.209	0.050	Not significant

Table 5.5 Mann-Kendall trend test for corrected annual temperature RCP4.5_2041-2070 and historical period of climate models for Forra catchment.

Climate Model	Kendall's Tau	Z	p-value	Alpha	Trend
CNRM_CCLM	0.540	6.091	0.000	0.050	Significantly increasing
CNRM_RCA	0.585	6.601	0.000	0.050	Significantly increasing
ECEARTH_CCLM	0.539	6.078	0.000	0.050	Significantly increasing
ECEARTH_HIRHAM	0.507	5.721	0.000	0.050	Significantly increasing
ECEARTH_RACMO	0.575	6.486	0.000	0.050	Significantly increasing
ECEARTH_RCA	0.588	6.627	0.000	0.050	Significantly increasing
HADGEM_RCA	0.719	8.106	0.000	0.050	Significantly increasing
IPSL_RCA	0.584	6.588	0.000	0.050	Significantly increasing
MPI_CCLM	0.354	3.986	0.000	0.050	Significantly increasing
MPI_RCA	0.384	4.331	0.000	0.050	Significantly increasing

Table 5.6 Mann-Kendall trend test for corrected annual temperature RCP4.5_2041-2070 and RCP4.5_2071-2099 for Forra catchment.

Climate Model	Kendall's Tau	Z	p-value	Alpha	Trend
CNRM_CCLM	0.259	2.891	0.004	0.050	Significantly increasing
CNRM_RCA	0.250	2.786	0.005	0.050	Significantly increasing
ECEARTH_CCLM	0.287	3.204	0.001	0.050	Significantly increasing
ECEARTH_HIRHAM	0.234	2.616	0.009	0.050	Significantly increasing
ECEARTH_RACMO	0.496	5.546	0.000	0.050	Significantly increasing
ECEARTH_RCA	0.364	4.068	0.000	0.050	Significantly increasing
HADGEM_RCA	0.382	4.270	0.000	0.050	Significantly increasing
IPSL_RCA	0.349	3.898	0.000	0.050	Significantly increasing
MPI_CCLM	0.241	2.694	0.007	0.050	Significantly increasing
MPI_RCA	0.219	2.446	0.014	0.050	Significantly increasing

Table 5.7 Mann-Kendall trend test for corrected annual temperature RCP8.5_2041-2070 and historical period of climate models for Forra catchment.

Climate Model	Kendall's Tau	Z	p-value	Alpha	Trend
CNRM_CCLM	0.593	6.690	0.000	0.050	Significantly increasing
CNRM_RCA	0.616	6.946	0.000	0.050	Significantly increasing
ECEARTH_CCLM	0.643	7.252	0.000	0.050	Significantly increasing
ECEARTH_HIRHAM	0.606	6.831	0.000	0.050	Significantly increasing
ECEARTH_RACMO	0.654	7.379	0.000	0.050	Significantly increasing
ECEARTH_RCA	0.663	7.481	0.000	0.050	Significantly increasing
HADGEM_RCA	0.740	8.349	0.000	0.050	Significantly increasing
IPSL_RCA	0.645	7.277	0.000	0.050	Significantly increasing
MPI_CCLM	0.507	5.721	0.000	0.050	Significantly increasing
MPI_RCA	0.527	5.938	0.000	0.050	Significantly increasing

Table 5.8 Mann-Kendall trend test for corrected annual temperature RCP8.5_2041-2070 and RCP8.5_2071-2099 for Forra catchment.

Climate Model	Kendall's Tau	Z	p-value	Alpha	Trend
CNRM_CCLM	0.604	6.749	0.000	0.050	Significantly increasing
CNRM_RCA	0.629	7.037	0.000	0.050	Significantly increasing
ECEARTH_CCLM	0.615	6.880	0.000	0.050	Significantly increasing
ECEARTH_HIRHAM	0.592	6.618	0.000	0.050	Significantly increasing
ECEARTH_RACMO	0.632	7.063	0.000	0.050	Significantly increasing
ECEARTH_RCA	0.629	7.037	0.000	0.050	Significantly increasing
HADGEM_RCA	0.686	7.664	0.000	0.050	Significantly increasing
IPSL_RCA	0.605	6.762	0.000	0.050	Significantly increasing
MPI_CCLM	0.555	6.199	0.000	0.050	Significantly increasing
MPI_RCA	0.553	6.186	0.000	0.050	Significantly increasing

For Lærdal catchment, three out of ten models predict that the precipitation of the catchment will significantly increase between the historical period (1971 – 2000) and medium term (2041-2071) for RCP4.5 (Table 5.9). On the other hand, seven models predict that there will be no significant change in the precipitation (Table 5.9). For the period between the medium term (2041 - 2071) and the long term (2071 – 2099), nine models predict that there would be no significant change in the precipitation of the Lærdal catchment for RCP4.5 (Table 5.10) while one model predicts that the precipitation would increase in the catchment. Four out of ten models predict that the precipitation of the catchment will significantly increase between the periods 1971 – 2000 and 2041-2070 as well as 2041 – 2070 and 2071 - 2099 for RCP4.5 (Table 5.11 and Table 5.12). On the other hand, six models predict that there will be no significant change in the precipitation (Table 5.11 and Table 5.12). For temperature, all the models predict that the temperature would significantly increase between the periods of 1971 – 2000 and 2041 - 2070 as well as 2041 – 2070 and 2071 – 2099 for both RCP4.5 and RCP8.5 scenarios (Tables 5.13 – 5.16).

Table 5.9 Mann-Kendall trend test for corrected annual precipitation RCP4.5_2041-2070 and historical period of climate models for Lærdal catchment.

Climate Model	Kendall's Tau	Z	p-value	Alpha	Trend
CNRM_CCLM	0.182	2.047	0.041	0.050	Significantly increasing
CNRM_RCA	0.183	2.060	0.039	0.050	Significantly increasing
ECEARTH_CCLM	-0.068	-0.759	0.448	0.050	Not significant
ECEARTH_HIRHAM	0.162	1.818	0.069	0.050	Not significant
ECEARTH_RACMO	0.019	0.210	0.833	0.050	Not significant
ECEARTH_RCA	0.008	0.083	0.934	0.050	Not significant
HADGEM_RCA	0.210	2.366	0.018	0.050	Significantly increasing
IPSL_RCA	0.151	1.703	0.089	0.050	Not significant
MPI_CCLM	0.058	0.644	0.520	0.050	Not significant
MPI_RCA	0.075	0.836	0.403	0.050	Not significant

Table 5.10 Mann-Kendall trend test for corrected annual precipitation RCP4.5_2041-2070 and RCP4.5_2071-2099 for Lærdal catchment.

Climate Model	Kendall's Tau	Z	p-value	Alpha	Trend
CNRM_CCLM	0.094	1.046	0.295	0.050	Not significant
CNRM_RCA	0.141	1.570	0.117	0.050	Not significant
ECEARTH_CCLM	0.023	0.249	0.804	0.050	Not significant
ECEARTH_HIRHAM	-0.056	-0.615	0.539	0.050	Not significant
ECEARTH_RACMO	-0.086	-0.955	0.340	0.050	Not significant
ECEARTH_RCA	0.080	0.889	0.374	0.050	Not significant
HADGEM_RCA	-0.081	-0.896	0.370	0.050	Not significant
IPSL_RCA	0.056	0.615	0.539	0.050	Not significant
MPI_CCLM	0.147	1.635	0.102	0.050	Not significant
MPI_RCA	0.217	2.420	0.016	0.050	Significantly increasing

Table 5.11 Mann-Kendall trend test for corrected annual precipitation RCP8.5_2041-2070 and historical period of climate models for Lærdal catchment.

Climate Model	Kendall's Tau	Z	p-value	Alpha	Trend
CNRM_CCLM	0.203	2.290	0.022	0.050	Significantly increasing
CNRM_RCA	0.175	1.971	0.049	0.050	Significantly increasing
ECEARTH_CCLM	-0.075	-0.836	0.403	0.050	Not significant
ECEARTH_HIRHAM	0.169	1.907	0.057	0.050	Not significant
ECEARTH_RACMO	-0.129	-1.448	0.148	0.050	Not significant
ECEARTH_RCA	0.058	0.644	0.520	0.050	Not significant
HADGEM_RCA	0.192	2.162	0.031	0.050	Significantly increasing
IPSL_RCA	0.166	1.869	0.062	0.050	Not significant
MPI_CCLM	0.113	1.269	0.204	0.050	Not significant
MPI_RCA	0.216	2.430	0.015	0.050	Significantly increasing

Table 5.12 Mann-Kendall trend test for corrected annual precipitation RCP8.5_2041-2070 and RCP8.5_2071-2099 for Lærdal catchment.

Climate Model	Kendall's Tau	Z	p-value	Alpha	Trend
CNRM_CCLM	0.168	1.870	0.061	0.050	Not significant
CNRM_RCA	0.316	3.531	0.000	0.050	Significantly increasing
ECEARTH_CCLM	0.168	1.870	0.061	0.050	Not significant
ECEARTH_HIRHAM	0.092	1.020	0.308	0.050	Not significant
ECEARTH_RACMO	0.167	1.857	0.063	0.050	Not significant
ECEARTH_RCA	0.290	3.244	0.001	0.050	Significantly increasing
HADGEM_RCA	0.220	2.459	0.014	0.050	Significantly increasing
IPSL_RCA	0.255	2.851	0.004	0.050	Significantly increasing
MPI_CCLM	0.043	0.471	0.638	0.050	Not significant
MPI_RCA	0.119	1.321	0.187	0.050	Not significant

Table 5.13 Mann-Kendall trend test for corrected annual temperature RCP4.5_2041-2070 and historical period of climate models for Lærdal catchment.

Climate Model	Kendall's Tau	Z	p-value	Alpha	Trend
CNRM_CCLM	0.549	6.193	0.000	0.050	Significantly increasing
CNRM_RCA	0.555	6.257	0.000	0.050	Significantly increasing
ECEARTH_CCLM	0.594	6.703	0.000	0.050	Significantly increasing
ECEARTH_HIRHAM	0.505	5.696	0.000	0.050	Significantly increasing
ECEARTH_RACMO	0.513	5.785	0.000	0.050	Significantly increasing
ECEARTH_RCA	0.636	7.175	0.000	0.050	Significantly increasing
HADGEM_RCA	0.676	7.622	0.000	0.050	Significantly increasing
IPSL_RCA	0.555	6.257	0.000	0.050	Significantly increasing
MPI_CCLM	0.386	4.356	0.000	0.050	Significantly increasing
MPI_RCA	0.415	4.675	0.000	0.050	Significantly increasing

Table 5.14 Mann-Kendall trend test for corrected annual temperature RCP4.5_2041-2070 and RCP4.5_2071-2099 for Lærdal catchment.

Climate Model	Kendall's Tau	Z	p-value	Alpha	Trend
CNRM_CCLM	0.244	2.720	0.007	0.050	Significantly increasing
CNRM_RCA	0.219	2.446	0.014	0.050	Significantly increasing
ECEARTH_CCLM	0.358	4.002	0.000	0.050	Significantly increasing
ECEARTH_HIRHAM	0.210	2.341	0.019	0.050	Significantly increasing
ECEARTH_RACMO	0.368	4.107	0.000	0.050	Significantly increasing
ECEARTH_RCA	0.385	4.303	0.000	0.050	Significantly increasing
HADGEM_RCA	0.348	3.891	0.000	0.050	Significantly increasing
IPSL_RCA	0.293	3.270	0.001	0.050	Significantly increasing
MPI_CCLM	0.250	2.786	0.005	0.050	Significantly increasing
MPI_RCA	0.189	2.106	0.035	0.050	Significantly increasing

Table 5.15 Mann-Kendall trend test for corrected annual temperature RCP8.5_2041-2070 and historical period of climate models for Lærdal catchment.

Climate Model	Kendall's Tau	Z	p-value	Alpha	Trend
CNRM_CCLM	0.603	6.805	0.000	0.050	Significantly increasing
CNRM_RCA	0.600	6.767	0.000	0.050	Significantly increasing
ECEARTH_CCLM	0.656	7.405	0.000	0.050	Significantly increasing
ECEARTH_HIRHAM	0.634	7.150	0.000	0.050	Significantly increasing
ECEARTH_RACMO	0.633	7.137	0.000	0.050	Significantly increasing
ECEARTH_RCA	0.692	7.800	0.000	0.050	Significantly increasing
HADGEM_RCA	0.749	8.451	0.000	0.050	Significantly increasing
IPSL_RCA	0.631	7.111	0.000	0.050	Significantly increasing
MPI_CCLM	0.560	6.321	0.000	0.050	Significantly increasing
MPI_RCA	0.581	6.550	0.000	0.050	Significantly increasing

Table 5.16 Mann-Kendall trend test for corrected annual temperature RCP8.5_2041-2070 and RCP8.5_2071-2099 for Lærdal catchment.

Climate Model	Kendall's Tau	Z	p-value	Alpha	Trend
CNRM_CCLM	0.599	6.696	0.000	0.050	Significantly increasing
CNRM_RCA	0.647	7.233	0.000	0.050	Significantly increasing
ECEARTH_CCLM	0.592	6.618	0.000	0.050	Significantly increasing
ECEARTH_HIRHAM	0.590	6.592	0.000	0.050	Significantly increasing
ECEARTH_RACMO	0.610	6.814	0.000	0.050	Significantly increasing
ECEARTH_RCA	0.608	6.801	0.000	0.050	Significantly increasing
HADGEM_RCA	0.715	7.991	0.000	0.050	Significantly increasing
IPSL_RCA	0.629	7.037	0.000	0.050	Significantly increasing
MPI_CCLM	0.557	6.226	0.000	0.050	Significantly increasing
MPI_RCA	0.560	6.265	0.000	0.050	Significantly increasing

5.2 HBV Model of Forra and Lærdal catchments

5.2.1 Calibration of HBV model Forra and Lærdal catchments

HBV models were setup for Forra and Lærdal catchments. For Forra catchment, the model was calibrated using discharge data ranging from 01.09.1971 – 31.08.1976 while Lærdel catchment was calibrated with data ranging from 01.09.1961 – 31.08.1966. The performance of Forra and Lærdal catchment models at calibration yielded NSE R2 values of 0.826 (Figure 5.5) and 0.895 (Figure 5.6), respectively. The evaluation of the performance of the models was carried out using the accumulation plot method. The comparison of the accumulated simulated and observed runoff for calibration period yielded an accumulated difference of -118.5mm and -144.1 mm for Forra and Lærdal

catchments, respectively (Figures 5.7 – 5.8). This implied that the results of the simulated runoff were comparable to the observed runoff.

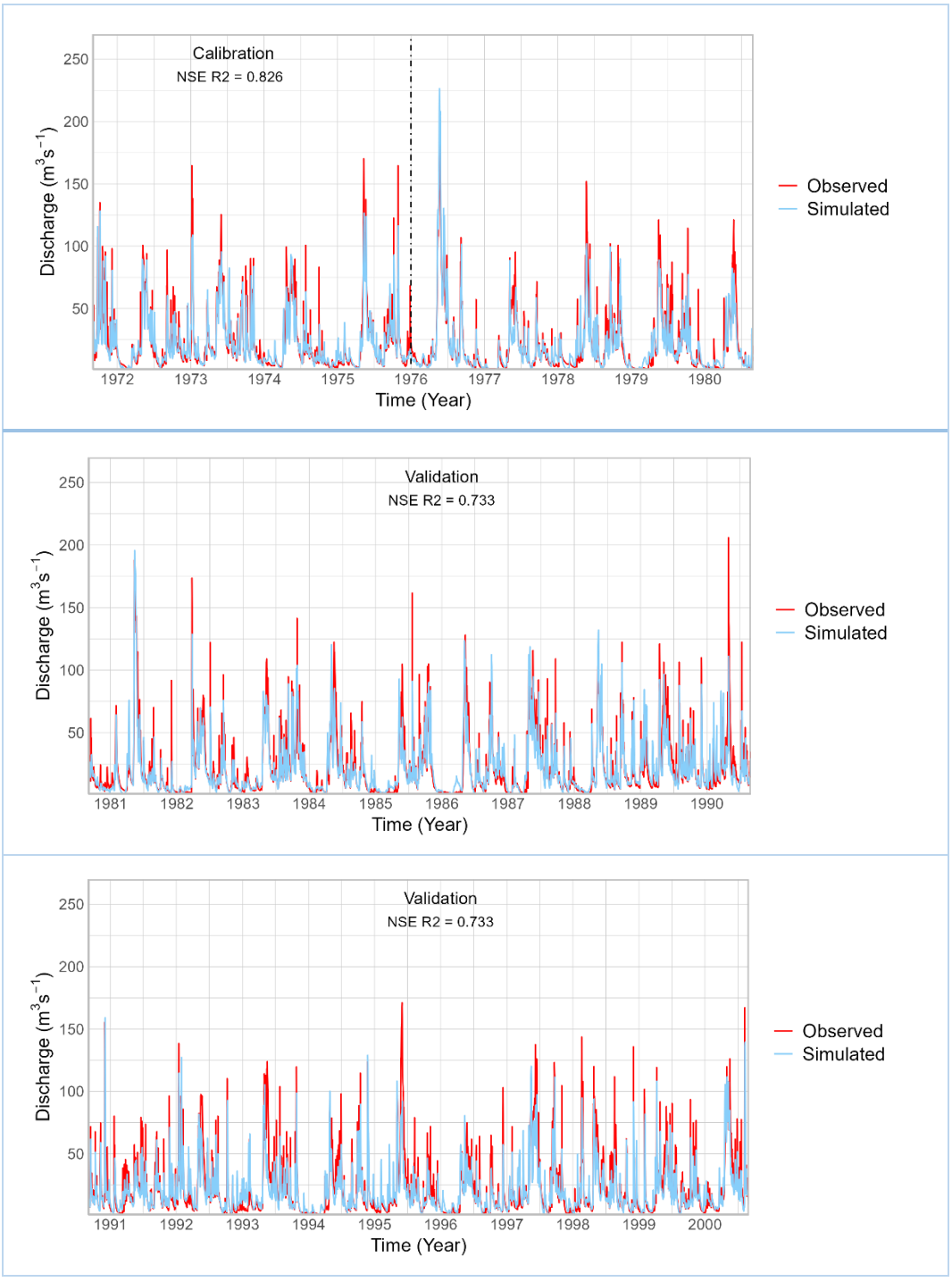

Figure 5.5 Simulated and observed runoff from Forra during calibration (01.09.1971 – 31.08.1976) and validation (01.09.1976 – 31.08.2000)

5.2.2 Validation of HBV model Forra and Lærdal catchments

To verify the performance of the calibrated models, validation was carried out

using the calibration parameters. The validation was carried out with the remaining datasets, not previously used in the calibration process. The Forra catchment model was validated using data ranging from and 01.09.1976 – 31.08.2000 while Lærdel catchment was validated with data ranging from 01.09.1966 – 31.08.1973. The performance of Forra catchment and Lærdal catchment models at validation yielded NSE R2 values of 0.733 (Figures 5.5) and 0.863 (Figure 5.6), respectively. The comparison of the accumulated simulated and observed runoff for the validation period yielded an accumulated difference of -1986.5 mm (Figures 5.7) and -348.1 mm (Figures 5.8) for Forra and Lærdal catchments, respectively.

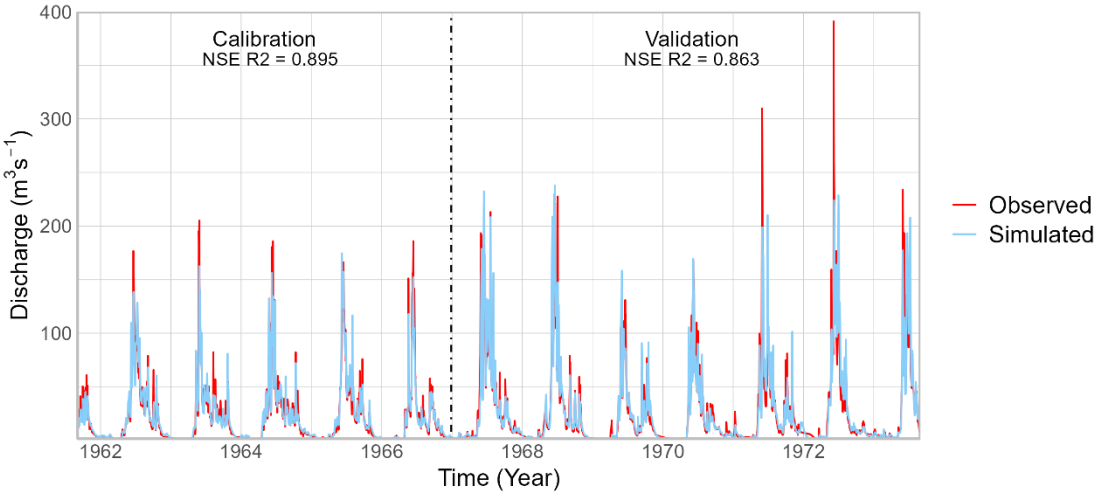

Figure 5.6 Simulated and observed runoff from Lærdal at calibration (01.09.1961 – 31.08.1966) and validation (01.09.1966 – 31.08.1973).

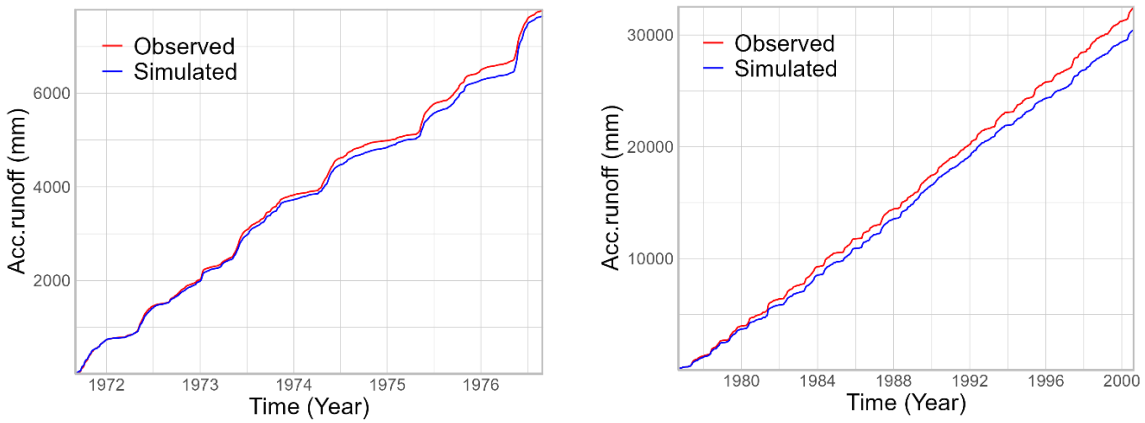

a **b**

Figure 5.7 Accumulated simulated and observed runoff from Forra during **a**. calibration (01.09.1971 – 31.08.1976) **b**. validation (01.09.1976 – 31.08.2000)

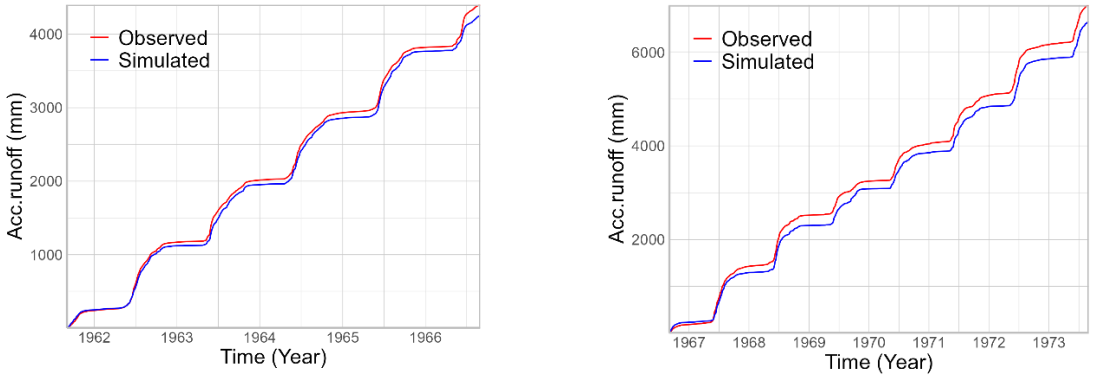

a **b**

Figure 5.8 Accumulated simulated and observed runoff from Lærdal during **a**. calibration (01.09.1961 – 31.08.1966) **b**. validation (01.09.1966 – 31.08.1973)

5.3 Effect of future climate scenarios on runoff and snowpack

The bias corrected datasets of the historical RCMs were simulated in hindcast. The results revealed that the corrected climate models' datasets could not be simulated in hindcast as the results of the Nash-Sutcliffe efficiency (objective function) were comparably too low. The inability of CMIP5 ensembles to capture variability in historical precipitation when run in hindcast have been reported (Mohammed et al., 2015). This necessitated the use of the delta change method. The effect of climate change on future snowpack and runoff, for RCP4.5 and RCP8.5 scenarios, were simulated via the perturbation of the observed time-series of precipitation and temperature.

5.3.1 Effects of climate change on the snowpack of Forra catchment

Figure 5.9 depicts the daily variability of the ensemble daily mean of future snowpack of various scenarios versus the baseline mean snowpack of Forra catchment while Figure 5.10 represents the ensemble mean of monthly snowpack of Forra catchment for future scenarios. The snowpack of Forra catchment is predicted to reduce between the historical period to the end of the century. The snowpack predictions of all the future scenarios were lower than the snowpack of the baseline scenario (Figure 5.9). The effects of warmer climate on snow accumulation of catchments in Finland have been reported (Veijalainen, 2012). The maximum mean monthly snowpack corresponding to the baseline,

RCP4.5_2041-2070, RCP4.5_2071-2099, RCP8.5_2041-2070, and RCP8.5_2071-2099 are 365.49 mm, 140.29 mm, 110.06 mm, 106.68 mm, and 34.65 mm, respectively. Also, the average of the ensemble mean monthly snowpack corresponding to the baseline, RCP4.5_2041-2070, RCP4.5_2071-2099, RCP8.5_2041-2070, and RCP8.5_2071-2099 are 140.49 mm, 49.02 mm, 38.03 mm, 37.39 mm and 11.07 mm, respectively. The order of decrease in snowpack was as follows: Baseline > RCP4.5_2041-2070 > RCP4.5_2071-2099 > RCP8.5_2041-2070 > RCP8.5_2071-2099.

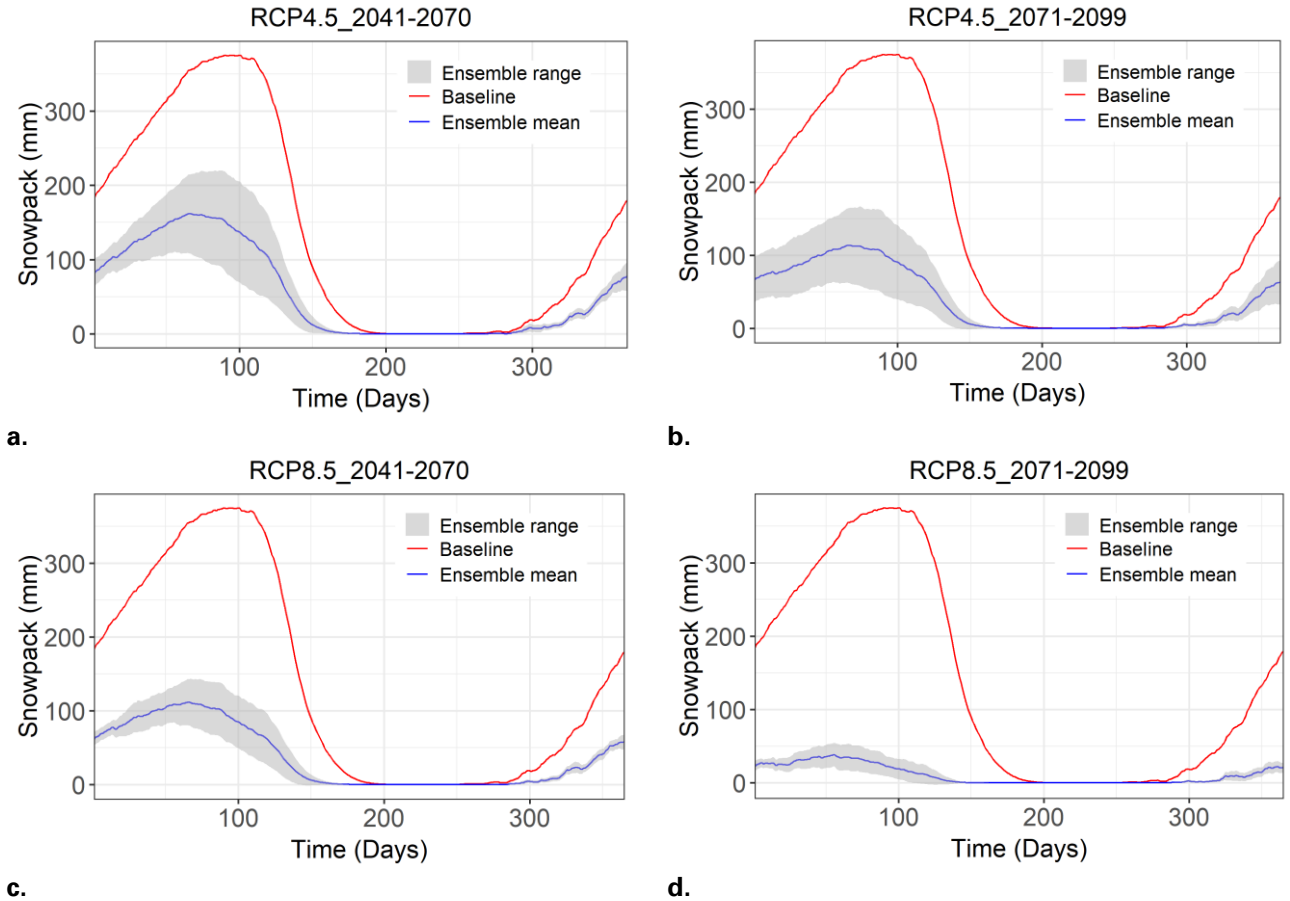

Figure 5.9 Ensemble daily mean snowpack of future scenarios versus baseline mean daily snowpack from Forra catchment. **a**. RCP4.5_2041-2070 **b**. RCP4.5_2071-2099 **c**. RCP8.5_2041-2070 **d**. RCP8.5_2071-2099.

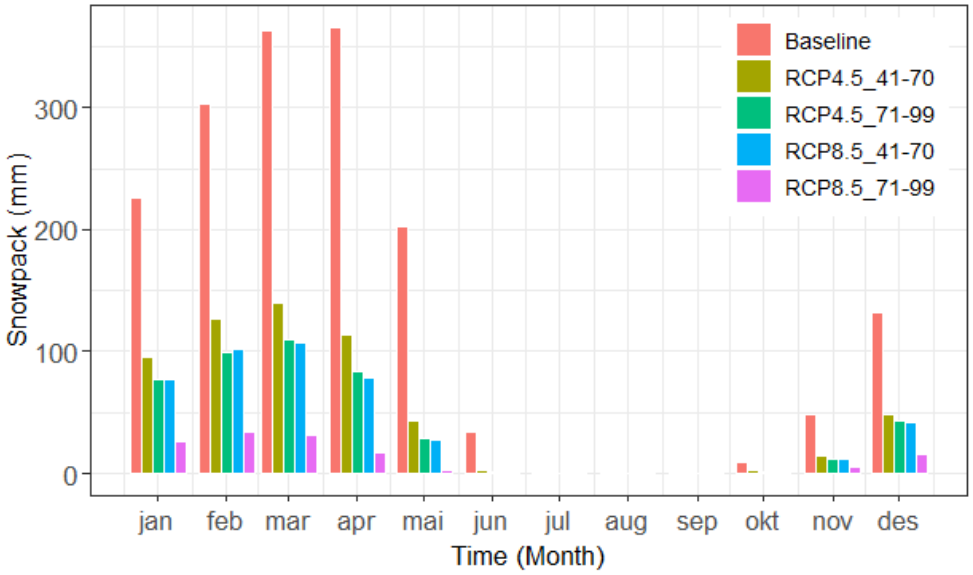

Figure 5.10 Ensemble Mean monthly snowpack of future scenarios versus baseline mean monthly snowpack from Forra catchment.

5.3.2 Effects of climate change on the daily runoff, spring, and autumn floods of Forra catchment

The results of the simulation of future runoff, considering the 10 climate models under review, are shown in Figure 5.11. A comparison of the peak runoff values of the future scenarios for spring/summer and autumn/winter vis-à-vis corresponding peaks for the baseline scenario was carried out (Table 5.17). The daily mean runoff shows that there would be changes in the timing as well as the magnitude of the future runoff from Forra catchment (Figure 5.11). A significant reduction of the spring floods and an increase in the winter discharge was observed for all the scenarios under review. However, the magnitude of the increase and reduction in runoff varied for different scenarios. The change in the hydrology is perhaps due to increase in temperature, which results to increased evapotranspiration and reduction in snowpack accumulation. Decrease in spring snowmelt and increase in winter discharge occasioned by increase in temperature have been reported (Veijalainen, 2012). Climate change resulted to the modification of the amplitude of flow hydrograph in Chute-du-Diable watershed (Minville et al., 2008). Reduction in snowpack and snowfall moderate spring melts influence and increases winter high flows (Capell et al., 2013). In

respect of the baseline and the ensemble mean, the peak of the spring runoff reduced from 61.94 m^3/s to 34.97 m^3/s while the peak of the winter runoff increased from 27.55 m^3/s to 35.87 m^3/s for RCP4.5_2041-2070 (Figure 5.11a and Table 5.17), considering the mean daily runoff. For RCP4.5_2071-2099, the peak of the spring runoff reduces from 61.94 m^3/s to 29.78 m^3/s while the peak of the winter runoff increases from 27.55 m^3/s to 33.55 m^3/s, for RCP4.5_2041-2070 (Figure 5.11b). Similarly, the peak of the spring runoff reduces from 61.94 m^3/s to 27.27 m^3/s while the peak of the rain runoff increases from 27.55 m^3/s to 33.84 m^3/s, for RCP8.5_2041-2070, considering the mean daily runoff (Figure 5.11c). For RCP8.5_2071-2099, the peak of the spring runoff reduces from 61.94 m^3/s to 27.20 m^3/s while the peak of the rain runoff increases from 27.55 m^3/s to 37.25 m^3/s (Figure 5.11d). The order of increase in autumn/winter flood, based on mean daily runoff, was as follows: RCP8.5_2071-2099 > RCP4.5_2041-2070 > RCP8.5_2041-2070 > RCP4.5_2071-2099. The order of decrease in spring flood, considering highest-to-least decrease, was as follows: RCP8.5_2071-2099 > RCP8.5_2041-2070 > RCP4.5_2071-2099 > RCP4.5_2041-2070 (Table 5.17).

The uncertainty in the predictions of the various GCM/RCM combination was assessed considering the average of all the daily mean of ensemble range. The averages of ensemble range corresponding to RCP4.5_2041-2070, RCP4.5_2071-2099, RCP8.5_2041-2070, and RCP8.5_2071-2099 were 11.34 m^3/s, 11.77 m^3/s, 11.44 m^3/s and 10.93 m^3/s, respectively. The uncertainties increased with time horizon for RCP4.5 scenario. Uncertainties due to GCM and RCM have been found to increase with time horizon of projections (Gelfan et al., 2017). However, the uncertainties decreased with time horizon for RCP8.5 scenario.

Table 5.17 Summary of flood peaks based on mean daily flow from Forra Catchment for the baseline and ensemble mean of scenarios.

	Peak flow (m^3/s)				
Season	Baseline	RCP4.5_2041-2070	RCP4.5_2071-2099	RCP8.5_2041-2070	RCP8.5_2071-2099
Spring/Summer	61.94	34.97	29.78	27.27	27.20
Autumn/Winter	27.55	35.87	33.55	33.84	37.25

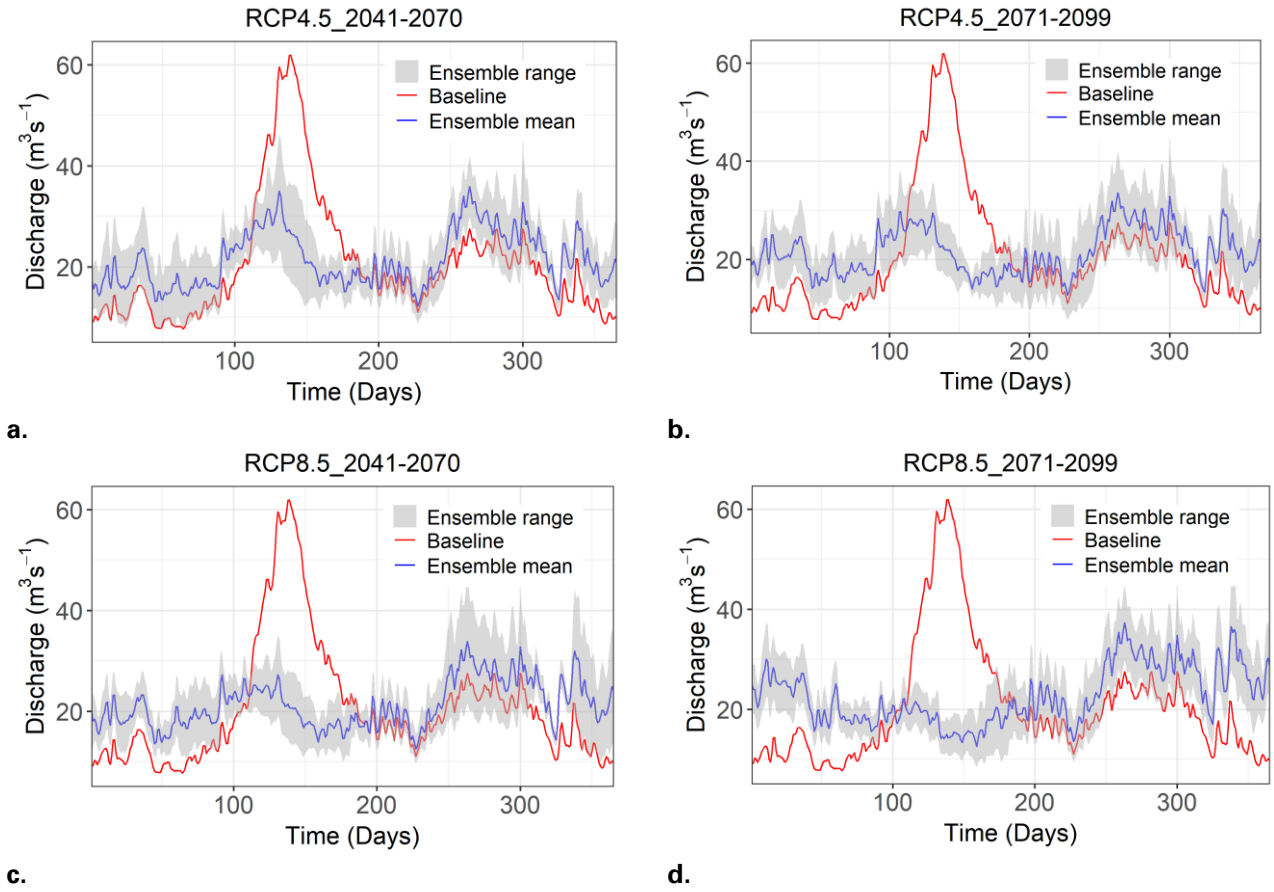

Figure 5.11 Mean daily runoff for the baseline and future scenarios **a.** RCP4.5_2041-2070 **b.** RCP4.5_2071-2099 **c.** RCP8.5_2041-2070 **d.** RCP8.5_2071-2099.

5.3.3 Effects of climate change on the seasonal runoff of Forra catchment.

The variability of the ensemble mean monthly runoff of future scenarios, vis-à-vis baseline scenario from Forra catchment is shown in Figure 5.12 while the average seasonal variations of future runoff for RCP4.5 and RCP8.5 scenarios in relation to the baseline runoff is shown in Table 5.18. The results revealed that RCP8.5_2071-2099 scenario yields the highest magnitude of runoff for 8 months (July – February). On the contrary, the baseline scenario yields the lowest magnitude of runoff for 9 months (July – March). A remarkable high magnitude of runoff occurs in the months of May and June for the baseline scenario (Figure 5.12). This can be attributed to the significant of amount of snowpack of the baseline scenario (Figure 5.9). The snowpack expectedly melts during the spring and summer due to increase in temperature, hence, high magnitude of melt floods. The increase in runoff, by the end of the 21st century for RCP8.5 scenario

is attributed to rain floods (Figure 5.11d). This assertion is buttressed by the decrease in snowpack during the end of the century (Figure 5.9d). In the past, projected changes in runoff due to changes in the snow regime have been reported (Beldring et al., 2008). The variability of the runoff for RCP4.5_2041-2070, RCP4.5_2071-2099, RCP8.5_2041-2070 scenarios was observed for all the months. Except for the months of May and June, RCP4.5_2041-2070, RCP4.5_2071-2099, RCP8.5_2041-2070 scenarios yielded higher runoff than the baseline.

The seasonal variability of future runoff vis-à-vis the baseline scenario were determined. Runoff is projected to increase for all the scenarios in the Autumn and Winter. The runoff is projected to decrease and increase for different scenarios for the months in spring and summer. In addition to the decrease is runoff in the month of April for RCP8.5_71-99, the runoff decreases for all future scenarios for the months of May and June. A maximum average seasonal variation in runoff of 111.19% occurred in Winter for RCP8.5_71-99 scenario while a minimum average seasonal variation in runoff of -9.38% occurred in the Summer for RCP4.5_71-99 scenario (Table 5.18).

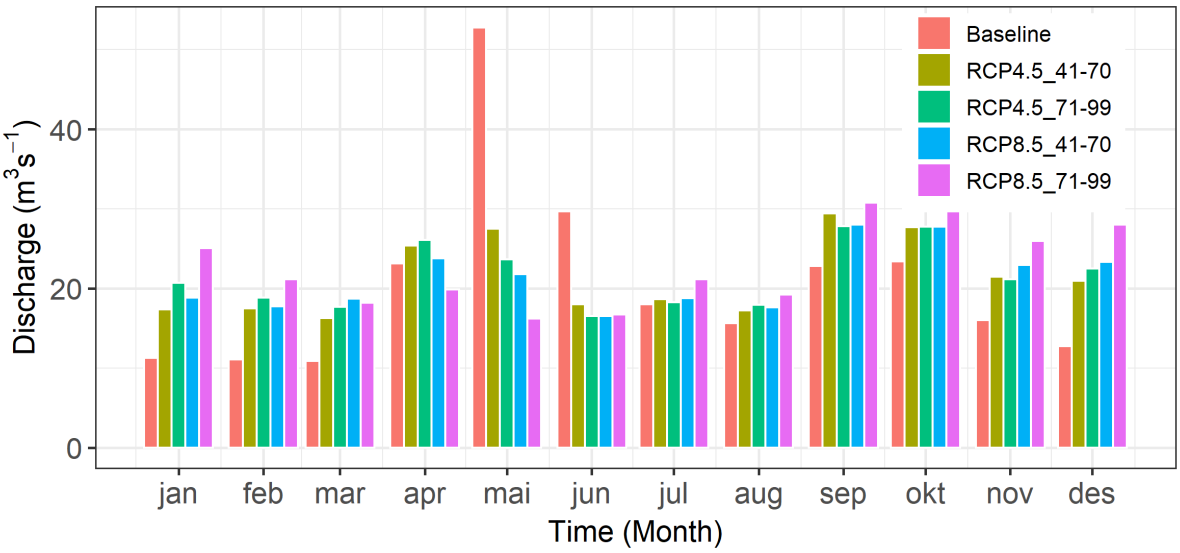

Figure 5.12 Ensemble Mean monthly runoff of future scenarios versus baseline mean monthly runoff from Forra catchment.

Table 5.18 Average seasonal variations of future runoff, in Forra catchment, for RCP4.5 and RCP8.5 scenarios in relation to the baseline runoff.

Season	Baseline average flow (m^3/s)	Average Seasonal variation (%)			
		RCP4.5_2041-2070	RCP4.5_2071-2099	RCP8.5_2041-2070	RCP8.5_2071-2099
Winter	11.68	58.88	76.92	70.33	111.19
Spring	28.94	3.80	6.78	5.52	-5.37
Summer	21.11	-8.51	-9.38	-9.12	-1.05
Autumn	20.76	26.99	24.03	28.14	41.45

5.3.4 Effect of climate change on mean annual runoff of Forra catchment.

The mean annual runoff was computed for the different scenarios of the various climate models (Table 5.19) as well as the baseline scenario. The baseline scenario yielded a mean annual runoff of 20.67 m^3/s. The mean annual runoff varied for different models and scenarios. A maximum mean annual runoff of 24.54 m^3/s was predicted by MPI_CCLM for RCP8.5_2071-2099 scenario while a minimum mean annual runoff of 19.33 m^3/s was predicted by ECEARTH_RACMO for RCP4.5_2071-2099 (Table 5.19). The ensemble mean was computed for different scenarios based on the mean annual runoff. The ensemble mean annual runoff, computed from the ten climate models, corresponding to RCP4.5_2041-2070, RCP4.5_2071-2099, RCP8.5_2041-2070, and RCP8.5_2071-2099 were 21.45 m^3/s, 21.58 m^3/s, 21.33 m^3/s, and 22.68 m^3/s, respectively.

Table 5.19 Mean annual runoff of future scenarios for Forra catchment.

Climate model	Mean annual runoff (m^3/s)			
	RCP4.5_2041-2070	RCP4.5_2071-2099	RCP8.5_2041-2070	RCP8.5_2071-2099
CNRM_CCLM	20.65	20.63	20.34	21.95
CNRM_RCA	22.39	21.94	21.14	24.08
ECEARTH_CCLM	20.01	20.70	20.60	22.64
ECEARTH_HIRHAM	22.07	21.19	19.93	19.73
ECEARTH_RACMO	21.71	19.33	19.71	20.15
ECEARTH_RCA	20.43	22.02	21.25	23.71
HADGEM_RCA	22.54	22.39	23.56	23.38
IPSL_RCA	21.86	22.02	21.98	24.08
MPI_CCLM	21.94	23.00	22.90	24.54
MPI_RCA	20.94	22.54	21.91	22.57

5.3.5 Future runoff and snowpack of Lærdal catchment

Figure 5.13 depicts the daily variability of the ensemble mean of future snowpack of various scenarios versus the baseline mean snowpack of Lærdal catchment while Figure 5.14 represents the ensemble mean of monthly snowpack of Lærdal catchment for future scenarios. The snowpack of Lærdal catchment is predicted to reduce between the historical period to the end of the century. The snowpack predictions of all the future scenarios were lower than the snowpack of the baseline scenario (Figure 5.13). The effects of warmer climate on snow accumulation of catchments in Finland have been reported (Veijalainen, 2012). The maximum mean monthly snowpack corresponding to the baseline, RCP4.5_2041-2070, RCP4.5_2071-2099, RCP8.5_2041-2070, and RCP8.5_2071-2099 are 608.01 mm, 461.97 mm, 428.74 mm, 418.27 mm, and 297.64 mm, respectively. Also, the average of the ensemble mean monthly snowpack corresponding to the baseline, RCP4.5_2041-2070, RCP4.5_2071-2099, RCP8.5_2041-2070, and RCP8.5_2071-2099 are 316.64 mm, 205.50 mm, 179.51 mm, 171.15 mm and 108.44 mm, respectively. The order of decrease in snowpack was as follows: Baseline > RCP4.5_2041-2070 > RCP4.5_2071-2099 > RCP8.5_2041-2070 > RCP8.5_2071-2099.

For the baseline scenario, the snowpack substantially melted (emptied) for most years except for years 1975, 1980, 1988, 1990, and 1991. This resulted to a minimum mean monthly snowpack of 34.65 mm (Figure 5.14).

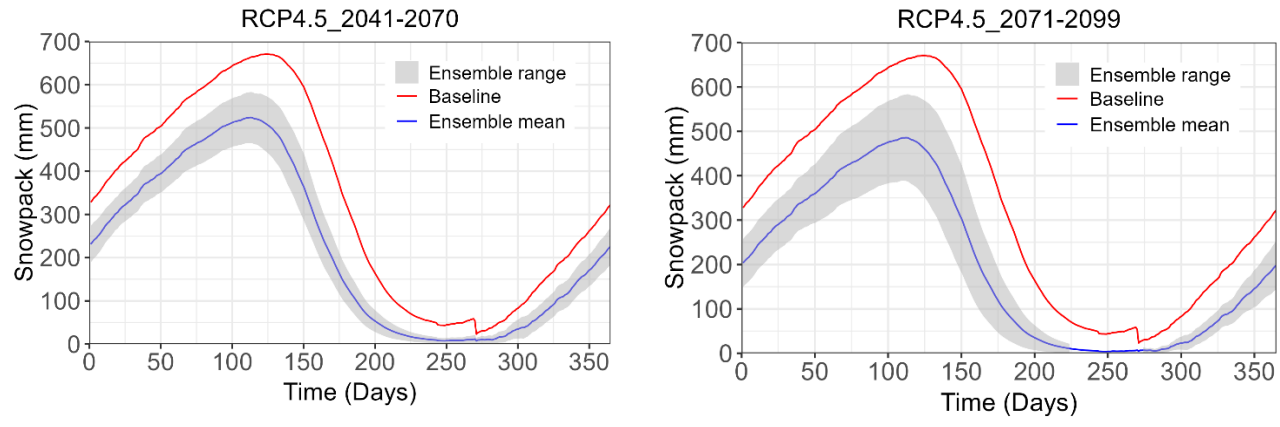

a. **b.**

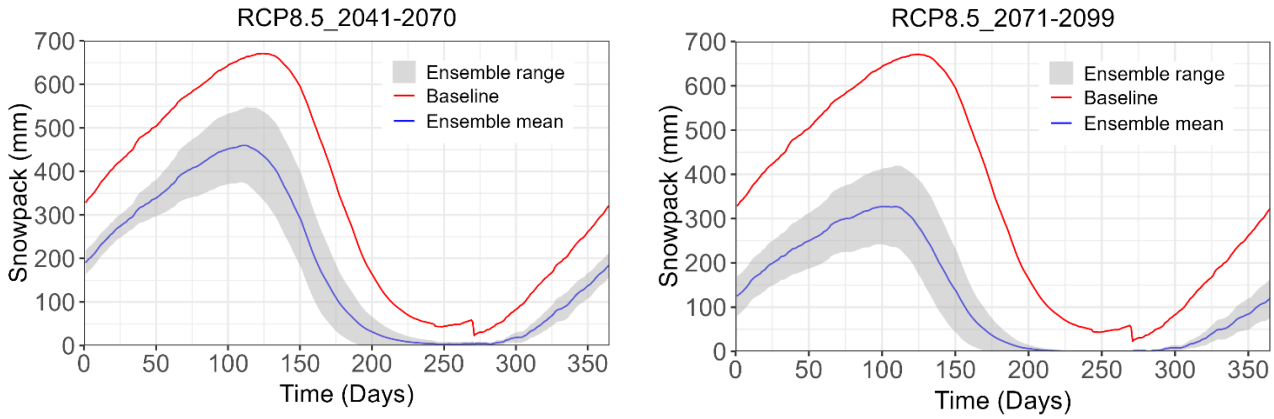

c. **d.**

Figure 5.13 Ensemble mean snowpack of future scenarios versus baseline mean snowpack from Lærdal catchment **a**. RCP4.5_2041-2070 **b**. RCP4.5_2071-2099 **c**. RCP8.5_2041-2070 **d**. RCP8.5_2071-2099.

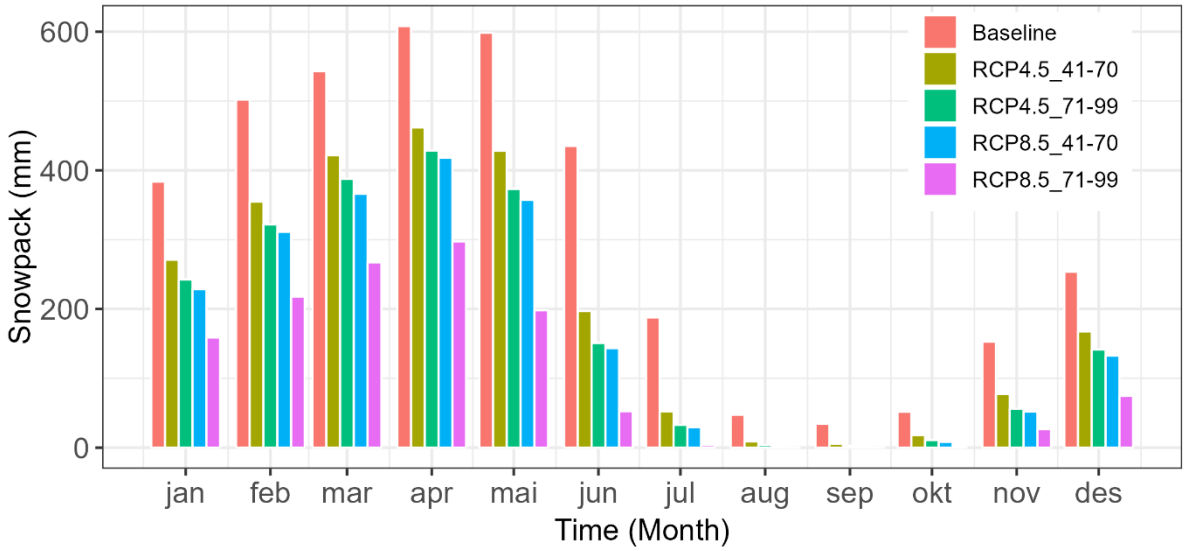

Figure 5.14 Ensemble mean monthly snowpack of future scenarios versus baseline median monthly snowpack from Lærdal catchment.

5.3.6 Effects of climate change on the daily runoff, Spring, and Autumn floods of Lærdal catchment

The results of the simulation of future flows, including the associated uncertainties, are shown in Figure 5.15. A comparison of the peak runoff values of the future scenarios for spring/summer and autumn/winter vis-à-vis corresponding peaks for the baseline scenario was carried out (Table 5.20). The daily mean runoff shows that there would be early occurrence of the future runoff from Lærdal catchment (Figure 5.15). Climate change has resulted to early

occurrence of spring peak flows, and overall increase in river flow have been reported (Graham et al., 2007). A comparison of the hydrographs of the baseline and the future scenarios revealed that a remarkable change in the peakedness of the hydrographs for RCP4.5_2041-2070, RCP4.5_2071-2099, and RCP8.5_2041-2070. A significant reduction of the peak runoff was observed for RCP8.5_2071-2099. In respect of the baseline and the ensemble mean, the peak of the spring runoff increased from 166.42 m^3/s to 168.75 m^3/s while the peak of the winter runoff increased from 49.97 m^3/s to 63.44 m^3/s for RCP4.5_2041-2070 (Figure 5.15a and Table 5.20), considering the mean daily runoff. For RCP4.5_2071-2099, the peak of the spring flood reduced from 166.42 m^3/s to 162.07 m^3/s while the peak of the rain runoff increased from 49.97 m^3/s to 69.61 m^3/s, for RCP4.5_2071-2099 (Figure 5.15b and Table 5.20). Similarly, the peak of the spring runoff reduced from 166.42 m^3/s to 160.57 m^3/s while the peak of the winter runoff increased from 49.97 m^3/s to 66.99 m^3/s, for RCP8.5_2041-2070, considering the mean daily runoff (Figure 5.15c and Table 5.20). For RCP8.5_2071-2099, the peak of the spring runoff reduced from 166.42 m^3/s to 118.68 m^3/s while the peak of the winter runoff increased from 49.97 m^3/s to 70.71 m^3/s (Figure 5.15d and Table 5.20). The order of decrease/increase in Spring runoff, considering highest-to-least magnitude, was as follows: RCP8.5_2071-2099 > RCP8.5_2041-2070 > RCP4.5_2071-2099 > RCP4.5_2041-2070 (Table 5.20). Comparatively, RCP8.5_2071-2099 yielded a lower peak runoff than the other scenarios due to the correspondingly smaller magnitude of snowpack (Figure 5.13d).

The peakedness of the hydrograph of can be attributed the impact of climate change on the watershed and perhaps, the geometry of the catchment. Comparatively, there is a significant amount of snowpack available for the baseline, RCP4.5_2041-2070, RCP4.5_2071-2099 and RCP8.5_2041-2070 scenarios compared to the RCP8.5_2071-2099 (Figure 5.13). Circular shaped catchments are associated with high peak discharge occurring over a short duration (Howard, 1990; Youssef et al., 2011). Snowpack expectedly melts during the spring and summer due to increase in temperature, hence, high magnitude of melt floods. The significant reduction in snowpack of RCP8.5_2071-2099

scenario resulted to the reduction in the peak discharge irrespective of the circularity of the catchment (Figure 5.13d).

The uncertainty in the predictions of the various GCM/RCM combination was assessed considering the average of all the daily mean of ensemble range. The averages of ensemble range corresponding to RCP4.5_2041-2070, RCP4.5_2071-2099, RCP8.5_2041-2070, and RCP8.5_2071-2099 were 22.59 m^3/s, 27.85 m^3/s, 28.46 m^3/s and 33.30 m^3/s, respectively. Uncertainties due to GCM and RCM have been found to increase with time horizon of projections (Gelfan et al., 2017).

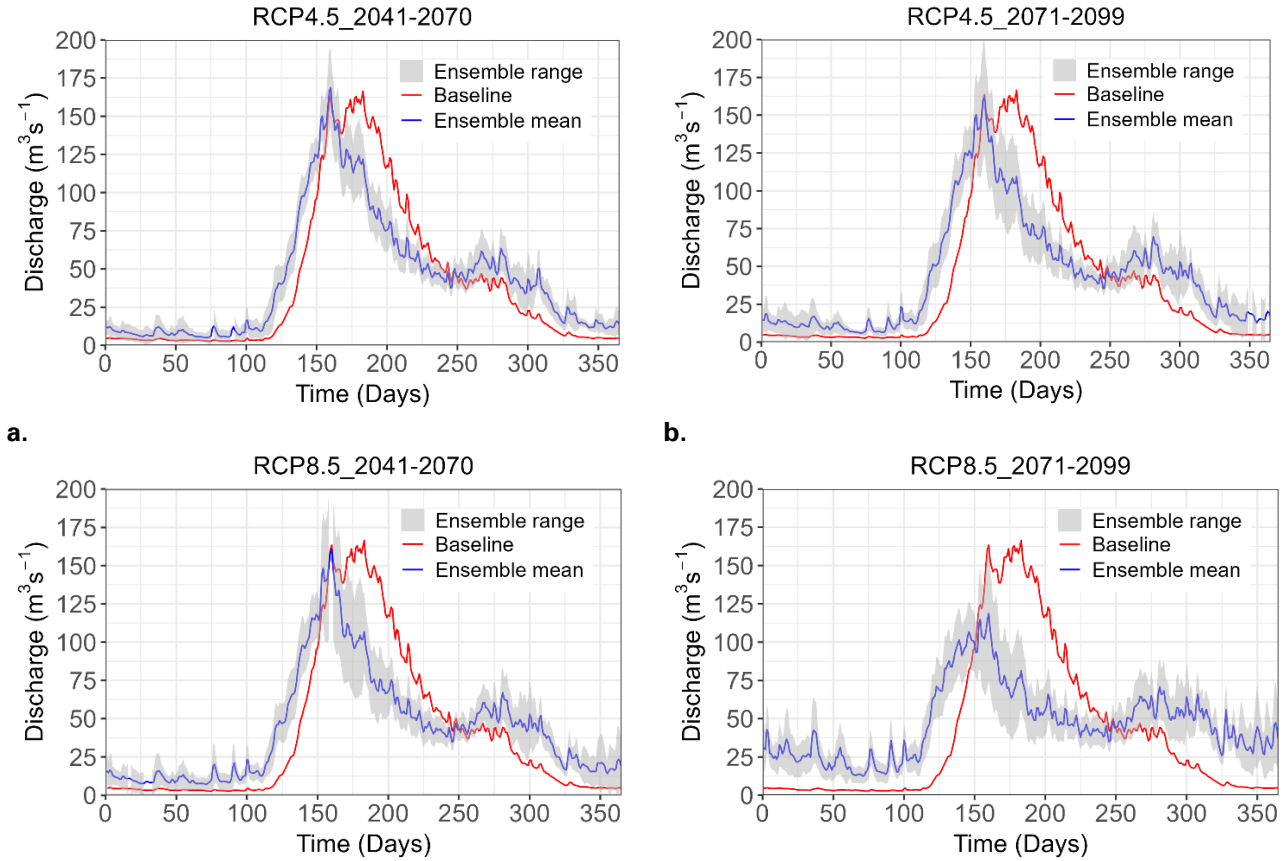

Figure 5.15 Mean daily runoff for the baseline and future scenarios for Lærdal catchment. **a**. RCP4.5_2041-2070 **b**. RCP4.5_2071-2099 **c**. RCP8.5_2041-2070 **d**. RCP8.5_2071-2099.

Table 5.20 Summary of flood peaks based on mean daily flow from Lærdal Catchment for the baseline and ensemble mean of scenarios.

	Peak flow (m^3/s)				
Season	Baseline	RCP4.5_2041-2070	RCP4.5_2071-2099	RCP8.5_2041-2070	RCP8.5_2071-2099
Spring/Summer	166.42	168.75	162.07	160.57	118.68
Autumn/Winter	49.97	63.44	69.61	66.99	70.71

5.3.7 Effects of climate change on the seasonal runoff of Lærdal catchment.

The variability of the ensemble mean monthly runoff of future scenarios, vis-à-vis baseline scenario from Lærdal catchment is shown in Figure 5.16 while the average seasonal variations of future runoff for RCP4.5 and RCP8.5 scenarios in relation to the baseline runoff is shown in Table 5.21. The results revealed that RCP8.5_2071-2099 scenario yielded the highest magnitude of runoff for 9 months (September – May). Also, the baseline scenario comparatively yielded the highest magnitude of runoff for 3 months (June – August) with the peak runoff occurring in June (Figure 5.16). On the contrary, the baseline scenario yields the lowest magnitude of runoff for 9 months (September – May).

The seasonal variability of future runoff vis-à-vis the baseline scenario were determined. Runoff is projected to increase for all the scenarios in the autumn, winter, and spring. The runoff is projected to decrease for all the scenarios in the summer. A maximum increase in average seasonal variation in runoff of 597.37% occurred in winter for RCP8.5_2071-2099 scenario while a minimum increase in average seasonal variation in runoff of 71.13% occurred in autumn for RCP4.5_2041-2070 (Table 5.21). A maximum decrease in average seasonal variation in runoff of 42.90% occurred in summer for RCP8.5_2071-2099 scenario (Table 5.21). It is noteworthy to state the large increases in winter are on comparatively small magnitude of flow.

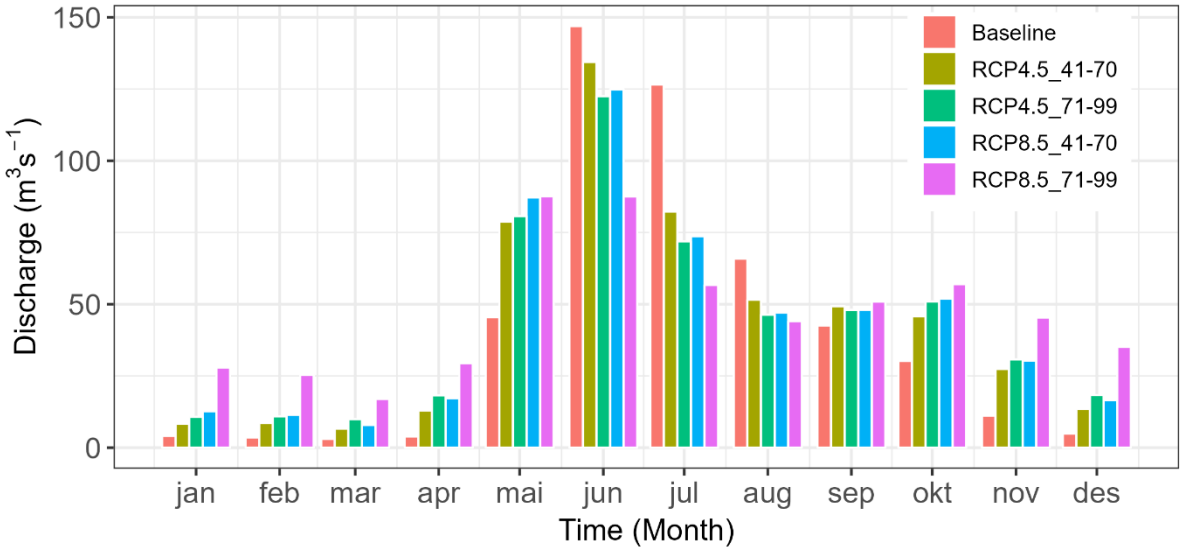

Figure 5.16 Ensemble Mean monthly runoff of future scenarios versus baseline mean monthly runoff from Lærdal catchment.

Table 5.21 Average seasonal variations of future runoff, in Lærdal catchment, for RCP4.5 and RCP8.5 scenarios in relation to the baseline runoff.

	Baseline	Average Seasonal variation (%)			
Season	average flow (m^3/s)	RCP4.5_2041-2070	RCP4.5_2071-2099	RCP8.5_2041-2070	RCP8.5_2071-2099
Winter	4.23	138.35	220.00	211.38	597.37
Spring	17.50	141.19	197.75	223.31	400.40
Summer	113.17	-21.74	-28.43	-29.82	-42.90
Autumn	28.00	71.13	85.50	85.76	138.25

5.3.8 Effect of climate change on mean annual runoff of Lærdal catchment.

The mean annual runoff was computed for the different scenarios of the various climate models (Table 5.22) as well as the baseline scenario. The baseline scenario yielded a mean annual runoff of 40.89 m^3/s. The mean annual runoff varied for different models and scenarios. A maximum mean annual runoff of 51.07 m^3/s was predicted by CNRM_RCA for RCP8.5_2071-2099 scenario while a minimum mean annual runoff of 37.96 m^3/s was predicted by ECEARTH_RACMO for RCP8.5_2041-2070 (Table 5.22). The ensemble mean was computed for different scenarios based on the mean annual runoff. The ensemble mean annual runoff, computed from the ten climate models, corresponding to RCP4.5_2041-2070, RCP4.5_2071-2099, RCP8.5_2041-2070, and RCP8.5_2071-2099 were 43.46 m^3/s, 44.24 m^3/s, 43.42 m^3/s, and 47.12 m^3/s, respectively. The

results revealed that runoff will increase in the future, especially for the end of century time horizon for RCP8.5 scenario.

Table 5.22 Mean annual runoff of future scenarios for Lærdal catchment.

	Mean annual runoff			
Climate model	RCP4.5_2041-2070	RCP4.5_2071-2099	RCP8.5_2041-2070	RCP8.5_2071-2099
CNRM_CCLM	45.17	45.48	45.73	46.85
CNRM_RCA	45.18	45.90	45.86	51.07
ECEARTH_CCLM	40.51	41.32	39.38	43.12
ECEARTH_HIRHAM	47.14	46.86	45.28	47.98
ECEARTH_RACMO	41.57	40.41	37.96	40.72
ECEARTH_RCA	42.16	43.21	42.56	48.66
HADGEM_RCA	47.64	45.29	46.04	49.75
IPSL_RCA	43.85	44.83	44.61	49.10
MPI_CCLM	40.21	42.62	42.22	45.03
MPI_RCA	41.13	46.45	44.54	48.91

5.4 Low flow and flood analyses of the future hydrologic regime of Forra and Lærdalselva

The variations in the characteristics of Forra and Lærdalselva were evaluated considering future low flow for the entire period, winter low flow, summer low flow, flood conditions, as well as trends in the occurrence of the annual minimum flow.

5.4.1 Future low flow (7Q10) and annual minimum runoff trend for the entire period for Forra catchment.

The distribution of the annual minimum series of runoff (Figure 5.17a) was computed for the baseline scenario (considering 1972 - 1999 data) while low flow frequency analysis of non-exceedance probability was fitted using the Log Pearson type III distribution (Figure 5.17b). Low flow was computed using the 7Q10 method. Table 5.23 depicts the low flow for various scenarios for Forra catchment. Figure 5.17a revealed that most of the minimum annual runoff occur within the first 96 days of the year and the after the 175th day of the year. No low flow was observed between the 96th day to 175th day due to spring floods, occasioned by snowmelt (Figure 5.17a). The baseline scenario yielded a low flow of 0.598 m^3/s. The low flow varied for different models and scenarios. A maximum low flow of 0.800 m^3/s was predicted by MPI_CCLM for RCP4.5_2071-

2099 scenario while a minimum low flow of 0.285 m^3/s was predicted by ECEARTH_HIRHAM for RCP8.5_2071-2099 (Table 5.23). Except for RCP4.5_2041-2070 scenario, the ensemble low flow will decrease in the future for the other scenarios and time horizons. The plots of the fitting of the non-exceedance probability of the low flows for all the ensembles mean runoff for scenarios RCP4.5 and RCP8.5 are shown in Appendix 4 (Figure S.4).

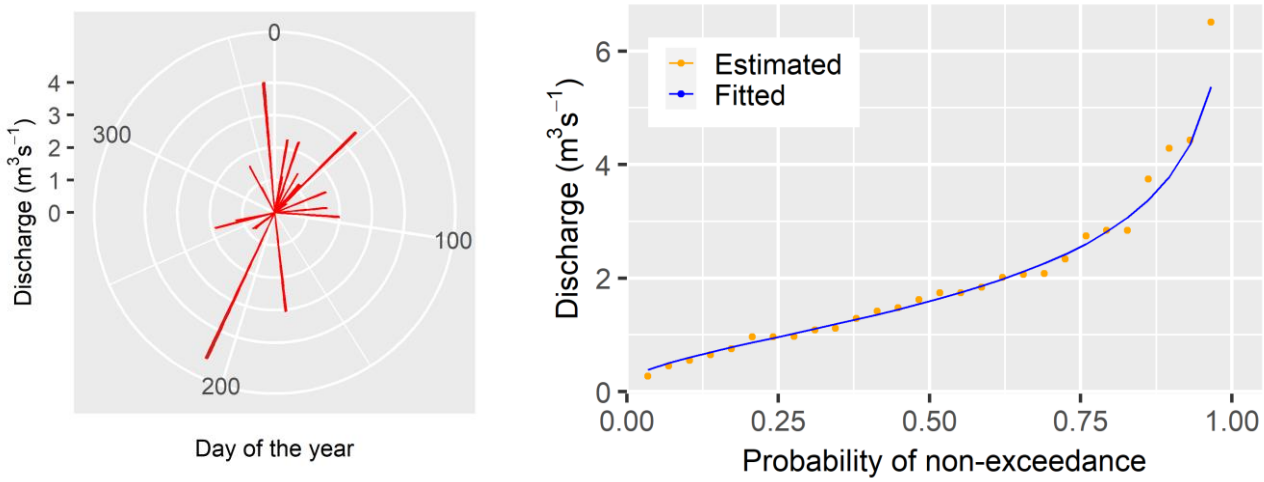

a. **b.**

Figure 5.17 Baseline scenario for Forra catchment **a.** annual minimum series (AMS) of runoff **b.** Fitting of AMS obtained from 7-day averages.

Figure 5.18 shows the future trend in the day of occurrence of annual minimum flow for RCP4.5 and RCP8.5 scenarios. For the RCP4.5_2041 – 2070 and RCP4.5_2071 – 2099 scenarios, no low flow occurred between the 97th day - 171st day and 97th day - 163rd day, respectively (Figure 5.18a and Figure 5.18b).

Table 5.23 Low flow for various scenarios for Forra catchment.

	Minimum flow (7Q10) in m^3/s			
Climate model	RCP4.5_2041-2070	RCP4.5_2071-2099	RCP8.5_2041-2070	RCP8.5_2071-2099
CNRM_CCLM	0.666	0.518	0.618	0.455
CNRM_RCA	0.714	0.592	0.569	0.658
ECEARTH_CCLM	0.690	0.647	0.638	0.683
ECEARTH_HIRHAM	0.616	0.513	0.411	0.285
ECEARTH_RACMO	0.667	0.459	0.590	0.501
ECEARTH_RCA	0.605	0.631	0.623	0.555
HADGEM_RCA	0.443	0.496	0.372	0.384
IPSL_RCA	0.610	0.552	0.506	0.605
MPI_CCLM	0.670	0.800	0.760	0.733
MPI_RCA	0.608	0.656	0.582	0.614

For the RCP8.5_2041 – 2070 and RCP8.5_2071 – 2099 scenarios, no low flow occurred between the 97th day - 163rd day and 62nd day - 114th, respectively (Figure 5.18c and Figure 5.18d).

A comparison of the historical and the future periods revealed that there would be frequent occurrence of annual minimum flow during the spring and summer. The increase in frequency of occurrence of minimum annual flow was significant for the end of century period (2071 – 2099) than the mid-century period (2041 – 2070), especially for RCP8.5_2071 – 2099 scenario. The range of an annual minimum flow corresponding to the baseline, RCP4.5_2041 – 2070, RCP4.5_2071 – 2099, RCP8.5_2041 – 2070, RCP8.5_2071 – 2099 are 0.24 – 4.95 m^3/s, 0.20 – 6.84 m^3/s, 0.00 – 6.04 m^3/s, 0.00 – 6.06 m^3/s, and 0.00 – 6.15 m^3/s, respectively. The results revealed that the range of the annual minimum runoff will increase in the future. This is indicative of increase in the future uncertainty of the minimum annual runoff.

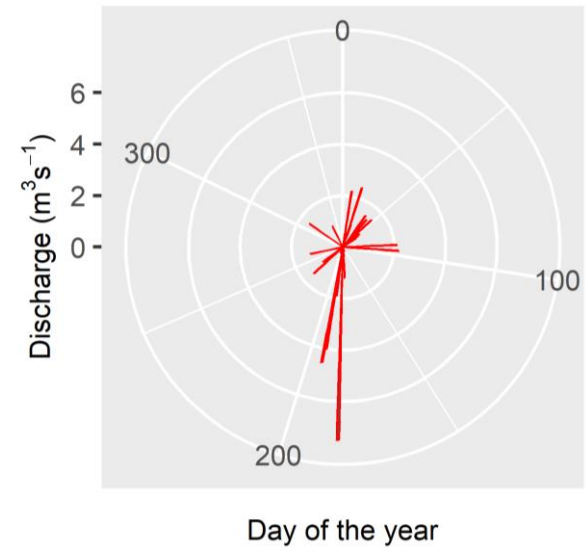

a.

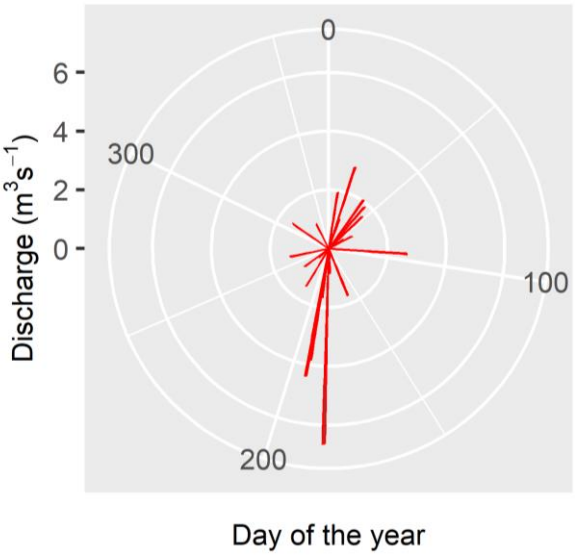

b.

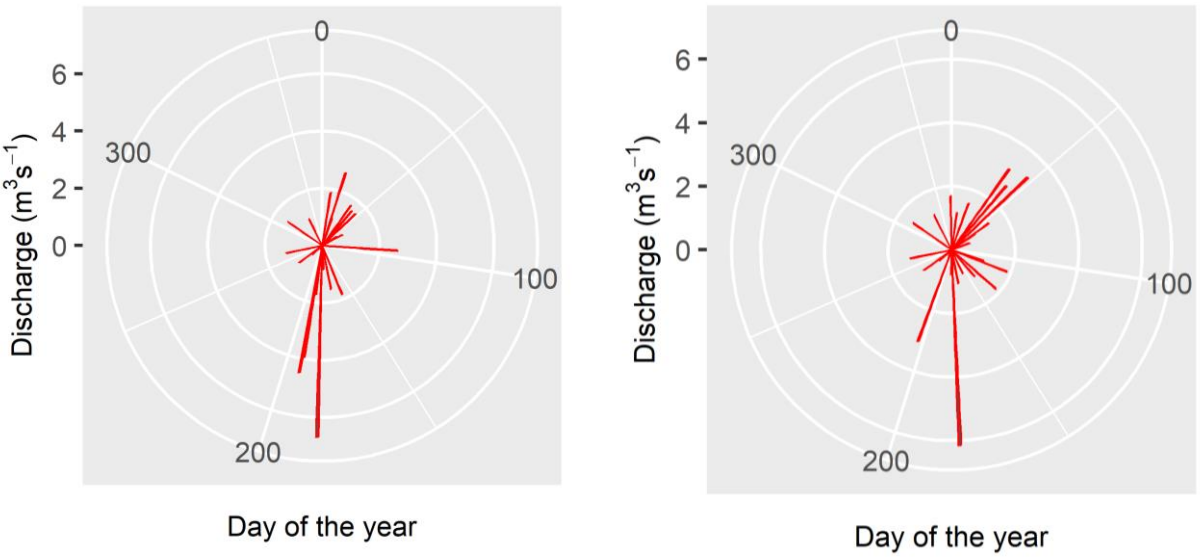

c. d.

Figure 5.18 Distribution of annual minimum series of runoff for Forra catchment **a**. RCP4.5_2041-2070 **b**. RCP4.5_2071-2099 **c**. RCP8.5_2041-2070 **d**. RCP8.5_2071-2099.

5.4.2 Future low flow and annual minimum runoff trend for the entire period for Lærdal catchment

The distribution of the annual minimum series of runoff (Figure 5.19a) was computed for the baseline scenario (considering 1972 - 1999 data) while low flow frequency analysis of non-exceedance probability was fitted using the Log Pearson type III distribution (Figure 5.19b). Table 5.24 depicts the minimum flow for various scenarios for Lærdal catchment. For the baseline scenarios, no low flow occurred between the 123rd day – 340th day (Figure 5.19a). The baseline scenario yielded a low flow of 0.251 m^3/s. The low flow varied for different models and scenarios. A maximum low flow of 0.614 m^3/s was predicted by CNRM_RCA for RCP8.5_2071-2099 scenario while a minimum low flow of 0.249 m^3/s was predicted by MPI_CCLM for RCP4.5_2041-2070 (Table 5.24). The ensemble low flow will increase in the future for all other scenarios and time horizons. The plots of the fitting of the non-exceedance probability of the low flows for all the ensembles mean runoff for scenarios RCP4.5 and RCP8.5 are shown in Appendix 4 (Figure S.5).

Figure 5.20 shows the future trend in the day of occurrence of annual minimum flow for RCP4.5 and RCP8.5. For the RCP4.5_2041 – 2070 and RCP4.5_2071 – 2099

scenarios, no low flow occurred between the 113th day – 340th day and 111th day – 310th, respectively (Figure 5.20a and Figure 5.20b).

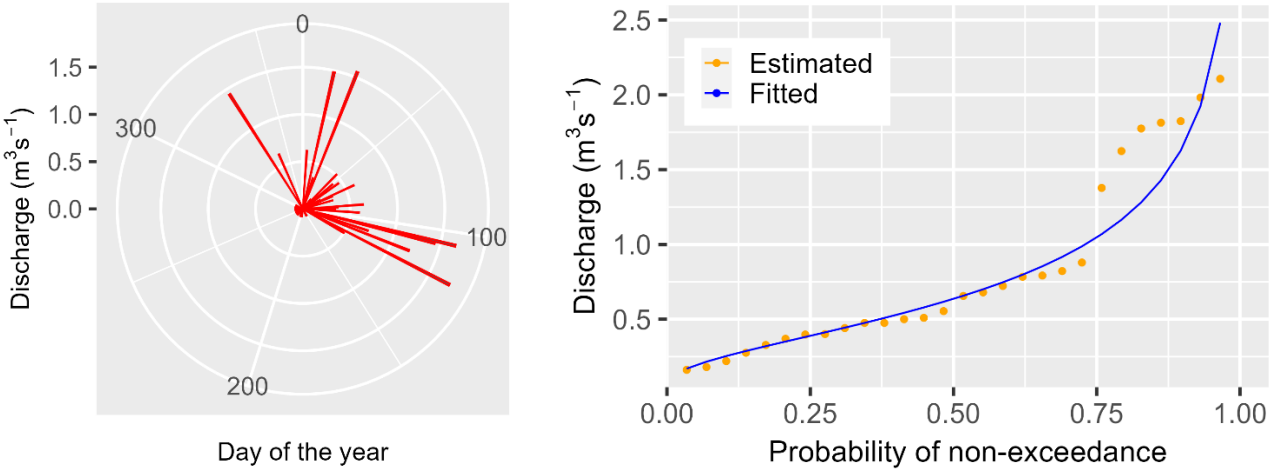

a. **b.**

Figure 5.19 Baseline scenario for Lærdal catchment **a.** annual minimum runoff **b.** Fitting of AMS obtained from 7-day averages.

For the RCP8.5_2041 – 2070 and RCP8.5_2071 – 2099 scenarios, no low flow occurred between the 95th day – 310th day and 110th day – 222nd day, respectively (Figure 5.20c and Figure 5.20d). A comparison of the historical and the future periods revealed that the erstwhile occurrence of low flow in winter up to spring would likely change in the future for RCP8.5_2071-2099 scenario. For the RCP8.5_2071-2099 scenario, low flow is likely to occur in Autumn up to spring. No remarkable change was observed in the range of day of occurrence of low flow for RCP4.5_2041-2070, vis-à-vis the baseline scenario.

Table 5.24 Low flow for various scenarios for Lærdal catchment.

	Low flow (7Q10) in m³/s			
Climate model	RCP4.5_41_70	RCP4.5_71_99	RCP8.5_41_70	RCP8.5_71_99
CNRM_CCLM	0.345	0.434	0.359	0.594
CNRM_RCA	0.352	0.392	0.376	0.614
ECEARTH_CCLM	0.309	0.323	0.321	0.466
ECEARTH_HIRHAM	0.328	0.291	0.336	0.386
ECEARTH_RACMO	0.255	0.356	0.252	0.343
ECEARTH_RCA	0.308	0.306	0.354	0.519
HADGEM_RCA	0.371	0.299	0.310	0.399
IPSL_RCA	0.334	0.381	0.391	0.578
MPI_CCLM	0.249	0.315	0.266	0.399
MPI_RCA	0.258	0.330	0.278	0.380

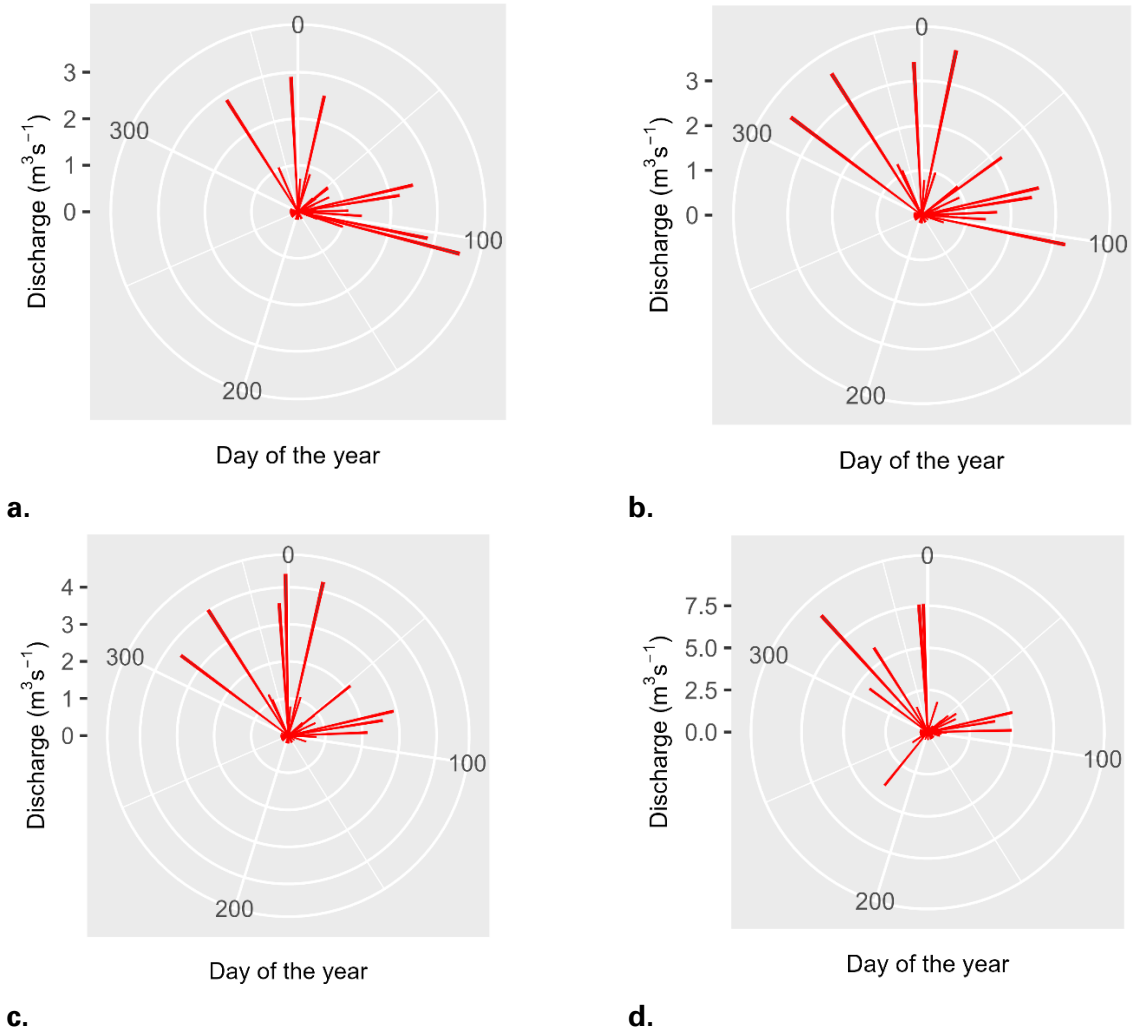

Figure 5.20 Distribution of minimum annual runoff for Lærdal catchment. **a**. RCP4.5_2041-2070 **b**. RCP4.5_2071-2099 **c**. RCP8.5_2041-2070 **d**. RCP8.5_2071-2099.

The range of an annual minimum flow (between 1972 – 1999) corresponding to the baseline, RCP4.5_2041 – 2070, RCP4.5_2071 – 2099, RCP8.5_2041 – 2070, RCP8.5_2071 – 2099 are 0.13 – 1.74 m^3/s, 0.16 – 3.58 m^3/s, 0.16 – 3.75 m^3/s, 0.15 – 4.34 m^3/s, and 0.22 – 9.33 m^3/s, respectively. The results revealed that the range of the annual minimum runoff will increase in the future. This is indicative of increase in the future uncertainty of the minimum annual runoff.

A designer interested in practicality and applicability of climate change impacts on runoff, climate change factors were computed using the average of the ensemble mean of various scenarios. Climate change factors, for Forra

catchment, corresponding to RCP4.5_2041-2070, RCP4.5_2071-2099, RCP8.5_2041-2070, RCP8.5_2071-2099 were 1.04, 1.04, 1.03 and 1.10. A minimum climate change factor of 0.94 was obtained for ECEARTH_RACMO for RCP4.5_71-99 while a maximum climate change factor of 1.19 was obtained for MPI_CCLM for RCP8.5_71-99 for Forra catchment. Climate change factors, for Lærdal catchment, corresponding to RCP4.5_2041-2070, RCP4.5_2071-2099, RCP8.5_2041-2070, RCP8.5_2071-2099 were 1.06, 1.08, 1.06 and 1.15. A minimum climate change factor of 0.93 was obtained for ECEARTH_RACMO for RCP8.5_41-70 while a maximum climate change factor of 1.25 was obtained for CNRM_RCA for RCP8.5_71-99 for Lærdal catchment.

5.4.3 Winter low flow, summer low flow, flood conditions

The winter low flow, summer low flow and flood conditions were computed, for Forra and Lærdal catchments, and presented in Tables 5.25 – 5.29. The results, for Forra and Lærdal catchmnents, revealed that the ensemble mean of winter low flow increased with time horizon of projections. On the contrary, the ensemble mean of summer low flow decreased with time horizon of projections. The ensemble mean winter low flow from Forra catchment, corresponding to RCP4.5_2041-2070, RCP4.5_2071-2099, RCP8.5_2041-2070, and RCP8.5_2071-2099 are 0.915 m^3/s, 1.083 m^3/s, 1.017 m^3/s and 1.515 m^3/s, respectively (Table 5.25), while the winter low flow of the baseline scenario yielded a value of 0.642 m^3/s. The ensemble mean summer low flow from Forra catchment, corresponding to RCP4.5_2041-2070, RCP4.5_2071-2099, RCP8.5_2041-2070, and RCP8.5_2071-2099 are 1.134 m^3/s, 0.892 m^3/s, 0.888 m^3/s and 0.757 m^3/s, respectively (Table 5.26), while the summer low flow of the baseline scenario yielded a value of 1.885 m^3/s. A maximum winter low flow of 1.771 m^3/s was predicted by HADGEM_RCA for RCP8.5_2071-2099 scenario while a minimum winter low flow of 0.707 m^3/s was predicted by MPI_RCA for RCP4.5_2041-2070 (Table 5.25). Also, a maximum summer low flow of 1.688 m^3/s was predicted by MPI_CCLM for RCP4.5_2041-2070 scenario while a minimum summer flow of 0.371 m^3/s was predicted by ECEARTH_HIRHAM for RCP8.5_2071-2099 scenario (Table 5.26). The ensemble winter low flow will increase while the ensemble

summer low flow will decrease in the future for all the scenarios and time horizons for Forra catchment.

The ensemble mean winter low flow from Lærdal catchment, corresponding to RCP4.5_2041-2070, RCP4.5_2071-2099, RCP8.5_2041-2070, and RCP8.5_2071-2099 are 0.378 m^3/s, 0.426 m^3/s, 0.389 m^3/s and 0.629 m^3/s, respectively (Table 5.27), while the winter low flow of the baseline scenario yielded a value of 0.299 m^3/s. The ensemble mean summer low flow from Lærdal catchment, corresponding to RCP4.5_2041-2070, RCP4.5_2071-2099, RCP8.5_2041-2070, and RCP8.5_2071-2099 are 10.634 m^3/s, 8.372 m^3/s, 7.814 m^3/s and 4.084 m^3/s, respectively (Table 5.28), while the summer low flow of the baseline scenario yielded a value of 19.759 m^3/s. A maximum winter low flow of 0.766 m^3/s was predicted by IPSL_RCA for RCP8.5_2071-2099 scenario while a minimum winter low flow of 0.306 m^3/s was predicted by MPI_CCLM for RCP4.5_71-99 (Table 5.27). Also, a maximum summer low flow of 12.950 m^3/s was predicted by CNRM_RCA for RCP4.5_2041-2070 scenario while a minimum summer flow of 2.399 m^3/s was predicted by HADGEM_RCA for RCP8.5_2071-2099 scenario (Table 5.28). The ensemble winter low flow will increase while the ensemble summer low flow will decrease in the future for all the scenarios and time horizons for Lærdal catchment. Comparatively, the change in winter and summer low flows of both catchments would be most significant for RCP8.5_2071-2099, vis-à-vis the other scenarios.

Table 5.25 Winter low flow for Forra

	Low flow (7Q10) in m^3/s			
Climate model	RCP4.5_2041-2070	RCP4.5_2071-2099	RCP8.5_2041-2070	RCP8.5_2071-2099
CNRM_CCLM	0.911	1.165	1.022	1.699
CNRM_RCA	0.858	1.052	0.995	1.576
ECEARTH_CCLM	1.007	1.145	1.154	1.668
ECEARTH_HIRHAM	0.875	0.776	0.876	1.134
ECEARTH_RACMO	0.890	1.105	0.912	1.190
ECEARTH_RCA	0.959	1.139	1.092	1.605
HADGEM_RCA	1.122	1.141	1.128	1.771
IPSL_RCA	1.087	1.151	1.199	1.632
MPI_CCLM	0.744	1.126	0.976	1.489
MPI_RCA	0.707	1.026	0.811	1.386

Table 5.26 Summer low flow for Forra

	Low flow (7Q10) in m^3/s			
Climate model	RCP4.5_2041-2070	RCP4.5_2071-2099	RCP8.5_2041-2070	RCP8.5_2071-2099
CNRM_CCLM	1.073	0.677	0.910	0.526
CNRM_RCA	1.331	0.878	0.834	0.860
ECEARTH_CCLM	0.993	0.888	0.877	0.954
ECEARTH_HIRHAM	1.002	0.872	0.638	0.371
ECEARTH_RACMO	1.233	0.586	0.962	0.647
ECEARTH_RCA	0.960	1.000	0.967	0.915
HADGEM_RCA	0.652	0.689	0.497	0.529
IPSL_RCA	1.076	0.913	0.812	0.913
MPI_CCLM	1.688	1.332	1.320	1.004
MPI_RCA	1.334	1.081	1.061	0.848

Table 5.27 Winter low flow for Lærdal

	Low flow (7Q10) in m^3/s			
Climate model	RCP4.5_2041-2070	RCP4.5_2071-2099	RCP8.5_2041-2070	RCP8.5_2071-2099
CNRM_CCLM	0.403	0.532	0.411	0.764
CNRM_RCA	0.414	0.467	0.427	0.748
ECEARTH_CCLM	0.383	0.393	0.399	0.718
ECEARTH_HIRHAM	0.387	0.329	0.398	0.485
ECEARTH_RACMO	0.315	0.466	0.316	0.424
ECEARTH_RCA	0.375	0.374	0.416	0.652
HADGEM_RCA	0.452	0.373	0.392	0.664
IPSL_RCA	0.428	0.499	0.499	0.766
MPI_CCLM	0.306	0.402	0.307	0.553
MPI_RCA	0.315	0.421	0.330	0.519

Table 5.28 Summer low flow for Lærdal

	Low flow (7Q10) in m3/s			
Climate model	RCP4.5_2041-2070	RCP4.5_2071-2099	RCP8.5_2041-2070	RCP8.5_2071-2099
CNRM_CCLM	12.149	10.367	10.344	5.052
CNRM_RCA	12.950	12.043	12.673	6.124
ECEARTH_CCLM	7.790	6.151	5.139	2.462
ECEARTH_HIRHAM	12.654	10.042	8.229	4.457
ECEARTH_RACMO	11.462	6.612	7.009	3.531
ECEARTH_RCA	10.399	7.748	5.985	3.547
HADGEM_RCA	8.548	3.881	4.480	2.399
IPSL_RCA	10.202	6.444	8.296	4.013
MPI_CCLM	10.934	10.039	8.249	5.033
MPI_RCA	9.253	10.393	7.738	4.219

The 200-year and 1000-year flood from Forra and Lærdal catchments were computed using the generalized extreme value (GEV). Comparatively, the future design flood of Forra catchment will decrease between the baseline and projected period for the various scenarios under review (Table 5.29). Similarly, the future design flood of Lærdal catchment will decrease between the baseline and projected period, for RCP4.5_41-70, RCP4.5_71-99, RCP8.5_41-70 scenarios. However, RCP8.5_71-99 yields higher design floods than the baseline 200- and 1000- year design floods. The deign floods of both catchments are likely to increase between the 2041 – 2070 and 2071 – 2099 time horizons for RCP4.5 and RCP8.5 scenarios (Table 5.29 and Appendix 5). It is noteworthy to state that the baseline under review is the modelled outcome of the observational gridded data.

Table 5.29 200- and 1000- year return period design flood

	Forral catchment		Lærdal catchment	
Climate model	Q200 (%)	Q1000 (%)	Q200 (%)	Q1000 (%)
RCP4.5_2041-70	-40.59	-54.80	-22.19	-29.36
RCP4.5_2071-99	-39.78	-53.92	-18.99	-25.39
RCP8.5_2041-70	-39.88	-53.80	-21.60	-28.85
RCP8.5_2071-99	-24.03	-37.46	17.29	18.09

5.5 Effect of climate change on the environment

A prognosis of the drought was carried out for various projections vis-à-vis the baseline scenario, for Lærdal catchment. Table 5.30 shows the summary of the water covered area (WCA) of the Lærdelselva reach for the baseline and projections while Figure 5.21shows the HEC-RAS simulation of winter low flow for the baseline scenario at maximum inundation boundary. Table 5.30 shows that the WCA of Lærdalselva will increase with increase in the future ensemble winter low flow for all the scenarios and time horizons. The increase in winter low flow is not significant compared to the average flow in the river. This portends grave consequences on the flora and fauna within the river and adjoining ecosystem. Measures to mitigate the adverse effects of drought in Lærdalselva should be implemented. The implementation of an enhanced minimum flow regime resulted to an increase in species richness (Travnichek et

al., 1995). Increase in flow velocity, achieved through increase in minimum flow, relatively resulted to an abundance of species preferring fast-flowing and/or deep microhabitats (Lamouroux et al., 2006).The HEC-RAS simulation of winter low flow for the future scenarios, at maximum depth, are shown in Appendix 6.

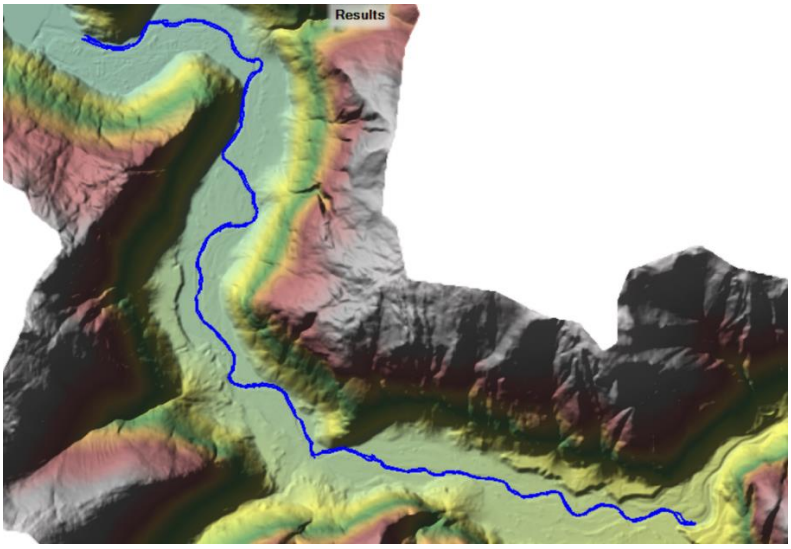

Figure 5.21 HEC-RAS simulation of winter low flow for the baseline scenario, at maximum inundation boundary, for Lærdal catchment

Table 5.30 Water covered areas of the Lærdelselva reach for the baseline and projections.

	Lærdal catchment	
Scenario	Flow (m^3/s)	WCA (Km^2)
Baseline	0.299	0.321
RCP4.5_2041-70	0.378	0.340
RCP4.5_2071-99	0.426	0.346
RCP8.5_2041-70	0.389	0.341
RCP8.5_2071-99	0.629	0.364

5.6 Effect of future climate scenarios on hydropower production of Stjørdal hydropower system

A prognosis of the current operational strategy on power production as well as spill of various scenarios was carried considering flow at Hoggås Bru as input. The storage and power production at Funna powerplant was evaluated. The results revealed that a significant decrease in storage is likely occur in the future, especially between day 120 to day 365 (Figure 5.22). On the contrary, a marginal increase in storage is likely to occur between day 1 to day 120 (Figure 5.22). The

mean annual reservoir volume corresponding to the baseline, RCP4.5_2041-2070, RCP4.5_2071-2099, RCP8.5_2041-2070, RCP8.5_2071-2099 scenarios are 12,105.20 Mm^3/yr, 10,580.79 Mm^3/yr, 10,422.04 Mm^3/yr, 10,282.36 Mm^3/yr and 10,076.30 Mm^3/yr, respectively (Figures 5.22). In general, a significant decrease in the reservoir volume occurs due to the variability in future flows (Figure 5.11) and the corresponding inability of the current operational strategy to maximize the future flows. The operational strategy, which was designed to maximize the incoming snowmelt spring flood, becomes inappropriate due to the drastic decrease in future snowmelt spring flood.

The increase in winter flows will likely result to higher energy production during the winter. Comparatively, there is a high possibility of decreased production of energy due to the significant decrease in storage after day 120 (Figure 5.23). The average annual energy production of Funna powerplant corresponding to the baseline, RCP4.5_2041-2070, RCP4.5_2071-2099, RCP8.5_2041-2070, RCP8.5_2071-2099 scenarios are 63.51 GWh/yr, 63.497 GWh/yr, 63.50 GWh/yr, 63.50 GWh/yr and 63.55 GWh/yr, respectively (Figure 5.23). The hydropower simulations show a marginal decrease in the future energy generation of 0.01–0.02% under the current reservoir operational strategies, for scenarios RCP4.5_2041-2070, RCP4.5_2071-2099 and RCP8.5_2041-2070. RCP8.5_2071-2099 yielded a marginal increase in hydropower generation of 0.06%. Increase in annual inflow resulted to an increase in energy generation for the current reservoir operational strategy (Chernet et al., 2013). The predictions of the various climate models in comparison to the ensemble mean revealed that there is low uncertainty in the future reservoir filling as well as the power production (Figures 5.22 and 5.23).

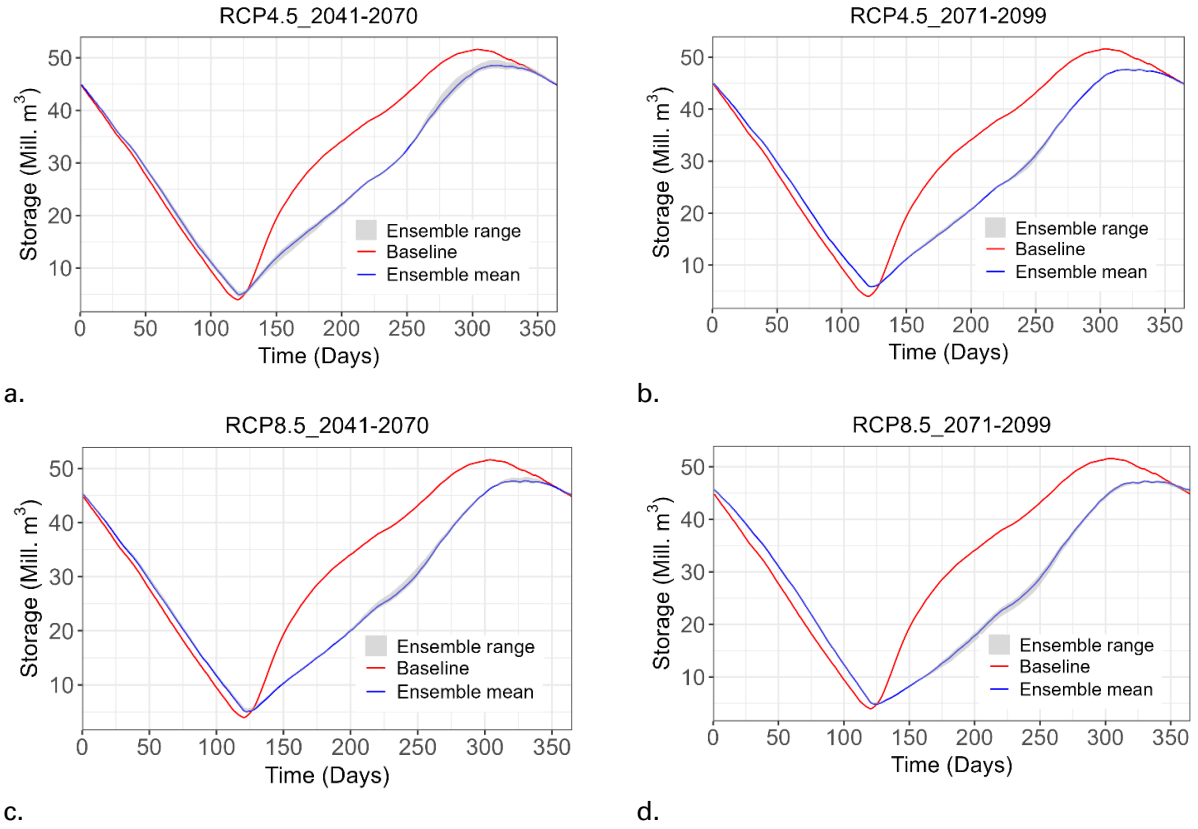

Figure 5.22 Mean daily reservoir volume of Funna powerplant using current operational strategy **a**. RCP4.5_2041-2070 **b**. RCP4.5_2071-2099 **c**. RCP8.5_2041-2070 **d**. RCP8.5_2071-2099.

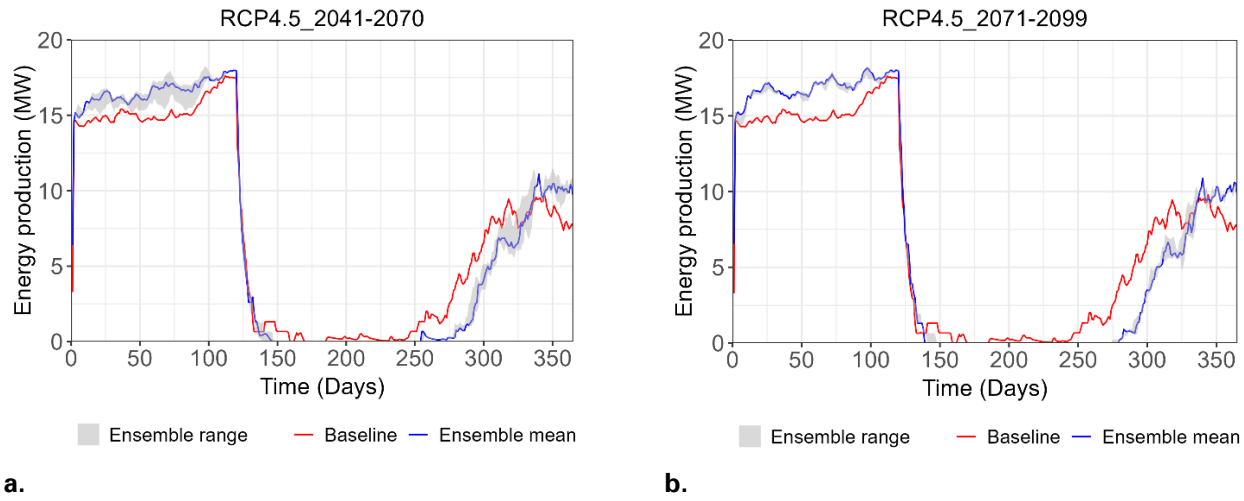

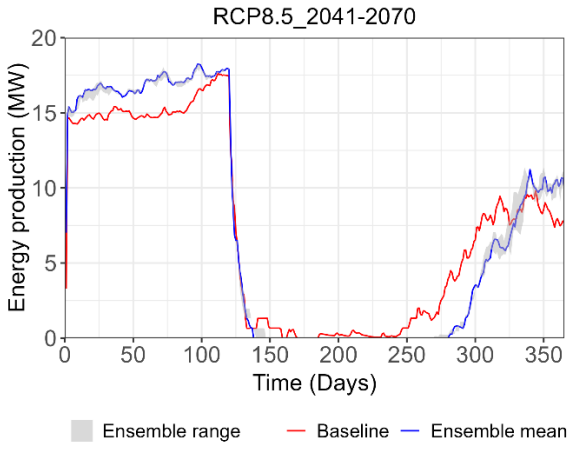

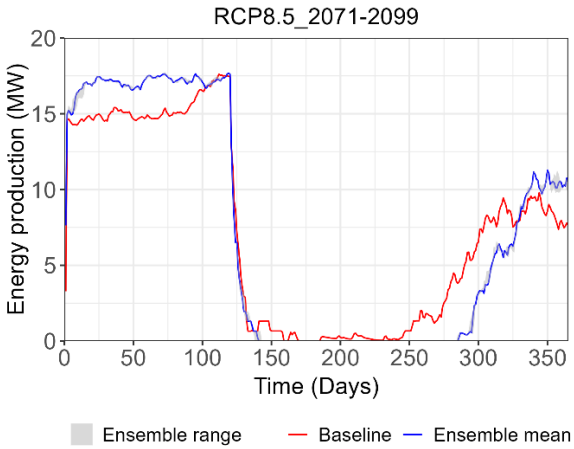

c. **d.**

Figure 5.23 Mean daily energy production of Funna powerplant using current operational strategy **a**. RCP4.5_2041-2070 **b**. RCP4.5_2071-2099 **c**. RCP8.5_2041-2070 **d**. RCP8.5_2071-2099.

The modification of the operational strategy was carried out considering two scenarios:

Scenario 1 - Changes in the timing and magnitude of filling.

Scenario 2 - Adjustment of the magnitude of filling only.

Changes in the timing and magnitude of filling (Figure 5.24a) as well as the modification of the magnitude of filling (Figure 5.24b) were proposed with a view to improving the reliability of energy production at Funna powerplant. It is noteworthy to state that both modified operational strategies were developed based on the inflow of RCP4.5_2041-2070 scenario.

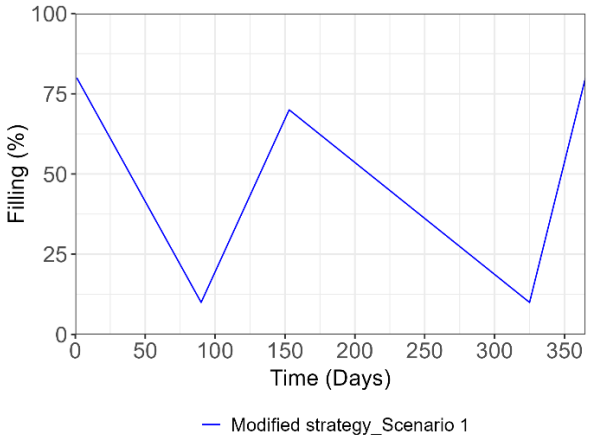

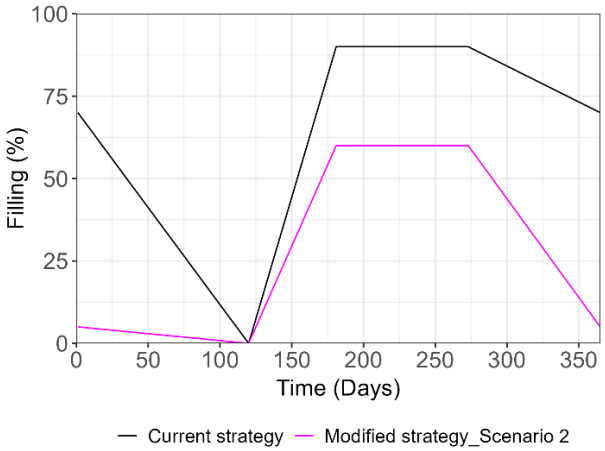

a. b.

Figure 5.24 Modified operational strategies **a**. scenario 1 **b**. scenario 2 and

current strategy.

For the first operational strategy (Scenario 1), the mean annual energy production corresponding to the baseline, RCP4.5_2041-2070, RCP4.5_2071-2099, RCP8.5_2041-2070, RCP8.5_2071-2099 scenarios are 63.51 GWh/yr, 64.01 GWh/yr, 63.99 GWh/yr, 63.97 GWh/yr and 63.96 GWh/yr, respectively. Also, the mean annual reservoir volume corresponding to the baseline, RCP4.5_2041-2070, RCP4.5_2071-2099, RCP8.5_2041-2070, RCP8.5_2071-2099 scenarios are 12,105.20 Mm^3/yr, 5,441.82 Mm^3/yr, 7,547.31 Mm^3/yr, 7,529.39 Mm^3/yr and 7,431.20 Mm^3/yr, respectively.

For the second operational strategy (Scenario 2), the mean annual energy production corresponding to the baseline, RCP4.5_2041-2070, RCP4.5_2071-2099, RCP8.5_2041-2070, RCP8.5_2071-2099 scenarios are 63.51 GWh/yr, 64.01 GWh/yr, 63.98 GWh/yr, 63.96 GWh/yr and 63.95 GWh/yr, respectively. Also, the mean annual reservoir volume corresponding to the baseline, RCP4.5_2041-2070, RCP4.5_2071-2099, RCP8.5_2041-2070, RCP8.5_2071-2099 scenarios are 12,105.20 Mm^3/yr, 5,441.82 Mm^3/yr, 5,208.41 Mm^3/yr, 5,223.68 Mm^3/yr and 5,043.00 Mm^3/yr, respectively.

The use of the current and modified strategies for the simulation of future hydropower production resulted to decrease in storage (Figure 5.24). A prognosis of future hydropower generation, using several trial operational strategies with greater filling capacities, resulted to lower energy production compared to those from the modified strategies under review. Perhaps, this can be attributed to higher inflows, fairly distributed over the year in the future. Consequently, the direct utilization of a proportion of the inflow without recourse to storage (Figure 5.25).

The variability of the availability of future energy production is shown in Figure 5.26. The modified operational strategy (Scenario 1) results to energy production for fewer days in the winter compared to the present realities (Figure 5.26). On the other hand, scenario 2 results to decrease in energy production during the winter and vice versa during the autumn (Figure 5.26).

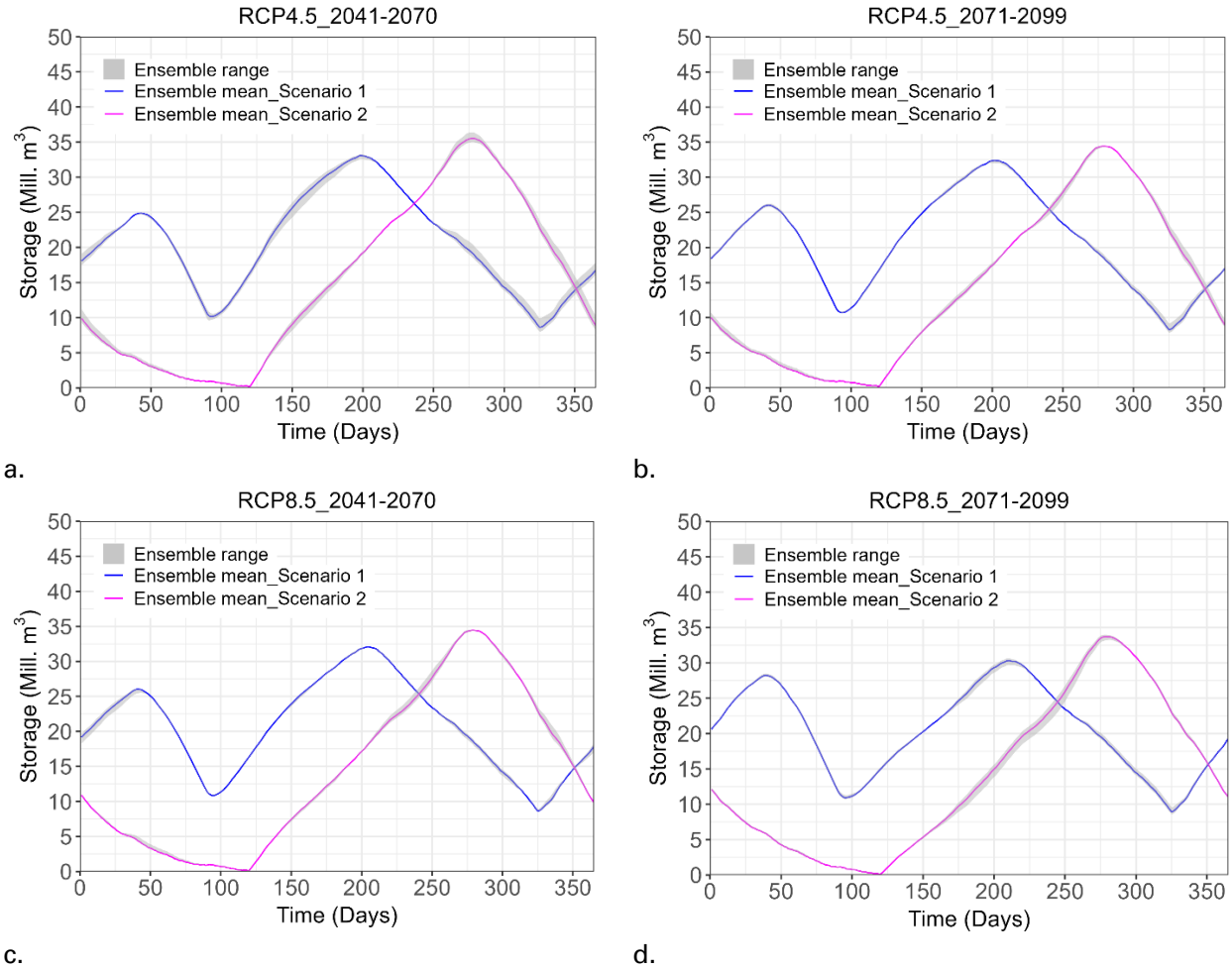

Figure 5.25 Mean daily reservoir volume of Funna hydropower system using modified operational strategies **a**. RCP4.5_2041 - 2070 **b**. RCP4.5_2071 – 2099 **c**. RCP8.5_2041 - 2070 **d**. RCP8.5_2071 – 2099.

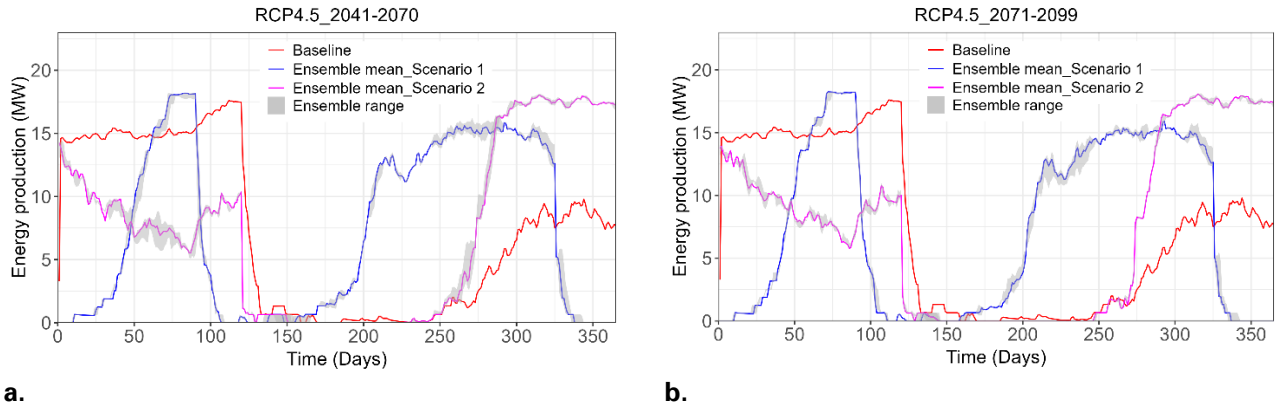

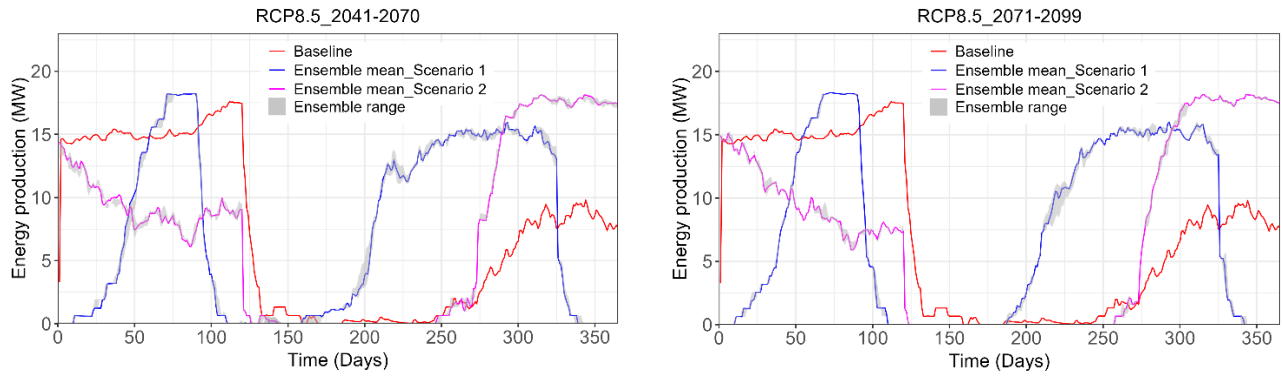

c. **d.**

Figure 5.26 Mean daily energy production of Funna hydropower system using modified operational strategies **a**. RCP4.5_2041 - 2070 **b**. RCP4.5_2071 – 2099 **c**. RCP8.5_2041 - 2070 **d**. RCP8.5_2071 – 2099.

The Stjørdal hydropower scheme, consisting of cascading hydropower systems was evaluated. The spill at Meråker was evaluated. The results corresponding to the observed flow, baseline and future scenarios are presented in Table 5.31. The average annual production based on observed data and baseline scenario, ranging for the period of 1972 to 1999, yielded an average annual production of 554.53 GWh/year and 554.94 GWh/year, respectively. The average annual productions for all future scenarios are lower than the baseline scenario (Table 5.31). The results revealed that the current operational strategy will not be adequate in the future. This assertion is based on the significant reduction in the future production irrespective of the comparable ensemble mean annual runoff (Table 5.19) of the future scenarios to the baseline and observed runoff, hence, the possibility of the unsuitability of the current operational strategy in the future.

The effect of the modified operational strategies on the power production of the Stjørdal hydropower system was evaluated. A prognosis of the future spill and energy generation vis-à-vis the historical period was carried out. On an average daily scale, the distribution of the spill, of the scenarios, vary over the year (Figure 5.27). The mean annual spill at Meråker, corresponding to the baseline current strategy was 70.29 Mm^3. The mean annual spill at Meråker for the ensemble mean current strategy (Figure 5.27), corresponding to RCP4.5_2041-2070, RCP4.5_2071-2099, RCP8.5_2041-2070, and RCP8.5_2071-2099 scenarios

are 79.99 Mm^3, 82.13 Mm^3, 83.19 Mm^3 and 90.78 Mm^3, respectively. Also, the mean annual spill at Meråker for the ensemble mean modified strategy (Scenario 1), corresponding to the RCP4.5_2041-2070, RCP4.5_2071-2099, RCP8.5_2041-2070, and RCP8.5_2071-2099 are 75.67 Mm^3, 77.96 Mm^3, 79.50 Mm^3 and 86.46 Mm^3, respectively. Also, the mean annual spill for Scenario 2 (Figure 5.27), corresponding to the RCP4.5_2041-2070, RCP4.5_2071-2099, RCP8.5_2041-2070, and RCP8.5_2071-2099 are 75.82 Mm^3, 77.85 Mm^3, 79.43 Mm^3 and 86.79 Mm^3, respectively. Therefore, the modification of the operational strategy resulted to the decrease in spill.

On average, the difference in average annual energy production between the baseline and projections considering current, modified (Scenario 1), modified (scenario 2) operational strategies were 4.97 GWh/yr, 0.06 GWh/yr, 1.51 GWh/yr, respectively, for RCP4.5_2041-2070. The modified operational strategy resulted to a marginal increase in future energy production for scenarios 1. Similarly, the difference in average annual energy production between the baseline and projections considering current, scenarios 1 and scenarios 2 for RCP4.5_2071-2099, RCP8.5_2041-2070 and RCP8.5_2071-2099 were 6.26 GWh/yr,1.53 GWh/yr and 2.94 GWh/yr, 6.92 GWh/yr, 2.52 GWh/yr and 3.91 GWh/yr, 12.20 GWh/yr, 7.63 GWh/yr and 9.05 GWh/yr, respectively. Comparatively, the use of the modified operational strategy (scenario 1) resulted to a remarkable increase in projected energy production than the current strategy. The modification of the operational strategy resulted to the decrease in spill, hence, increase in energy generation (Figure 5.27 and Table 5.31). The deterioration in the performance of the operational strategy with increase in the time horizon is perhaps due to the need for the modification of the strategy on a pro rata basis.

Table 5.31 Average annual production of current and modified operational strategies for Stjørdal hydropower system.

Scenario	Description	Status quo operational strategy	Modified operational strategy - Scenario 1	Modified operational strategy - Scenario 2
		Average annual production (GWh/yr)	Average annual production (GWh/yr)	Average annual production (GWh/yr)
Baseline/observed	Observed	554.53		
	Baseline	554.94		
RCP4.5_2041-2070	Ensemble lower limit	545.66	549.74	547.90
	Ensemle mean	549.97	555.00	553.43
	Ensemble upper limit	549.88	555.80	554.24
RCP4.5_2071-2099	Ensemble lower limit	544.83	548.69	547.77
	Ensemle mean	548.68	553.41	552.00
	Ensemble upper limit	548.98	555.04	552.98
RCP8.5_2041-2070	Ensemble lower limit	546.58	550.06	549.23
	Ensemle mean	548.02	552.42	551.03
	Ensemble upper limit	546.43	552.08	549.83
RCP8.5_2071-2099	Ensemble lower limit	540.62	544.53	543.17
	Ensemle mean	542.74	547.31	545.89
	Ensemble upper limit	543.23	548.47	546.76

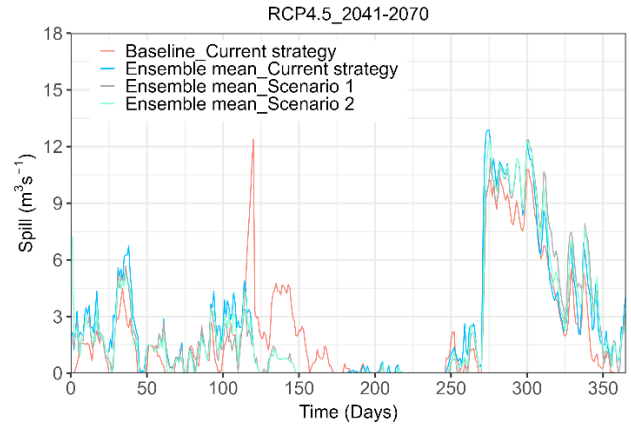

a.

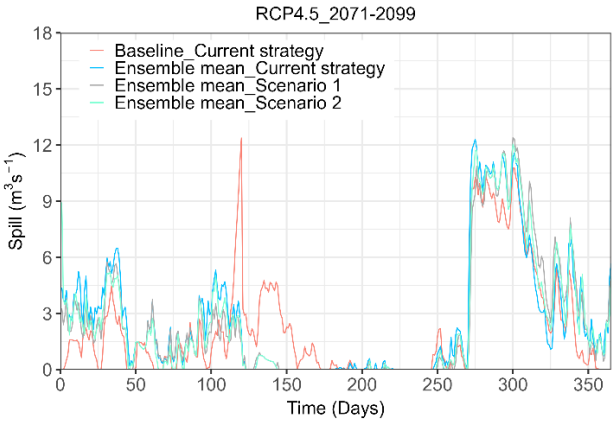

b.

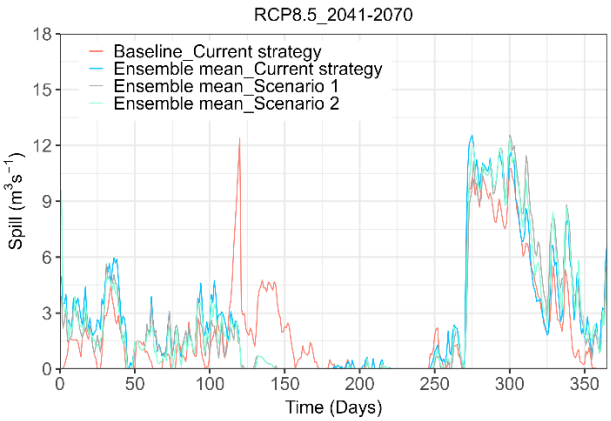

c.

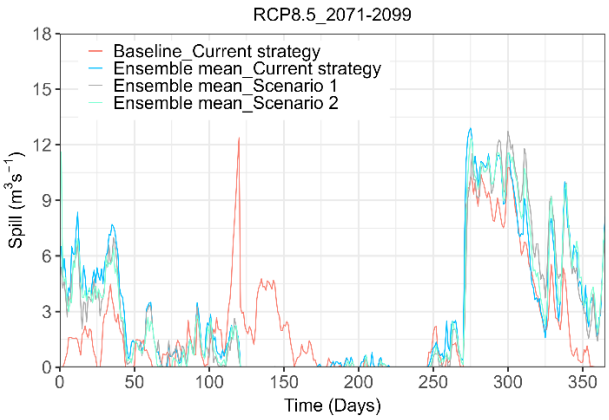

d.

Figure 5.27 Mean daily spill at Meråker module using current and modified operational strategies **a**. RCP4.5_2041 - 2070 **b**. RCP4.5_2071 – 2099 **c**. RCP8.5_2041 - 2070 **d**. RCP8.5_2071 – 2099.

6.0 CONCLUSION AND RECOMMENDATION

The future impact of climate on hydrology and hydropower production on two Nordic catchments (Forra and Laerdal catchments) were evaluated. The impact studies were carried out on a full range of climate models. On an ensemble basis, the average annual precipitation and average temperature of Forra and Laerdal catchments will increase in the future. The increase in precipitation and temperature was higher for RCP8.5 scenario during the end-of-century period the other scenarios and time horizons.

The corrected historical climate models' datasets could not be simulated in hindcast as the results of the objective function were comparably too low. Hence, the inability of CMIP5 ensembles to capture the variability in historical precipitation and temperature of the study area. The simulations of the future runoff using the delta change method indicate that the temporal variability of runoff in Forra catchment is likely to change from the current snowmelt-based spring flood to higher winter runoff while early occurrence of snowmelt-based spring flood will become prevalent in Laerdal catchment. A significant increase in runoff as well as potential evaporation will occur for RCP8.5 scenario during the end of century period compared to other scenarios and time horizons. On the contrary, the snowpack is projected to decline for both catchments.

For a designer interested in practicality and applicability of climate change impacts on runoff, the climate change factors for future runoff of Forra and Lærdal catchment are projected to increase by 10% and 15%, respectively, by the end of the 21st century. The uncertainties due to GCM/RCM combinations increased with time horizon of projections. In comparison to the baseline, the ensemble winter low flow will increase while the ensemble summer low flow will decrease in the future for all the scenarios and time horizons for both catchments. A remarkable change in the timing of occurrence of low flow will likely occur, for both catchments, particularly for RCP8.5_2071-2099, vis-à-vis the baseline scenario.

For Funna hydropower system, the continued use of the current operational strategy ("Do Nothing" alternative) will in the medium-term result to a marginal

loss in energy production capacity as well as a marginal increase for RCP8.5_2071-2099. The improvements in the energy production occasioned by the modification of the reservoir operational strategy presents a dilemma: increased production during the autumn and start of winter and reduced production for a greater proportion of winter. The decision on reservoir management strategy for Funna hydropower system must be balance with other considerations such as target consumers (residential, commercial, or industrial), firm power demand, environmental constraints etc.

The modified operational strategies comparatively improved the future energy production of Stjørdal hydropower system. The increase in energy production was most significant for the scenario whose inflow was used in the development of the strategy. Hence, the development of future operational strategies on pro rata basis should be considered for flow within Forra catchment. In the future, comparatively higher inflows, fairly distributed over the year, will play an important role in the hydropower production in Forra catchment and its environs. This will, perhaps, affect future reservoir management within and around Forra catchment.

References

Adera, A. G., & Alfredsen, K. T. (2020). Climate change and hydrological analysis of Tekeze river basin Ethiopia: implication for potential hydropower production. *Journal of Water and Climate Change*, *11*(3), 744-759.

Alfredsen, K., Júarez, A., Limpens, E., & Sivakumar, A. (2019). Simulering av vassdekt areal i Lærdalselva. *Simulation of water covered area in Lærdalselva)(In Norwegian) Norwegian University of Science and Technology B1-2019-5*.

Andréasson, J., Bergström, S., Carlsson, B., Graham, L. P., & Lindström, G. (2004). Hydrological change–climate change impact simulations for Sweden. *AMBIO: A Journal of the Human Environment*, *33*(4), 228-234.

Beldring, S., Engen-Skaugen, T., Førland, E. J., & Roald, L. A. (2008). Climate change impacts on hydrological processes in Norway based on two methods for transferring regional climate model results to meteorological station sites. *Tellus A: Dynamic Meteorology and Oceanography*, *60*(3), 439-450.

Berga, L. (2016). The role of hydropower in climate change mitigation and adaptation: a review. *Engineering*, *2*(3), 313-318.

Bergström, S. (1976). *Development and application of a conceptual runoff model for Scandinavian catchments*.

Buser, C. M., Künsch, H. R., & Weber, A. (2010). Biases and uncertainty in climate projections. *Scandinavian Journal of Statistics*, *37*(2), 179-199.

Capell, R., Tetzlaff, D., & Soulsby, C. (2013). Will catchment characteristics moderate the projected effects of climate change on flow regimes in the Scottish Highlands? *Hydrological Processes*, *27*(5), 687-699.

Chernet, H. H., Alfredsen, K., & Killingtveit, Å. (2013). The impacts of climate change on a Norwegian high-head hydropower system. *Journal of Water and Climate Change*, *4*(1), 17-37.

Collins, M., Knutti, R., Arblaster, J., Dufresne, J.-L., Fichefet, T., Friedlingstein, P., Gao, X., Gutowski, W. J., Johns, T., & Krinner, G. (2013). Long-term climate change: projections, commitments and irreversibility.

Committee, W. R. C. H. (1967). *A uniform technique for determining flood flow frequencies*. The Council.

Enayati, M., Bozorg-Haddad, O., Bazrafshan, J., Hejabi, S., & Chu, X. (2021). Bias correction capabilities of quantile mapping methods for rainfall and temperature variables. *Journal of Water and Climate Change*, *12*(2), 401-419.

Fang, G., Yang, J., Chen, Y., & Zammit, C. (2015). Comparing bias correction methods in downscaling meteorological variables for a hydrologic impact study in an arid area in China. *Hydrology and Earth System Sciences*, *19*(6), 2547-2559.

Ficklin, D. L., Stewart, I. T., & Maurer, E. P. (2013). Climate change impacts on streamflow and subbasin-scale hydrology in the Upper Colorado River Basin. *Plos one*, *8*(8), e71297.

Gelfan, A., Gustafsson, D., Motovilov, Y., Arheimer, B., Kalugin, A., Krylenko, I., & Lavrenov, A. (2017). Climate change impact on the water regime of two

great Arctic rivers: modeling and uncertainty issues. *Climatic Change*, *141*, 499-515.
Giorgi, F., & Gutowski Jr, W. J. (2015). Regional dynamical downscaling and the CORDEX initiative. *Annual review of environment and resources*, *40*, 467-490.
Giorgi, F., & Gutowski, W. J. (2016). Coordinated experiments for projections of regional climate change. *Current Climate Change Reports*, *2*, 202-210.
Gippel, C. J., & Stewardson, M. J. (1998). Use of wetted perimeter in defining minimum environmental flows. *Regulated Rivers: Research & Management: An International Journal Devoted to River Research and Management*, *14*(1), 53-67.
Graham, L. P. (2004). Climate change effects on river flow to the Baltic Sea. *AMBIO: A Journal of the Human Environment*, *33*(4), 235-241.
Graham, L. P., Andréasson, J., & Carlsson, B. (2007). Assessing climate change impacts on hydrology from an ensemble of regional climate models, model scales and linking methods–a case study on the Lule River basin. *Climatic Change*, *81*(Suppl 1), 293-307.
Guo, Q., Chen, J., Zhang, X., Shen, M., Chen, H., & Guo, S. (2019). A new two-stage multivariate quantile mapping method for bias correcting climate model outputs. *Climate dynamics*, *53*, 3603-3623.
Hailegeorgis, T., Alfredsen, K., & Killingtveit, Å. Appraisal of a comprehensive framework of decision support system (DSS) for hydropower in Africa: The influential roles of hydrology for optimal and sustainable planning-management and potential conflict resolution among water uses/users and case studies for catchments in Ethiopia and Norway.
Harby, A., Olivier, J. M., Merigoux, S., & Malet, E. (2007). A mesohabitat method used to assess minimum flow changes and impacts on the invertebrate and fish fauna in the Rhône River, France. *River Research and Applications*, *23*(5), 525-543.
Hattermann, F. F., Huang, S., & Koch, H. (2015). Climate change impacts on hydrology and water resources.
Hay, L. E., Wilby, R. L., & Leavesley, G. H. (2000). A comparison of delta change and downscaled GCM scenarios for three mountainous basins in the United States 1. *JAWRA Journal of the American Water Resources Association*, *36*(2), 387-397.
Howard, A. D. (1990). Role of hypsometry and planform in basin hydrologic response. *Hydrological Processes*, *4*(4), 373-385.
Lamouroux, N., OLIVIER, J. M., Capra, H., Zylberblat, M., Chandesris, A., & Roger, P. (2006). Fish community changes after minimum flow increase: testing quantitative predictions in the Rhône River at Pierre-Bénite, France. *Freshwater Biology*, *51*(9), 1730-1743.
Lawrence, D., & Haddeland, I. (2011). Uncertainty in hydrological modelling of climate change impacts in four Norwegian catchments. *Hydrology Research*, *42*(6), 457-471.
Li, J., Wang, Z., Wu, X., Ming, B., Chen, L., & Chen, X. (2020). Evident response of future hydropower generation to climate change. *Journal of Hydrology*,

590, 125385.
Lussana, C., Saloranta, T., Skaugen, T., Magnusson, J., Tveito, O. E., & Andersen, J. (2018). seNorge2 daily precipitation, an observational gridded dataset over Norway from 1957 to the present day. *Earth System Science Data*, *10*(1), 235-249.
Markoff, M. S., & Cullen, A. C. (2008). Impact of climate change on Pacific Northwest hydropower. *Climatic Change*, *87*(3-4), 451-469.
Masson-Delmotte, V., Zhai, P., Pirani, A., Connors, S. L., Péan, C., Berger, S., Caud, N., Chen, Y., Goldfarb, L., & Gomis, M. (2021). Climate change 2021: the physical science basis. *Contribution of working group I to the sixth assessment report of the intergovernmental panel on climate change*, *2*.
Masson-Delmotte, V., Zhai, P., Pörtner, H.-O., Roberts, D., Skea, J., & Shukla, P. R. (2022). *Global Warming of 1.5° C: IPCC Special Report on Impacts of Global Warming of 1.5° C above Pre-industrial Levels in Context of Strengthening Response to Climate Change, Sustainable Development, and Efforts to Eradicate Poverty*. Cambridge University Press.
Meehl, G. A., Covey, C., Delworth, T., Latif, M., McAvaney, B., Mitchell, J. F., Stouffer, R. J., & Taylor, K. E. (2007). The WCRP CMIP3 multimodel dataset: A new era in climate change research. *Bulletin of the American meteorological society*, *88*(9), 1383-1394.
Meehl, G. A., Moss, R., Taylor, K. E., Eyring, V., Stouffer, R. J., Bony, S., & Stevens, B. (2014). Climate model intercomparisons: Preparing for the next phase. *Eos, Transactions American Geophysical Union*, *95*(9), 77-78.
Minville, M., Brissette, F., & Leconte, R. (2008). Uncertainty of the impact of climate change on the hydrology of a nordic watershed. *Journal of Hydrology*, *358*(1-2), 70-83.
Mohammed, I. N., Bomblies, A., & Wemple, B. C. (2015). The use of CMIP5 data to simulate climate change impacts on flow regime within the Lake Champlain Basin. *Journal of Hydrology: Regional Studies*, *3*, 160-186.

Norges geologiske undersøkelse (2022) (https://www.ngu.no)

Ouyang, F., Zhu, Y., Fu, G., Lü, H., Zhang, A., Yu, Z., & Chen, X. (2015). Impacts of climate change under CMIP5 RCP scenarios on streamflow in the Huangnizhuang catchment. *Stochastic environmental research and risk assessment*, *29*, 1781-1795.
Perez, J., Menendez, M., Mendez, F. J., & Losada, I. J. (2014). Evaluating the performance of CMIP3 and CMIP5 global climate models over the north-east Atlantic region. *Climate dynamics*, *43*, 2663-2680.
Pörtner, H.-O., Roberts, D. C., Adams, H., Adler, C., Aldunce, P., Ali, E., Begum, R. A., Betts, R., Kerr, R. B., & Biesbroek, R. (2022). *Climate change 2022: Impacts, adaptation and vulnerability*. IPCC Geneva, Switzerland:.
Richter, B. D., Baumgartner, J. V., Powell, J., & Braun, D. P. (1996). A method for assessing hydrologic alteration within ecosystems. *Conservation biology*, *10*(4), 1163-1174.
Räty, O., Räisänen, J., & Ylhäisi, J. S. (2014). Evaluation of delta change and bias

correction methods for future daily precipitation: intermodel cross-validation using ENSEMBLES simulations. *Climate dynamics*, *42*, 2287-2303.

Schaefli, B., Hingray, B., & Musy, A. (2007). Climate change and hydropower production in the Swiss Alps: quantification of potential impacts and related modelling uncertainties. *Hydrology and Earth System Sciences*, *11*(3), 1191-1205.

Shen, M., Chen, J., Zhuan, M., Chen, H., Xu, C.-Y., & Xiong, L. (2018). Estimating uncertainty and its temporal variation related to global climate models in quantifying climate change impacts on hydrology. *Journal of Hydrology*, *556*, 10-24.

Shine, K. P. (2000). Radiative forcing of climate change. *Space Science Reviews*, *94*(1-2), 363-373.

Shrestha, A., Shrestha, S., Tingsanchali, T., Budhathoki, A., & Ninsawat, S. (2021). Adapting hydropower production to climate change: A case study of Kulekhani Hydropower Project in Nepal. *Journal of Cleaner Production*, *279*, 123483.

Smakhtin, V. U. (2001). Low flow hydrology: a review. *Journal of Hydrology*, *240*(3-4), 147-186.

Smitha, P., Narasimhan, B., Sudheer, K., & Annamalai, H. (2018). An improved bias correction method of daily rainfall data using a sliding window technique for climate change impact assessment. *Journal of Hydrology*, *556*, 100-118.

Stedinger, J. R. (1993). Frequency analysis of extreme events. *Handbook of hydrology*.

Stocker, T. F., Qin, D., Plattner, G.-K., Tignor, M. M., Allen, S. K., Boschung, J., Nauels, A., Xia, Y., Bex, V., & Midgley, P. M. (2014). Climate Change 2013: The physical science basis. contribution of working group I to the fifth assessment report of IPCC the intergovernmental panel on climate change.

Sunde, M. G., He, H. S., Hubbart, J. A., & Urban, M. A. (2017). Integrating downscaled CMIP5 data with a physically based hydrologic model to estimate potential climate change impacts on streamflow processes in a mixed-use watershed. *Hydrological Processes*, *31*(9), 1790-1803.

Teutschbein, C., & Seibert, J. (2010). Regional climate models for hydrological impact studies at the catchment scale: a review of recent modeling strategies. *Geography Compass*, *4*(7), 834-860.

Teutschbein, C., & Seibert, J. (2012). Bias correction of regional climate model simulations for hydrological climate-change impact studies: Review and evaluation of different methods. *Journal of Hydrology*, *456*, 12-29.

Thornthwaite, C. W. (1948). An approach toward a rational classification of climate. *Geographical review*, *38*(1), 55-94.

Timalsina, N. P., Alfredsen, K. T., & Killingtveit, Å. (2015). Impact of climate change on ice regime in a river regulated for hydropower. *Canadian Journal of Civil Engineering*, *42*(9), 634-644.

Travnichek, V. H., Bain, M. B., & Maceina, M. J. (1995). Recovery of a warmwater

fish assemblage after the initiation of a minimum-flow release downstream from a hydroelectric dam. *Transactions of the American Fisheries Society*, *124*(6), 836-844.

Tryhorn, L., & DeGaetano, A. (2011). A comparison of techniques for downscaling extreme precipitation over the Northeastern United States. *International journal of climatology*, *31*(13), 1975-1989.

Veijalainen, N. (2012). Estimation of climate change impacts on hydrology and floods in Finland.

Vicuña, S., Garreaud, R. D., & McPhee, J. (2011). Climate change impacts on the hydrology of a snowmelt driven basin in semiarid Chile. *Climatic Change*, *105*, 469-488.

Wasti, A., Ray, P., Wi, S., Folch, C., Ubierna, M., & Karki, P. (2022). Climate change and the hydropower sector: A global review. *Wiley Interdisciplinary Reviews: Climate Change*, *13*(2), e757.

Wong, W. K., Haddeland, I., Lawrence, D., & Beldring, S. (2016). Gridded 1 x 1 km climate and hydrological projections for Norway.

Youssef, A. M., Pradhan, B., & Hassan, A. M. (2011). Flash flood risk estimation along the St. Katherine road, southern Sinai, Egypt using GIS based morphometry and satellite imagery. *Environmental Earth Sciences*, *62*(3), 611-623.

Yuan, F., Tung, Y.-K., & Ren, L. (2016). Projection of future streamflow changes of the Pearl River basin in China using two delta-change methods. *Hydrology Research*, *47*(1), 217-238.

Appendix 1: Hypsographic characteristics of delineated catchments

Norges vassdrags- og energidirektorat

Kartbakgrunn: Statens Kartverk
Kartdatum: EUREF89 WGS84
Projeksjon: UTM 33N
Beregn.punkt: 318698 E 7045667 N

Nedbørfeltgrenser og feltparametere er automatisk generert og kan inneholde feil. Resultatene må kvalitetssikres.

Nedbørfeltparametere

Vassdragsnr.:	124.AB0
Kommune.:	Stjørdal
Fylke.:	Trøndelag
Vassdrag.:	Forra

Feltparametere		
Areal (A)	495	km²
Effektiv sjø (A_{SE})	2.37	%
Elvleengde (E_L)	57.9	km
Elvegradient (E_G)	8.8	m/km
Elvegradient $_{1085}$($E_{G,1085}$)	7	m/km
Helning	7.7	°
Dreneringstetthet (D_T)	2.4	km^{-1}
Feltlengde (F_L)	39.8	km

Arealklasse		
Bre (A_{BRE})	0	%
Dyrket mark (A_{JORD})	0.5	%
Myr (A_{MYR})	28.3	%
Leire (A_{LEIRE})	0.2	%
Skog (A_{SKOG})	31.9	%
Sjø (A_{SJO})	8.2	%
Snaufjell (A_{SF})	25.2	%
Urban (A_U)	0	%
Uklassifisert areal (A_{REST})	6.0	%

Hypsografisk kurve		
$Høyde_{MIN}$	95	m
$Høyde_{10}$	377	m
$Høyde_{20}$	402	m
$Høyde_{30}$	434	m
$Høyde_{40}$	469	m
$Høyde_{50}$	505	m
$Høyde_{60}$	547	m
$Høyde_{70}$	596	m
$Høyde_{80}$	647	m
$Høyde_{90}$	749	m
$Høyde_{MAX}$	1246	m

Klima- /hydrologiske parametere		
Avrenning 1961-90 (Q_N)	41.7	l/s*km²
Sommernedbør	462	mm
Vinternedbør	641	mm
Årstemperatur	1.6	°C
Sommertemperatur	8.1	°C
Vintertemperatur	-3.0	°C

Figure S.1 Hypsographic characteristics of Forra catchment considering outlet at Høggås bru gauging station location.

Norges vassdrags- og energidirektorat

Kartbakgrunn: Statens Kartverk
Kartdatum: EUREF89 WGS84
Projeksjon: UTM 33N
Beregn.punkt: 106328 E 6790536 N

Nedbørfeltgrenser og feltparametere er automatisk generert og kan inneholde feil. Resultatene må kvalitetssikres.

Nedbørfeltparametere

Vassdragsnr.:	073.B3
Kommune.:	Lærdal
Fylke.:	Vestland
Vassdrag.:	Lærdalsvassdraget

Feltparametere		
Areal (A)	789	km²
Effektiv sjø (A_{SE})	0.21	%
Elvleengde (E_L)	60.2	km
Elvegradient (E_G)	21.7	m/km
Elvegradient $_{1085}$($E_{G,1085}$)	21.6	m/km
Helning	14.0	°
Dreneringstetthet (D_T)	1.7	km^{-1}
Feltlengde (F_L)	32.5	km

Arealklasse		
Bre (A_{BRE})	0.1	%
Dyrket mark (A_{JORD})	0.3	%
Myr (A_{MYR})	0.9	%
Leire (A_{LEIRE})	0	%
Skog (A_{SKOG})	11.1	%
Sjø (A_{SJO})	7	%
Snaufjell (A_{SF})	78.1	%
Urban (A_U)	0	%
Uklassifisert areal (A_{REST})	2.5	%

Hypsografisk kurve		
$Høyde_{MIN}$	180	m
$Høyde_{10}$	956	m
$Høyde_{20}$	1135	m
$Høyde_{30}$	1228	m
$Høyde_{40}$	1287	m
$Høyde_{50}$	1335	m
$Høyde_{60}$	1378	m
$Høyde_{70}$	1424	m
$Høyde_{80}$	1479	m
$Høyde_{90}$	1563	m
$Høyde_{MAX}$	1917	m

Klima- /hydrologiske parametere		
Avrenning 1961-90 (Q_N)	30.7	l/s*km²
Sommernedbør	414	mm
Vinternedbør	498	mm
Årstemperatur	-1.7	°C
Sommertemperatur	3.9	°C
Vintertemperatur	-5.8	°C

Figure S.2 Hypsographic characteristics of Lærdal catchment considering outlet at Sælthun gauging station location.

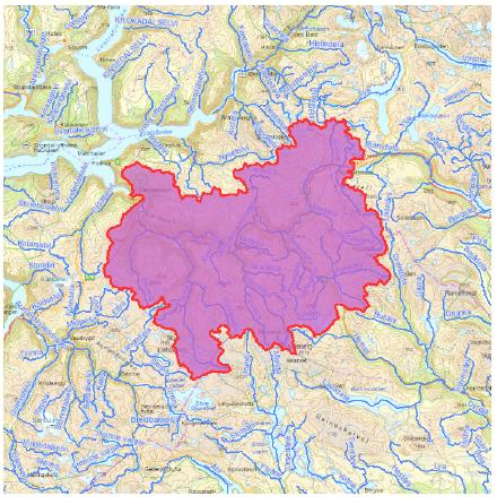

Norges vassdrags- og energidirektorat

Kartbakgrunn:	Statens Kartverk
Kartdatum:	EUREF89 WGS84
Projeksjon:	UTM 33N
Beregn.punkt:	94969 E 6797512 N

Nedbørfeltgrenser og feltparametere er automatisk generert og kan inneholde feil. Resultatene må kvalitetssikres.

Nedbørfeltparametere

Vassdragsnr.:	**073.A2**
Kommune.:	**Lærdal**
Fylke.:	**Vestland**
Vassdrag.:	**Lærdalsvassdraget**

Feltparametere

Areal (A)	1182	km²
Effektiv sjø (A_{SE})	0.11	%
Elvleengde (E_L)	80.9	km
Elvegradient (E_G)	18.4	m/km
Elvegradient $_{1085}$ ($E_{G,1085}$)	19.3	m/km
Helning	15.5	°
Dreneringstetthet (D_T)	1.5	km^{-1}
Feltlengde (F_L)	45.3	km

Arealklasse

Bre (A_{BRE})	0.1	%
Dyrket mark (A_{JORD})	0.8	%
Myr (A_{MYR})	0.7	%
Leire (A_{LEIRE})	0	%
Skog (A_{SKOG})	14.2	%
Sjø (A_{SJO})	6.4	%
Snaufjell (A_{SF})	75.0	%
Urban (A_U)	0.0	%
Uklassifisert areal (A_{REST})	2.9	%

Hypsografisk kurve

$Høyde_{MIN}$	1	m
$Høyde_{10}$	819	m
$Høyde_{20}$	1079	m
$Høyde_{30}$	1208	m
$Høyde_{40}$	1285	m
$Høyde_{50}$	1341	m
$Høyde_{60}$	1395	m
$Høyde_{70}$	1448	m
$Høyde_{80}$	1498	m
$Høyde_{90}$	1566	m
$Høyde_{MAX}$	1917	m

Klima- /hydrologiske parametere

Avrenning 1961-90 (Q_N)	30.7	l/s*km²
Sommernedbør	424	mm
Vinternedbør	521	mm
Årstemperatur	-1.4	°C
Sommertemperatur	4.1	°C
Vintertemperatur	-5.3	°C

Figure S.3 Hypsographic characteristics of Lærdal catchment considering outlet close to Lærdalsfjorden

Appendix 2: Potential evaporation of the catchments for different time horizons

Table S.1 Mean monthly potential evaporation for the baseline and RCP4.5_2041 - 2070 scenario for Forra catchment.

Month	Baseline	CNRM_CCLM	CNRM_RCA	ECEARTH_CCLM	ECEARTH_HIRHAM	ECEARTH_RACMO	ECEARTH_RCA	HADGEM_RCA	IPSL_RCA	MPI_CCLM	MPI_RCA
	mm/day	mm/day	mm/day	mm/day	mm/day	mm/day	mm/day	mm/day	mm/day	mm/day	mm/day
Jan	0.00	0.02	0.01	0.01	0.02	0.03	0.02	0.02	0.04	0.01	0.01
Feb	0.01	0.03	0.03	0.10	0.02	0.01	0.07	0.07	0.03	0.03	0.02
Mar	0.00	0.15	0.16	0.08	0.09	0.05	0.08	0.23	0.12	0.03	0.03
Apr	0.33	0.57	0.60	0.68	0.74	0.52	0.72	1.10	0.71	0.53	0.72
May	2.23	2.46	2.45	2.58	2.79	2.29	2.77	2.87	2.68	2.57	2.83
Jun	3.73	3.76	4.10	3.81	3.89	4.26	4.23	3.96	4.28	3.95	4.04
Jul	4.11	4.06	4.24	4.23	4.10	4.44	4.21	4.24	4.49	3.98	4.06
Aug	3.24	3.44	3.39	3.36	3.36	3.23	3.32	3.45	3.42	3.24	3.18
Sep	1.82	1.91	1.89	2.00	1.89	1.92	1.95	1.98	1.96	1.87	1.85
Oct	0.68	0.96	0.90	0.95	0.82	0.91	0.90	0.94	0.92	0.85	0.75
Nov	0.04	0.16	0.17	0.15	0.12	0.17	0.13	0.07	0.13	0.15	0.13
Dec	0.00	0.03	0.03	0.03	0.04	0.00	0.02	0.05	0.01	0.02	0.01

Table S.2 Mean monthly potential evaporation for RCP4.5_2071 - 2099 scenario for Forra catchment.

Month	CNRM_CCLM	CNRM_RCA	ECEARTH_CCLM	ECEARTH_HIRHAM	ECEARTH_RACMO	ECEARTH_RCA	HADGEM_RCA	IPSL_RCA	MPI_CCLM	MPI_RCA
	mm/day	mm/day	mm/day	mm/day	mm/day	mm/day	mm/day	mm/day	mm/day	mm/day
Jan	0.05	0.03	0.03	0.02	0.07	0.03	0.03	0.09	0.03	0.03
Feb	0.05	0.03	0.09	0.02	0.03	0.07	0.05	0.07	0.09	0.03
Mar	0.18	0.17	0.13	0.11	0.11	0.12	0.22	0.11	0.05	0.06
Apr	0.62	0.68	0.91	0.78	0.60	0.92	1.07	0.86	0.77	0.93
May	2.43	2.72	2.67	2.83	2.53	3.05	3.01	2.85	2.55	2.79
Jun	3.89	4.26	4.02	3.90	4.70	4.44	4.07	4.41	4.02	4.13

Jul	4.37	4.40	4.12	4.18	4.52	4.21	4.49	4.50	3.96	4.00
Aug	3.39	3.29	3.31	3.46	3.31	3.23	3.51	3.50	3.25	3.16
Sep	1.92	1.86	2.02	1.90	1.89	1.96	2.02	2.09	1.85	1.88
Oct	0.94	0.87	1.00	0.96	1.00	0.99	0.97	0.98	1.00	0.91
Nov	0.17	0.16	0.26	0.12	0.21	0.23	0.17	0.13	0.11	0.14
Dec	0.03	0.03	0.04	0.03	0.02	0.02	0.08	0.02	0.02	0.02

Table S.3 Mean monthly potential evaporation for RCP8.5_2041 - 2070 scenario for Forra catchment.

Month	CNRM_CCLM	CNRM_RCA	ECEARTH_CCLM	ECEARTH_HIRHAM	ECEARTH_RACMO	ECEARTH_RCA	HADGEM_RCA	IPSL_RCA	MPI_CCLM	MPI_RCA
	mm/day	mm/day	mm/day	mm/day	mm/day	mm/day	mm/day	mm/day	mm/day	mm/day
Jan	0.02	0.02	0.03	0.02	0.04	0.03	0.03	0.07	0.02	0.01
Feb	0.06	0.05	0.08	0.03	0.02	0.07	0.04	0.06	0.07	0.03
Mar	0.17	0.23	0.11	0.14	0.06	0.18	0.20	0.21	0.08	0.11
Apr	0.57	0.57	0.84	1.05	0.59	0.76	1.19	0.83	0.75	1.01
May	2.45	2.42	2.64	2.89	2.29	2.92	2.88	2.67	2.58	2.82
Jun	3.91	4.21	4.10	3.88	4.64	4.53	4.12	4.37	3.85	3.95
Jul	4.19	4.33	4.17	4.09	4.47	4.32	4.32	4.53	4.00	4.07
Aug	3.39	3.35	3.40	3.42	3.28	3.30	3.36	3.52	3.31	3.20
Sep	1.96	1.98	2.06	1.98	2.01	2.01	2.01	2.02	1.93	1.95
Oct	0.95	0.88	1.05	1.00	0.97	1.00	1.14	0.92	1.09	0.98
Nov	0.14	0.13	0.20	0.14	0.17	0.19	0.15	0.20	0.15	0.16
Dec	0.04	0.05	0.03	0.03	0.02	0.02	0.07	0.02	0.05	0.04

Table S.4 Mean monthly potential evaporation for RCP8.5_2071 - 2099 scenario for Forra catchment.

Month	CNRM_CCLM	CNRM_RCA	ECEARTH_CCLM	ECEARTH_HIRHAM	ECEARTH_RACMO	ECEARTH_RCA	HADGEM_RCA	IPSL_RCA	MPI_CCLM	MPI_RCA
	mm/day	mm/day	mm/day	mm/day	mm/day	mm/day	mm/day	mm/day	mm/day	mm/day
Jan	0.12	0.10	0.12	0.05	0.07	0.10	0.08	0.10	0.10	0.09
Feb	0.16	0.12	0.21	0.04	0.09	0.18	0.13	0.12	0.13	0.09
Mar	0.23	0.36	0.33	0.22	0.19	0.41	0.42	0.26	0.15	0.28
Apr	0.84	1.03	1.30	1.32	0.86	1.44	1.27	1.04	0.97	1.26
May	2.64	2.95	2.85	3.05	3.09	3.35	3.10	3.11	2.72	3.07
Jun	3.99	4.42	3.89	4.06	5.07	4.44	4.48	4.70	3.91	4.05
Jul	4.35	4.56	4.25	4.37	4.48	4.38	4.66	4.73	4.08	4.15
Aug	3.54	3.50	3.44	3.59	3.43	3.46	3.62	3.86	3.41	3.36
Sep	2.01	2.01	2.13	2.13	2.10	2.11	2.30	2.28	2.00	2.00
Oct	1.04	0.92	1.16	1.04	1.09	1.08	1.21	0.98	1.14	0.99
Nov	0.25	0.23	0.38	0.24	0.29	0.32	0.29	0.27	0.31	0.30
Dec	0.09	0.07	0.11	0.10	0.04	0.08	0.14	0.06	0.10	0.09

Table S.5 Mean monthly potential evaporation for the baseline and RCP4.5_2041 - 2070 scenario for Lærdal catchment.

Month	Baseline_calib	Baseline	CNRM_CCLM	CNRM_RCA	ECEARTH_CCLM	ECEARTH_HIRHAM	ECEARTH_RACMO	ECEARTH_RCA	HADGEM_RCA	IPSL_RCA	MPI_CCLM	MPI_RCA
	mm/day	mm/day	mm/day	mm/day	mm/day	mm/day	mm/day	mm/day	mm/day	mm/day	mm/day	
Jan	0.00	0.00	0.00	0.00	0.00	0.00	0.00	0.00	0.00	0.00	0.00	0.00
Feb	0.00	0.00	0.00	0.00	0.00	0.00	0.00	0.00	0.00	0.00	0.00	0.00
Mar	0.00	0.00	0.00	0.00	0.00	0.00	0.00	0.00	0.00	0.00	0.00	0.00
Apr	0.00	0.00	0.00	0.00	0.00	0.07	0.02	0.02	0.08	0.09	0.00	0.00
May	0.99	0.98	1.19	1.08	1.14	1.43	1.40	1.35	1.24	1.35	1.20	1.12
Jun	3.43	3.36	3.43	3.10	3.45	3.52	3.45	3.09	3.09	3.14	3.70	3.30
Jul	3.86	4.10	4.13	3.86	4.30	4.08	4.10	3.99	4.05	3.97	4.10	4.15

Aug	3.11	3.25	3.24	3.45	3.16	3.20	3.14	3.33	3.50	3.38	3.01	3.39
Sep	1.39	1.44	1.68	1.87	1.72	1.64	1.66	1.90	2.03	1.87	1.69	1.62
Oct	0.14	0.11	0.30	0.31	0.28	0.18	0.30	0.34	0.52	0.42	0.13	0.15
Nov	0.00	0.00	0.01	0.01	0.01	0.01	0.03	0.00	0.02	0.01	0.01	0.00
Dec	0.00	0.00	0.00	0.00	0.00	0.00	0.00	0.00	0.00	0.00	0.00	0.00

Table S.6 Mean monthly potential evaporation for RCP4.5_2071 - 2099 scenario for Lærdal catchment.

Month	CNRM_CCLM	CNRM_RCA	ECEARTH_CCLM	ECEARTH_HIRHAM	ECEARTH_RACMO	ECEARTH_RCA	HADGEM_RCA	IPSL_RCA	MPI_CCLM	MPI_RCA
	mm/day	mm/day	mm/day	mm/day	mm/day	mm/day	mm/day	mm/day	mm/day	mm/day
Jan	0.00	0.00	0.00	0.00	0.00	0.00	0.00	0.01	0.00	0.00
Feb	0.00	0.00	0.00	0.00	0.00	0.00	0.00	0.00	0.00	0.00
Mar	0.00	0.00	0.00	0.00	0.00	0.00	0.00	0.00	0.00	0.00
Apr	0.00	0.01	0.00	0.01	0.05	0.06	0.01	0.10	0.01	0.00
May	1.17	1.36	1.39	1.58	1.72	1.33	1.40	1.50	1.35	1.10
Jun	3.54	3.15	3.70	3.46	3.54	3.14	3.32	3.10	3.79	3.35
Jul	4.30	4.00	4.15	4.06	4.18	3.97	4.48	3.86	4.04	4.06
Aug	3.10	3.41	3.13	3.29	3.15	3.41	3.72	3.41	2.99	3.40
Sep	1.72	1.88	1.82	1.73	1.58	2.04	1.99	2.07	1.69	1.73
Oct	0.32	0.29	0.45	0.38	0.43	0.57	0.54	0.63	0.42	0.40
Nov	0.01	0.00	0.02	0.01	0.03	0.02	0.07	0.02	0.02	0.03
Dec	0.00	0.00	0.00	0.00	0.01	0.00	0.00	0.00	0.00	0.00

Table S.7 Mean monthly potential evaporation for RCP8.5_2041 - 2070 scenario for Lærdal catchment.

Month	CNRM_CCLM	CNRM_RCA	ECEARTH_CCLM	ECEARTH_HIRHAM	ECEARTH_RACMO	ECEARTH_RCA	HADGEM_RCA	IPSL_RCA	MPI_CCLM	MPI_RCA
	mm/day	mm/day	mm/day	mm/day	mm/day	mm/day	mm/day	mm/day	mm/day	mm/day
Jan	0.00	0.00	0.00	0.00	0.00	0.00	0.00	0.00	0.01	0.00
Feb	0.00	0.00	0.00	0.00	0.00	0.00	0.00	0.00	0.00	0.00
Mar	0.00	0.00	0.00	0.00	0.00	0.00	0.00	0.00	0.00	0.00
Apr	0.00	0.02	0.00	0.05	0.05	0.00	0.06	0.10	0.02	0.00
May	1.06	1.03	1.29	1.58	1.39	1.38	1.22	1.27	1.39	1.09
Jun	3.64	3.17	3.72	3.57	3.50	3.25	3.34	3.07	3.70	3.20
Jul	4.19	3.91	4.14	4.03	4.10	4.04	4.35	3.89	4.02	4.21
Aug	3.13	3.35	3.19	3.25	3.19	3.33	3.51	3.45	3.06	3.43
Sep	1.79	1.97	1.84	1.75	1.76	2.00	1.99	2.05	1.77	1.79
Oct	0.34	0.37	0.55	0.47	0.38	0.61	0.80	0.55	0.59	0.53
Nov	0.00	0.00	0.05	0.01	0.01	0.07	0.04	0.01	0.03	0.03
Dec	0.00	0.00	0.01	0.00	0.00	0.00	0.01	0.00	0.00	0.00

Table S.8 Mean monthly potential evaporation for RCP8.5_2071 - 2099 scenario for Lærdal catchment.

Month	CNRM_CCLM	CNRM_RCA	ECEARTH_CCLM	ECEARTH_HIRHAM	ECEARTH_RACMO	ECEARTH_RCA	HADGEM_RCA	IPSL_RCA	MPI_CCLM	MPI_RCA
	mm/day	mm/day	mm/day	mm/day	mm/day	mm/day	mm/day	mm/day	mm/day	mm/day
Jan	0.00	0.01	0.01	0.01	0.00	0.01	0.01	0.00	0.00	0.00
Feb	0.00	0.00	0.00	0.00	0.00	0.00	0.01	0.00	0.00	0.00
Mar	0.00	0.00	0.00	0.00	0.00	0.00	0.00	0.02	0.00	0.00
Apr	0.00	0.10	0.11	0.12	0.12	0.12	0.11	0.14	0.02	0.05
May	1.48	1.44	1.73	1.87	1.88	1.53	1.72	1.45	1.65	1.55
Jun	3.74	3.11	3.81	3.81	3.67	3.34	4.34	3.07	3.65	3.62
Jul	4.18	4.20	4.23	4.13	4.06	4.38	4.95	4.03	4.12	4.46

Aug	3.26	3.69	3.18	3.31	3.23	3.68	3.84	3.89	3.18	3.62
Sep	1.86	2.06	1.93	1.98	1.85	2.20	2.34	2.39	1.83	1.81
Oct	0.60	0.55	0.74	0.65	0.73	0.77	0.86	0.68	0.67	0.57
Nov	0.06	0.05	0.10	0.05	0.11	0.09	0.15	0.08	0.03	0.07
Dec	0.01	0.00	0.00	0.01	0.01	0.01	0.01	0.01	0.01	0.01

Appendix 3: Script for computation of potential evaporation

```
#Script fo computation of monthly evapotranspiration
library(readxl)
library(tidyverse)
library(xts)
library(hydroTSM)
library(dplyr)
library(SPEI)
setwd("C:/r_files/thornthwaite")
pathh <- "C:/r_files/thornthwaite/thorn_inp.xlsx"
data1 <- excel_sheets(pathh)
data1 <- read_excel(pathh,sheet = 4,
                    col_types = c("date", "numeric", "numeric", "numeric", "numeric", "numeric",
"numeric", "numeric", "numeric", "numeric", "numeric", "numeric"),
                    skip = 0)
#Compute monthly temperature
snf <- as.data.frame(data1)
nc <- ncol(snf)
name <- names(snf)
data1 = as.data.frame(data1)
for (i in 2:nc){
  xtssn <- xts(snf[,i],order.by=as.Date(snf[,1]))
  msnow_check <- daily2monthly(xtssn,FUN="mean")  #Runoff = mean
  allsnow_check <- monthlyfunction(msnow_check,FUN="mean")
    if (i==2){
    print(name[i])
    result <- data.frame(date=index(msnow_check), coredata(msnow_check))
    names(result) <- c(name[1],name[i])
  }
  else {
    print(name[i])
    temp <-  data.frame(coredata(msnow_check))
    names(temp) <- c(name[i])
    result <- cbind(result,temp)
  }
}
#view(result)
write.csv(result,"monthly_temperature.csv")
#Compute PET using Thornthwaite at monthly timescale
for (i in 2:nc){
  xtssn <- thornthwaite(result[,i],lat = 63.568345)

  if (i==2){
    print(name[i])
    result2 <- data.frame(date=index(xtssn), coredata(xtssn))
    names(result2) <- c(name[1],name[i])
  }
  else {
    print(name[i])
    temp <-  data.frame(coredata(xtssn))
    names(temp) <- c(name[i])
    result2 <- cbind(result2,temp)
  }
}
write.csv(result2,"monthly_PET.csv")
################################
```

Appendix 4: Fitting of 7-day minimum flow frequency analysis of non-exceedance probability

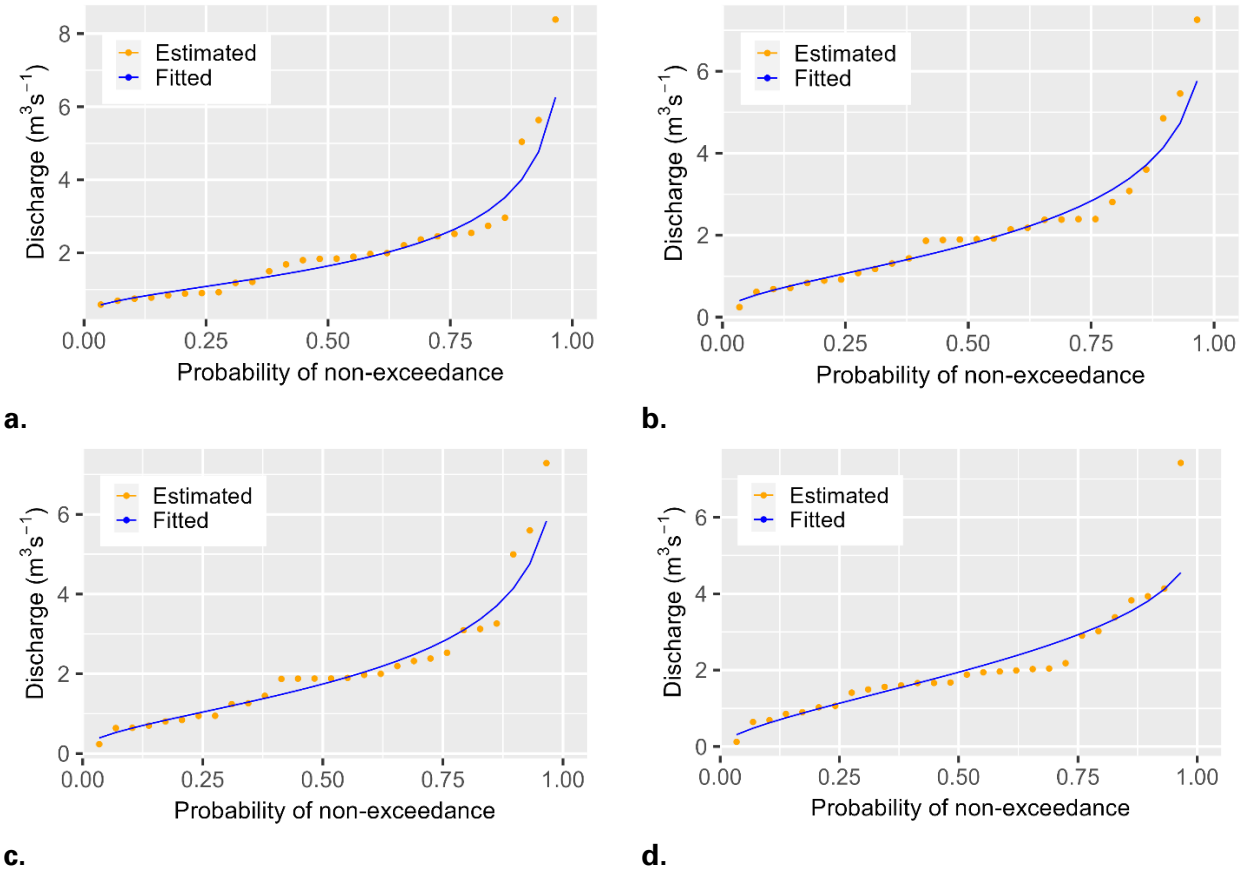

Figure S.4 Fitting of 7-day minimum flow frequency analysis of non-exceedance probability for Forra catchment **a.** RCP4.5_2041 - 2070 **b.** RCP4.5_2071 – 2099 **c.** RCP8.5_2041 - 2070 **d.** RCP8.5_2071 – 2099 for Forra catchment

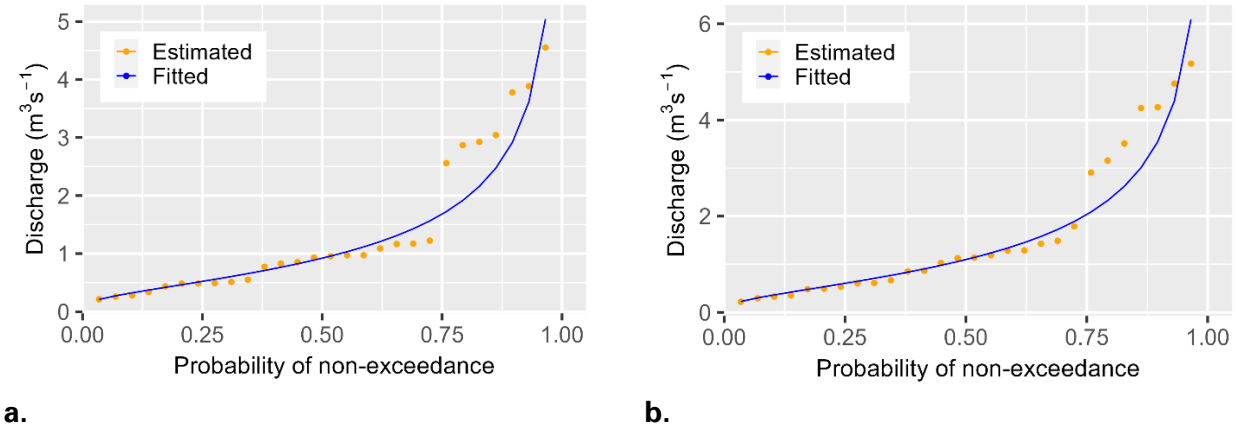

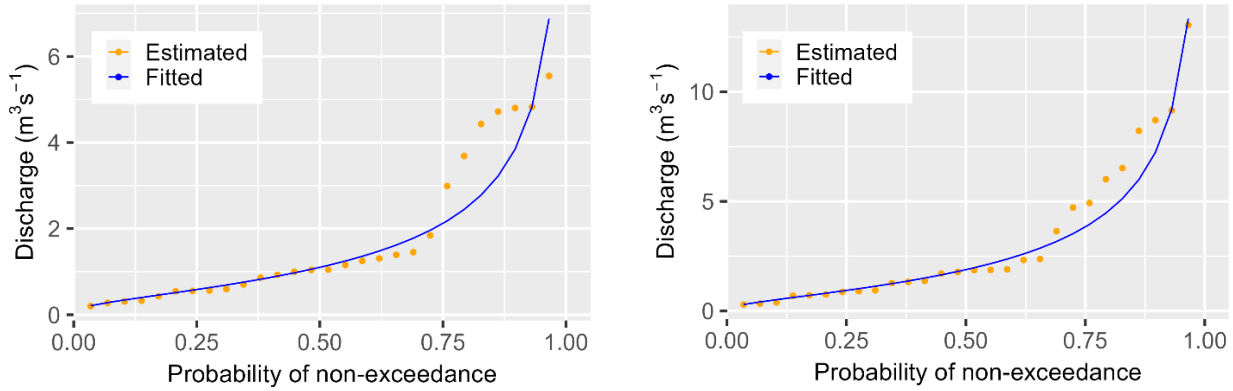

c. **d.**

Figure S.5 Fitting of 7-day minimum flow frequency analysis of non-exceedance probability for Lærdal catchment a. RCP4.5_2041 - 2070 b. RCP4.5_2071 – 2099 c. RCP8.5_2041 - 2070 d. RCP8.5_2071 – 2099 for Lærdal catchment

Appendix 5: Summary of design flood for various probability distribution functions and return period.

Table S9: Design flood for baseline scenario in m^3/s (Forra catchment)

FF	Q5	Q10	Q15	Q20	Q50	Q100	Q200	Q500	Q1000
GEV	133.98	155.17	168.42	178.31	212.99	242.98	276.79	328.23	373.05
GNo	134.97	156.65	169.82	179.44	211.82	238.29	266.64	307.23	340.45
P3	136.76	158.83	171.51	180.44	208.57	229.62	250.53	278.01	298.70
Gum	137.78	156.20	166.59	173.87	196.74	213.88	230.96	253.49	270.51

Table S10: Design flood for RCP4.5_2041-2070 scenario in m^3/s (Forra catchment)

FF	Q5	Q10	Q15	Q20	Q50	Q100	Q200	Q500	Q1000
GEV	133.79	143.88	148.40	151.14	157.94	161.64	164.44	167.13	168.61
GNo	132.93	143.21	148.14	151.30	159.99	165.55	170.48	176.26	180.19
P3	132.99	143.25	148.15	151.28	159.85	165.29	170.09	175.67	179.43
Gum	130.14	146.46	155.67	162.12	182.39	197.58	212.71	232.68	247.77

Table S11: Design flood for RCP4.5_2071-2099 scenario in m^3/s (Forra catchment)

FF	Q5	Q10	Q15	Q20	Q50	Q100	Q200	Q500	Q1000
GEV	133.19	143.70	148.53	151.50	159.08	163.35	166.68	170.00	171.90
GNo	132.42	143.04	148.21	151.56	160.87	166.93	172.37	178.83	183.27
P3	132.44	143.06	148.22	151.55	160.82	166.83	172.22	178.60	182.98
Gum	129.81	145.78	154.79	161.10	180.94	195.80	210.60	230.14	244.90

Table S12: Design flood for RCP8.5_2071-2099 scenario in m^3/s (Forra catchment)

FF	Q5	Q10	Q15	Q20	Q50	Q100	Q200	Q500	Q1000
GEV	130.48	141.49	146.60	149.78	157.98	162.68	166.40	170.17	172.36
GNo	129.74	140.82	146.25	149.78	159.68	166.17	172.03	179.04	183.89
P3	129.75	140.82	146.26	149.78	159.66	166.12	171.96	178.93	183.75
Gum	127.16	143.39	152.54	158.96	179.11	194.21	209.25	229.10	244.10

Table S13: Design flood for RCP8.5_2071-2099 scenario in m^3/s (Forra catchment)

FF	Q5	Q10	Q15	Q20	Q50	Q100	Q200	Q500	Q1000
GEV	139.08	155.36	164.02	169.87	187.19	199.16	210.29	223.85	233.31
GNo	138.92	155.01	163.64	169.53	187.33	200.13	212.54	228.52	240.39
P3	139.16	155.22	163.76	169.54	186.81	199.01	210.68	225.46	236.25
Gum	137.57	155.59	165.76	172.88	195.25	212.02	228.72	250.76	267.42

Table S14: Design flood for baseline scenario in m^3/s (Lærdal catchment)

FF	Q5	Q10	Q15	Q20	Q50	Q100	Q200	Q500	Q1000
GEV	380.15	423.66	448.22	465.43	519.55	560.15	600.64	654.11	694.57
GNo	380.69	423.91	448.12	465.01	518.01	557.83	597.77	651.11	692.06
P3	382.18	425.40	449.05	465.30	514.92	550.83	585.72	630.63	663.88
Gum	380.21	423.66	448.17	465.34	519.29	559.71	599.99	653.14	693.30

Table S15: Design flood for RCP4.5_2041-2070 scenario in m^3/s (Lærdal catchment)

FF	Q5	Q10	Q15	Q20	Q50	Q100	Q200	Q500	Q1000
GEV	349.97	383.49	399.62	409.88	437.27	453.75	467.37	481.85	490.66
GNo	348.24	381.69	398.48	409.51	441.04	462.19	481.63	505.30	521.99
P3	348.24	381.70	398.48	409.51	441.03	462.17	481.60	505.26	521.93
Gum	341.68	387.27	412.99	431.00	487.60	530.02	572.28	628.04	670.18

Table S16: Design flood for RCP4.5_2071-2099 scenario in m^3/s (Lærdal catchment)

FF	Q5	Q10	Q15	Q20	Q50	Q100	Q200	Q500	Q1000
GEV	348.12	385.35	403.79	415.71	448.51	469.03	486.56	505.94	518.20
GNo	346.65	383.63	402.53	415.08	451.50	476.40	499.62	528.35	548.88
P3	346.71	383.68	402.56	415.07	451.35	476.09	499.13	527.56	547.84
Gum	340.53	388.13	414.98	433.78	492.88	537.16	581.28	639.49	683.49

Table S17: Design flood for RCP8.5_2041-2070 scenario in m^3/s (Lærdal catchment)

FF	Q5	Q10	Q15	Q20	Q50	Q100	Q200	Q500	Q1000
GEV	349.20	384.45	401.30	411.96	440.25	457.10	470.91	485.45	494.22
GNo	347.27	382.51	400.11	411.65	444.50	466.43	486.53	510.90	528.02
P3	347.28	382.51	400.11	411.65	444.50	466.43	486.53	510.90	528.02
Gum	340.10	388.81	416.29	435.53	496.01	541.33	586.49	646.06	691.09

Table S18: Design flood for RCP8.5_2071-2099 scenario in m^3/s (Lærdal catchment)

FF	Q5	Q10	Q15	Q20	Q50	Q100	Q200	Q500	Q1000
GEV	404.48	467.00	501.56	525.45	598.94	652.45	704.48	771.21	820.22
GNo	404.75	466.71	500.86	524.49	597.61	651.65	705.19	775.74	829.24
P3	406.40	468.28	501.79	524.70	594.12	643.96	692.12	753.77	799.21
Gum	402.40	467.11	503.62	529.19	609.54	669.75	729.75	808.90	868.72

Appendix 6: HEC-RAS simulation of winter low flow for the future scenarios

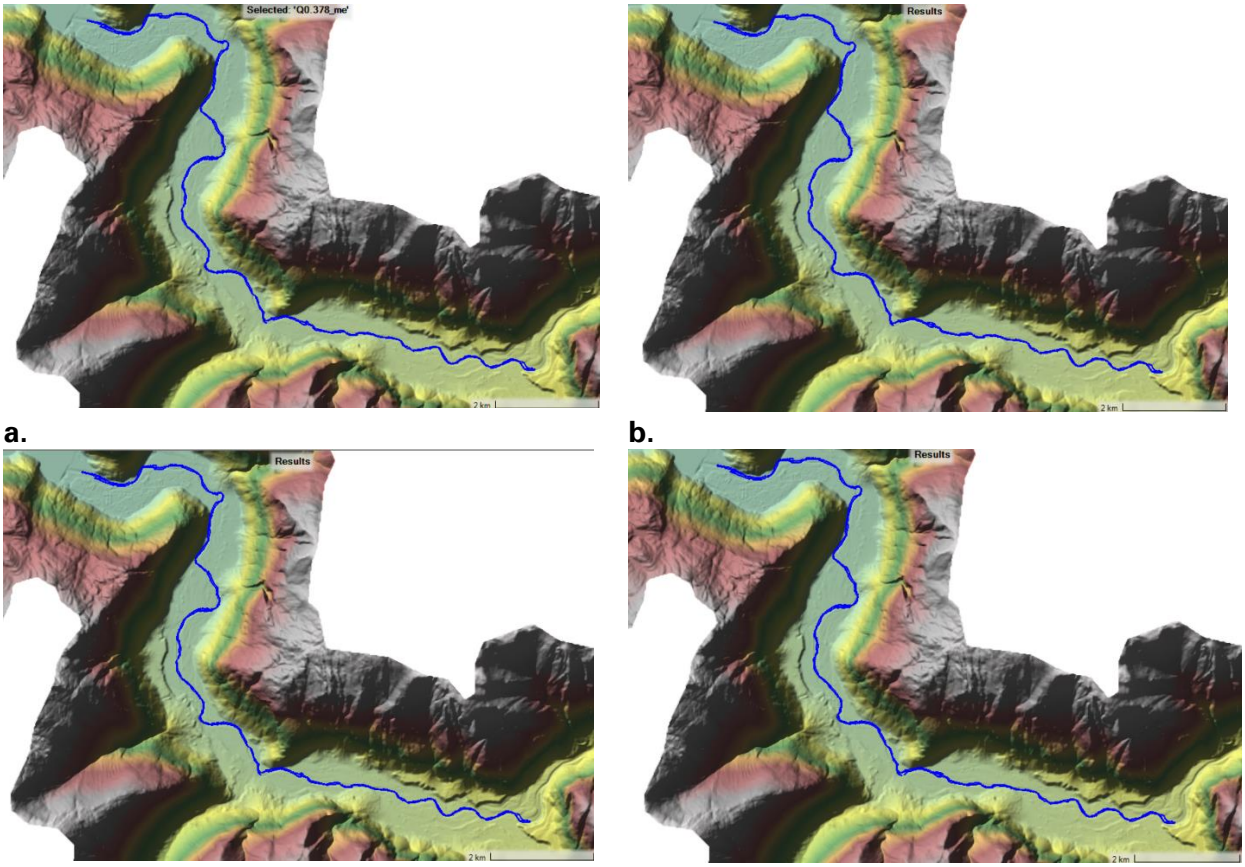

Figure S.6 HEC-RAS simulation of winter low flow for the baseline scenario, at maximum inundation boundary, for Lærdal catchment **a.** RCP4.5_2041 - 2070 **b.** RCP4.5_2071 – 2099 **c.** RCP8.5_2041 - 2070 **d.** RCP8.5_2071 – 2099